Dissertation

The Role of 15-Prostaglandindehydrogenase in Idiopathic Pulmonary Fibrosis

submitted by

Dr.med.univ.

Thomas BÄRNTHALER

For the Academic Degree of

Doctor of Philosophy (PhD)

at the

Medical University of Graz

Otto Loewi Research Center, Division of Pharmacology

under the Supervision of

Prof. Dr. Akos HEINEMANN

and

Prof. Dr. Rufina SCHULIGOI

2019

Declaration

I hereby declare that this dissertation is my own original work and that I have fully acknowledged by name all of those individuals and organizations that have contributed to the research for this dissertation. Due acknowledgement has been made in the text to all other material used. Throughout this dissertation and in all related publications I followed the guidelines of “Good Scientific Practice”.

Graz, am 10.7.2019, eh

Disclosures

This dissertations contains materials previously published in:
Bärnthaler, T; Maric, J; Platzer, W; Konya, V; Theiler, A; Hasenöhrl, C; Gottschalk, B; Trautmann, S; Schreiber, Y; Graier, WF; Schicho, R; Marsche, G; Olschewski, A; Thomas, D; Schuligoi, R; Heinemann, A. "**The Role of PGE2 in Alveolar Epithelial and Lung Microvascular Endothelial Crosstalk**." Scientific Reports (2017) 7 (1): 7923. doi: 10.1038/s41598-017-08228-y.

Furthermore, the data contained within the second chapter are currently under review as:

Bärnthaler, Th.; Theiler A. ; Zabini D. ; Trautmann S. ; Stacher-Priehse E. ; Lanz I. ; Klepetko W. ; Sinn K. ; Flick H. ; Scheidl S. ; Thomas D. ; Olschewski H. ; Kwapiszewska G.; Schuligoi R. ; Heinemann A. "**Inhibiting eicosanoid degradation exerts antifibrotic effects in a pulmonary fibrosis mouse model and human tissue**".

All necessary permissions have been obtained.All co-authors who contributed to the research in this thesis agreed to the use of their data.

These include:

Dominique Thomas, Sandra Trautmann and Yannick Schreiber

Institute of Clinical Pharmacology, Goethe-University Frankfurt, Frankfurt, Germany

Andrea Olschewski, Diana Zabini, Elvira Stacher-Priehse, Grazyna Kwapiszewska

Ludwig Boltzmann Institute for Lung Vascular Research, Graz, Austria

Holger Flick, Stefan Scheidl, Horst Olschewski,

Department of Internal Medicine, Division of Pulmonology, Graz, Austria

Benjamin Gottschalk, Wolfgang Graier

Division of Molecular Biology and Biochemistry, Gottfried Schatz Research Center, Graz, Austria

Katharina Sinn, Walter Klepetko

Division of Thoracic Surgery, Department of Surgery, Medical University of Vienna, Austria

Technical assistance: I thank Markus Absenger-Novak and Eleonore Fröhlich from the core facility for microscopy of the Medical University Graz, for their expert assistance in image acquisition. I am particularly grateful to Ilse Lanz, Martina Ofner, Sabine Kern, Sabine Halsegger, Daniela Kleinschek, Wolfgang Platzer and Kathrin Rohrer for their expert technical assistance.

Acknowledgements

First of all, I want to thank my supervisors, Akos Heinemann and Rufina Schuligoi, for their incredible support and for the opportunity to work with them. It was an amazing experience and I wouldn't want to miss a day of it. Thank you Rufina, for always having an open door, no matter the time, and for endless inspiring discussions and never-ceasing encouragement. It cannot be overstated what it means to have someone who is as enthusiastic about data and science as you are. While I am confident that I will not forget your lessons about scientific rigor and method, I am absolutely sure that I will always remember the fun we had in science.

Thank you Akos, for the unbelievable freedom you gave me in my project and in exploring my own scientific ways, while at the same time being always available for both help and advice.

Furthermore, I want to express my gratitude to the other members of my thesis committee, Andrea Olschewski and Grazyna Kwapiszewska, for their helpful inputs and fascinating discussions.

I also need to thank the Austrian Science Fund (FWF W1241), the Austrian Academy of Science (ÖAW, Doc-Stipendium) and the Medical University of Graz (Start Funding) for funding me during my PhD, and the DK-Molin, for providing the framework of my studies.

It is surprising how many remarkable people can work at one single place; Ilse, Wolfi, Carina, Ida, David, Sabine, Sonja, Kathrin, Geraldine and all the others, this experience would not have been the same without you. Everybody who can leave this institute and these people without feeling sad is obviously also capable of cold-blooded murder. Ilse and Wolfi, I need to thank you again, because without our conversations and lunch breaks, I would have starved long before even thinking about writing my dissertation.

Thank you Marc, Flo and Basti for providing support and distraction when needed.

I want to thank my family, especially my parents Judith and Manfred, my sister Kathrin, my grandparents Günther and Rosemarie, and Gernot and Bärbel; for your support, for being there for me and your interest in "what I am actually doing" ☺. I would not be where and who I am without you.

Last but not least, I can hardly express how much I owe to you Julia, for your unwavering support and belief in me. I am so happy to have you. Finally, thank you Nora, for being the best daughter one could wish for; I hope you enjoyed our excursions to the "Piepseschrank" as much as I did.

Table of Contents

Abbreviations

PG	prostaglandin
LX	lipoxin
RS	resolvins
TX	thromboxane
LT	leukotrienes
PUFA	polyunsaturated fatty acids
AA	arachidonic acid
cPLA	cytosolic phospholipase A
COX	cyclooxygenase
NSAIDs	non-steroidal, anti-inflammatory drugs
TNFα	tumor necrosis factor alpha
LPS	lipopolysaccharide
mPGES	microsomal prostaglandin E synthase
cPGES	cytosolic prostaglandin E synthase
PG…S	prostaglandin… synthase
…P receptor	…-type prostanoid receptor
GPCR	G-protein-coupled receptor
MRP	multridrug resistant protein
ATP	adenosine triphosphate
cAMP	cyclic adenosine monophosphate
GTP	guanosine triphosphate
GDP	guanosine diphosphate
PLC	phospholipase C
GEF	guanine nucleotide exchange factors

PI3K	phosphoinositol 3 kinase
IP3	inositol-1,4,5-trisphosphate
ERK	extracellular signal regulated kinase
PKC	protein kinase C
CRTH	chemoattractant receptor-homologous molecule expressed on T-helper type 2 cells
GPR	G-protein-coupled receptor
PGT	prostaglandin transporter
SLCO	solute carrier organic anion transporters
OATP	organic anion transporting polypeptides
15-PGDH	15-prostaglandindehydrogenase
NAD	nicotinamide adenine dinucleotide
K_m	Michaelis constant
V_{max}	maximal velocity
NADP	nicotinamide adenine dinucleotide phosphate
PHO	primary hypertrophic osteoarthropathy
HPGD	hydroxyprostaglandindehydrogenase (name of gene coding 15-PGDH)
PPARγ	peroxisome proliferator-activated receptor gamma
PGE-MUM	prostaglandin E-major urinary metabolite
IPF	idiopathic pulmonary fibrosis
ILD	interstitial lung diseases
HRCT	high resolution computed tomography
UIP	usual interstitial pneumonia
ECM	extracellular matrix
AEC	alveolar epithelial cells

ATI cells	type I alveolar epithelial cells
ATII cells	type II alveolar epithelial cells
FIF	familial interstitial fibrosis
aSMA	alpha-smooth muscle actin
TGFβ1	transforming growth factor beta 1
PDGF	platelet derived growth factor
CTGF	connective tissue growth factor
CD	cluster of differentiation
VEGFR	vascular endothelial growth factor receptor
FGFR	fibroblast growth factor receptor
BAL	bronchoalveolar lavage
NaOH	sodium hydroxide
HCl	hydrochloric acid
EtOH	ethanol
IHC	immunohistochemistry
HRP	horseradish peroxidase
AP	alkaline phosphatase
DAB	3,3'-diaminobenzidin
IF	immunofluorescence
DAPI	4′,6-diamidino-2-phenylindole
F'ab	antigen-binding fragment
ISH	*In situ* hybridization
miRNA	micro ribonucleic acid
TSA	tyramide signal amplification
EDTA	ethylenediaminetetraacetic acid

FBS	fetal bovine serum
DMEM	Dulbecco’s modified eagle medium
OPTI-MEM	optimized eagle’s minimal essential medium
KO	knock-out
PBMCs	peripheral blood mononuclear cells
HEPES	4-(2-hydroxyethyl)-1-piperazineethanesulfonic acid
HMVEC-L	human lung microvascular endothelial cells
NaCl	sodium chloride
SW	SW003291 (15-PGDH inhibitor)
DMAB	p-dimethylaminobenzaldehyde
NH_4Cl	ammonium chloride
BCA	bichinonic acid
RIPA	radio-immuno-precipitation
PCLS	precision cut lung slices
EBSS	Earle’s balanced salt solution
ELISA	enzyme linked immunosorbent assay
MAEC	mouse alveolar epithelial cells
ECIS	Electrical Cell-Substrate Impendance Sensing
AQP5	aquaporin 5
SP-C	surfactant protein C
vWF	von Willebrand Factor
mRNA	messenger ribonucleic acid
FSP	fibroblast specific protein
qPCR	quantitative polymerase chain reaction
SPM	specialized pro resolving mediators

Figures

Abstract

Idiopathic pulmonary fibrosis (IPF) is a disease linked to a high 5-year mortality, with few therapeutic options. Prostaglandin (PG)E_2 exhibits antifibrotic properties and is reduced in the broncho-alveolar lavage from IPF patients. 15-prostaglandin dehydrogenase (15-PGDH) is a key enzyme in PGE_2 metabolism under the control of transforming growth factor-β and microRNA 218.

We observed that expression patterns of 15-PGDH differ between healthy and IPF lungs, with areas of more pronounced expression in IPF. Treatment of mice with SW033291, an inhibitor of 15-PGDH, was beneficial against bleomycin-induced lung fibrosis in mice, reducing collagen content and improving lung function. These favorable effects were also observed when treatment was started after lung injury and established fibrosis. Fibrocytes are bone marrow derived cells that have been implicated in fibrotic remodeling. We found that PGE_2 inhibited human fibrocyte differentiation *in vitro* both in healthy donors and IPF patients, and observed a reduction of fibrocyte counts in bleomycin treated mice after treatment with 15-PGDH inhibitor, along with decreased alveolar epithelial cell apoptosis and fibroblast proliferation. In precision-cut lung slices from IPF patients, 15-PGDH inhibition increased PGE_2 levels and decreased collagen secretion. Finally, microRNA 218-5p, which is downregulated in IPF patients, suppressed 15-PGDH expression *in vivo* and *in vitro.*

In summary, these data suggest that 15-PGDH plays a crucial role in the metabolism of PGE_2 and inhibition of its activity positively affects the development of lung fibrosis through the antifibrotic effects of PGE_2. Thus 15-PGDH inhibition might be a promising novel approach for the treatment of IPF.

Zusammenfassung

Bei der idiopathischen pulmonalen Fibrose (IPF) handelt es sich um eine Erkrankung mit einer sehr niedrigen 5-Jahres-Überlebensrate und nur eingeschränkten therapeutischen Möglichkeiten. Prostaglandin E_2, ein Gewebshormon aus der Klasse der Eikosanoide zeigt deutliche antifibrotische Wirkungen und seine Spiegel sind in der bronchoalveolären Lavage von IPF-Patienten reduziert. Der Abbau dieses Mediators wird durch die 15-Prostaglandindehydrogenase (15-PGDH) vermittelt und dieses Enzym steht unter dem Einfluss des transformierenden Wachstumsfaktors β sowie der microRNA 218-5p.

Unsere Untersuchungen zeigten deutliche Veränderungen in den Expressionsmustern der 15-PGDH, mit einer markanten Steigerung der Expression in gewissen Arealen in IPF Lungen. Die Behandlung von Mäusen mit einem spezifischen Hemmstoff der 15-PGDH, SW033291 verhinderte die Entwicklung einer durch Bleomycin ausgelösten Lungenfibrose, was sich vor allem in einer verbesserten Lungenfunktion, und reduzierten Kollagenablagerungen widerspiegelte. Selbst wenn die Behandlung mit SW033291 erst begonnen wurde, nachdem sich bereits eine Fibrose entwickelt hatte, konnten wir diese Ergebnisse reproduzieren. Fibrozyten sind Zellen die dem Knochenmark entstammen und wurden mit dem fibrotischen Umbau verschiedener Gewebe in Verbindung gebracht. Wir konnten die Entstehung dieser Zellen aus Leukozyten von IPF-Patienten und gesunden Spendern in *in vitro* Versuchen mittels PGE_2 verhindern. Darüber hinaus reduzierte die zusätzliche Behandlung mit SW033291 die Fibrozytenzahlen in den Lungen im Vergleich zu den nur mit Bleomycin behandelten Mäusen und senkte die Apoptose von alveolaren Epithelzellen sowie die Proliferation von Fibroblasten. Die Expression der 15-PGDH wurde sowohl *in vitro* als auch *in vivo* durch die microRNA-218-5p supprimiert. Dies ist von besonderer Bedeutung, weil diese microRNA in IPF-Lungen erniedrigt ist. In *ex vivo* Kulturen von Lungengewebsproben (precision cut lung slices), die aus den Lungen von IPF-Patienten gewonnen wurden, konnten wir einen deutlichen Anstieg der Eikosanoide und ein Absinken der Kollagensynthese nach 15-PGDH-Inhibitorbehandlung nachweisen.

Unsere Daten zeigen, dass die 15-PGDH eine zentrale Rolle im PGE_2-Katabolismus spielt, und dass eine Inhibierung dieses Enzyms zu erhöhten PGE_2-Spiegeln führt, welche wiederum antifibrotische Wirkungen entfalten. Daher könnte die 15-PGDH einen neuen Angriffspunkt in der Therapie der IPF darstellen.

1 Introduction

1.1 Prostaglandins

Prostaglandins (PG) are a class of lipid mediators that belong to the larger group of eicosanoids. Besides prostaglandins, lipoxins (LX), some resolvins (RS), thromboxanes (TX) and leukotrienes (LT) are also classified as eicosanoids (Greek "*eikosi*", twenty). The term prostanoids in turn comprises PGs and TXs. As all eicosanoids, prostaglandins are derived from 20 carbon units long, polyunsaturated fatty acids (PUFA) and have great importance as signaling molecules under both physiological and pathological conditions. They have first been isolated and investigated in the 1930s (1, 2) and have since been extensively studied. PGs have been named according to being first isolated from the prostate gland (2) while thromboxane received its name in acknowledgment of its critical role in thrombosis and platelet aggregation (3). The subscripts (e.g. PGE_2) describe the number of double bonds in the molecule that depends upon the PUFA from which they are formed. Series 1 prostaglandins (e.g. PGE_1) are derived from dihomo-γ-linolenic acid, series 2 from arachidonic acid, and series 3 from eicosapentanoic acid (4, 5).

1.1.1 Prostaglandin synthesis

The first step in the synthesis of prostaglandins is the liberation of arachidonic acid (AA) (or other PUFAs) from membrane phospholipids by cytosolic phospholipase A2 (cPLA2). This is followed by oxygenation via cyclooxygenase (COX) 1 or 2 and resulting first in the formation of PGG_2 and afterwards PGH_2. PGH_2 is then metabolized via terminal prostaglandin synthases to the respective PGs, i.e. PGD_2, PGE_2, PGF_{2alpha}, PGI_2 or TXA_2. The most abundant series-2 PGs are in general considered to be pro-inflammatory. Due to their potent effects, levels of PGs need to be tightly controlled, either by hydrolysis or by specific enzymes mediating their degradation.

1.1.1.1 Cyclooxygenases

COX-1 and -2 are considered the key enzymes of PG synthesis as they are thought to be the rate limiting step in PG-generation (6). The fact that PGs play a crucial role in inflammation (as illustrated by their contribution to the 4 classic hallmarks of inflammation, which were first described by Celsus) is the reason that COX inhibitors are widely used for the symptomatic treatment of pain (7). Although this may lead to a wide range of adverse effects (7), COX

inhibitors, also referred to as non-steroidal, anti-inflammatory drugs (NSAIDs) are still first-line agents for this indication.

COX-1 and -2 each have two separate activities: cyclooxygenase activity, leading to formation of PGG_2 from AA, and subsequent peroxidase activity, catalyzing the reaction from PGG_2 to PGH_2. While these two isoforms have an amino acid sequence similarity of approximately 60-65%, they differ only slightly in their structure, the catalytic center is highly conserved and affinity for AA is almost the same (8). Furthermore, they do act as functional and structural dimers and present multiple glycosylation sites as confirmed by data from Western blot (8). Of note, COX-2 has an additional “side pocket” that allows for the metabolisation of a wider variety of substrates, especially endocannabinoids (9). The prostaglandin-endoperoxide synthase (PTGS) 1 and 2 genes that encode the two COXs are located on chromosome 9 and 1 respectively and are conserved in vertebrates (10). As COX-2 can be induced by a variety of stimuli, the classical paradigm is that while COX-1 is responsible for the basal synthesis of PGs in resting cells, COX-2 is expressed predominantly under inflammatory/activated conditions (6). Common stimulators of COX-2 expression include cytokines (e.g. tumor necrosis factor (TNF)α) or microbial components (such as lipopolysaccharide (LPS)) (11, 12). Although this might be true for a variety of tissues, some organs show considerable COX-2 expression already under baseline conditions, among them the lung and the kidney (12, 13). Furthermore, a recent study found expression of COX-2 at baseline conditions in the parenchymal cells of most organs, including the gastrointestinal tract, the nervous system, endocrine and exocrine glands and the reproductive organs, although sometimes at low levels (14). However, the notion that the gastro-protective effects of prostanoids depend upon COX-1-mediated synthesis resulted in the introduction of selective COX-2 inhibitors (coxibs) that show less gastrointestinal adverse events than classic NSAIDs (15), although these so-called Coxibs showed cardiovascular side effects, severely limiting their use (16). The development of selective COX-2 inhibitors was facilitated by the larger size of the active site in COX-2 and small amino acid differences of the enzymes (17). In the lung, both isoforms are present under physiologic conditions, both in mice and men, with predominant expression in alveolar epithelial cells (12, 18, 19). The fact that the respiratory tract lining fluid contains extensive levels of PGs, predominantly PGE_2, reflects the potent biosynthetic capacity of the lungs (20).

The first widely marketed medication that targeted COX enzymes was acetylsalicylic acid, synthesized by Felix Hoffman (21). However, it was not until 1971 that this mechanism was unraveled as the reason for its analgesic, anti-inflammatory and antipyretic actions (21, 22).

1.1.1.2 Terminal synthases

The last step towards the formation of the different PGs is catalyzed by the respective terminal synthases. Interestingly, most of them were shown to preferentially couple to one of the COX isoenzymes (as reviewed in (23)). While the three terminal synthases for PGE_2 received the most attention (microsomal PGE synthase (mPGES)1, linked to COX-2; mPGES2, no preference; cytosolic PGES, linked to COX-1), two synthases for PGD_2 have also been described (haematopoietic PGDS, linked to COX-1; lipocalin dependent PGDS, no preference) (24, 25). For both TXA_2 and PGI_2 only one terminal synthase exists (both preferentially linked to COX-2) (24, 25). In contrast, there are still doubts about specific PGF synthases, as enzymes from different families might contribute to PGF_{2alpha} synthesis and this might furthermore depend upon the specific tissue (23, 25, 26).

mPGES1 is, in contrast to mPGES2 and cPGES, considered to be the inducible isoform (25). Of note, studies have failed to show *in vivo* involvement in PGE_2 synthesis of mPGES2 and cPGES, providing some evidence that mPGES1 is the primary source of PGE_2 (27, 28). As mPGES1 is coupled preferentially (but not exclusively) to COX-2, it is responsible for the increases in PGE_2 seen upon stimulation and is also the primary source of PGE_2 in the lung under basal conditions (29). However, mPGES1 knockout mice lack the phenotype of COX and EP4 deficient mice, most notable the patent ductus arteriosus (30), meaning that residual synthesis seems to occur.

1.1.2 Prostaglandin release

As PGs mostly exert their effects via G-protein-coupled receptors (GPCR) with extracellular binding domains, but are synthetized in the cell, they have to cross the cell membrane. Although PGs are derived from lipids, they show very limited penetration through intact cell membranes (31) as they are charged ions at physiological pH (32). Despite this fact, they were widely believed to exit the cell mainly via passive diffusion until the prostaglandin efflux transporter multridrug resistant protein (MRP) 4 was shown to transport PGE_2 and other PGs with high affinity (33). This protein belongs to the subfamily C of ATP-binding cassette transporters and, besides prostaglandins, transports a variety of other endogenous compounds (e.g. cyclic nucleotides, such as cAMP, bile acids and steroids) but also drugs (e.g. antibiotics or diuretics) (34). The hydrolysis of ATP provides the necessary energy for the transport of its substrates across membranes. Most of the work concerning its role as a prostaglandin efflux transporter focuses on PGE_2 and there is evidence that increased MRP4 expression might play a role in the pro-carcinogenic effects of PGE_2 via increasing its extracellular levels (35). However, there is evidence that also in the absence of MRP4, PGs

can still exit the producer cells, possibly via other MRPs (36). The process of PG synthesis and release is illustrated in Figure 1.

1.1.3 Prostaglandin receptors

PGs exert the majority of their wide effects via activation of multiple receptors. All PG receptors are GPCRs and as such, are characterized by their seven transmembrane spanning domain and their binding of heterotrimeric G-proteins (mainly Gα, Gβ and Gγ). If not activated, the Gα-subunit is bound to GDP and associates with Gβ and Gγ. Binding of the ligand leads to conformational changes that in turn cause dissociation of GDP and, owing to the high GTP concentrations in living cells, its replacement by GTP. In response to this, the Gα and the Gβγ separate and induce their respective downstream effects. As the Gα subunit has an intrinsic GTPase activity, GTP is hydrolyzed to GDP and the subunits reunite. Activated Gα and Gβγ can regulate adenylyl cyclases and phospholipase C (PLC) while Gα subunits also affect cGMP, phosphodiesterases and guanine nucleotide exchange factors (GEF). In contrast, the Gβγ subunit can activate GPCR kinases, thereby regulating GPCR signaling, and controls some potassium and calcium channels, as well as phosphoinositol 3 kinase (PI3K) and mitogen activated protein kinases (37). In order to “fine-tune” GPCR-signaling, a complex machinery exists, consisting for example of GTPase accelerating proteins, or activators of G-protein signaling (38).

The Gα subunits can be divided into four families depending upon their primary function. $G\alpha_s$ activation stimulates adenylyl cyclase, thereby increasing cAMP formation while $G\alpha_i$ activation has the opposite effect. $G\alpha_q$/ $G\alpha_{11}$ activates phospholipase C, resulting in the formation of diacyl glycerol and inositol trisphosphate. $G\alpha_{12}$/ $G\alpha_{13}$ results in the activation RhoGEF (39). Prostanoid receptors can be coupled to any of these G subunits. The prostanoid receptors are named for the endogenous substrate that binds with the highest affinity, for example I-type prostanoid receptor (IP) preferentially binds PGI_2. Of note, most prostanoid receptors do show cross reactivity with other prostanoids as well, being reflective of their close structural resemblance. Interestingly, receptors for the very same prostanoid can be coupled to opposing $G\alpha_s$ and $G\alpha_i$ subunits, as it is for example the case for DP1 and 2 and EP3 as opposed to 2 and 4 receptors. For a graphic summary of G-protein coupling of the receptors see Figure 2.

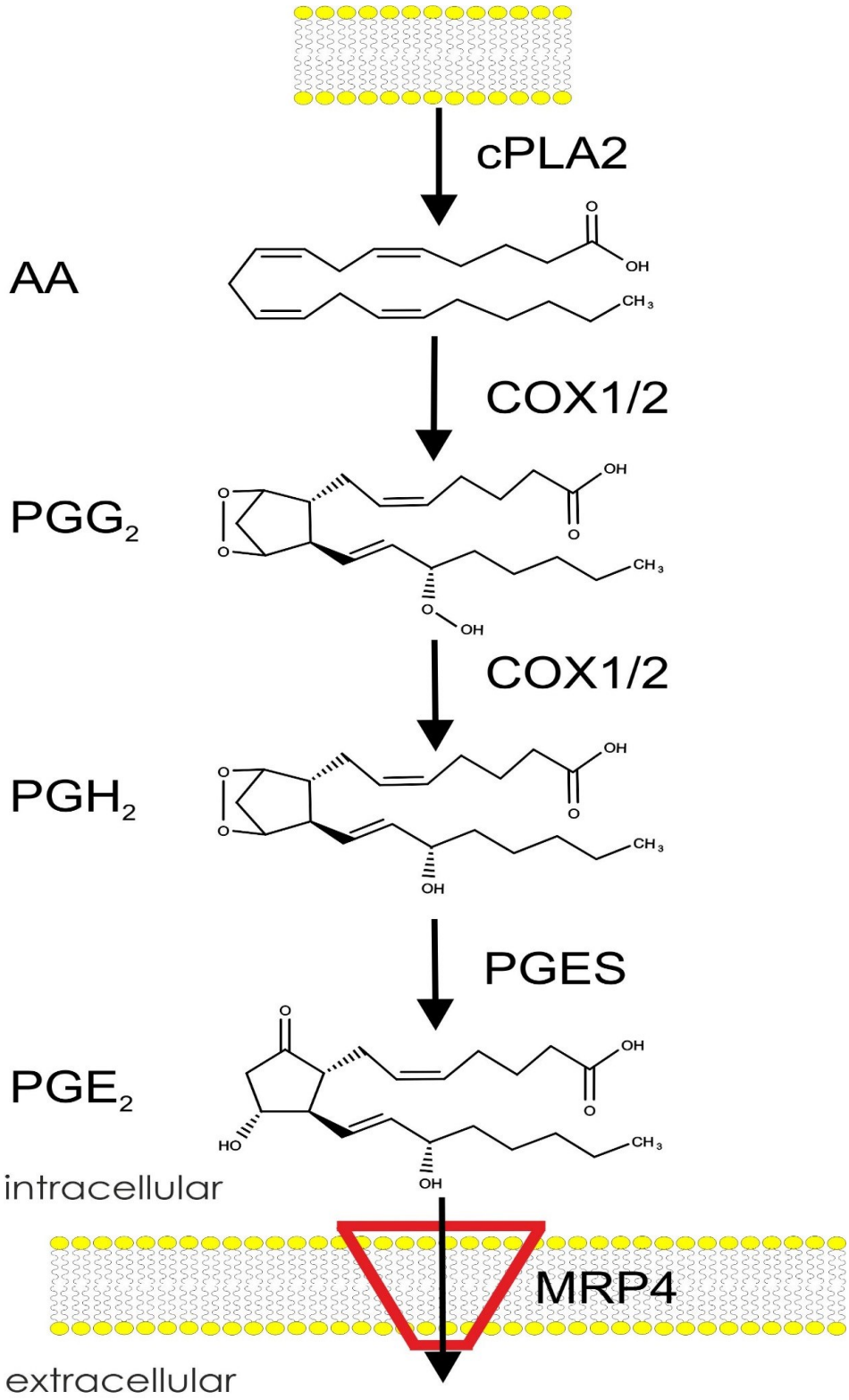

Figure 1. Biosynthetic pathway of prostaglandins as illustrated by the example of PGE_2. *The first step consists of the cleavage of arachidonic acid (AA) from membrane phospholipids by cytosolic phospholipase A2 (cPLA2) and is followed by its metabolisation via cyclooxygenase (COX) 1 or 2 to PGG_2 and PGH_2.Afterwards, microsomal PGE-synthase 1 (PGES) catalyzes the final reaction to PGE_2 which is then transported out of the cell via multi-drug-resistant protein (MRP) 4 to the extracellular space.*

1.1.3.1 EP-receptors

EP1 receptor activation has been shown to result in an increase in intracellular Ca^{2+} presumably via activation of $G_{q/11}$ protein, subsequent recruitment of PLC and inositol-1,4,5-trisphosphate (IP3) formation (40). Nevertheless, some authors suggest different mechanisms, possibly involving protein kinase C mediated Ca^{2+} increases (41). Under physiologic conditions, the EP1 receptor is, besides other functions, involved in pain responses and blood pressure regulation (40). Pulmonary functions include vasoconstriction in human pulmonary veins (42), stimulation of surfactant production in rats (43) and wound healing in airway epithelial cells (44).

EP2 receptor activation predominantly leads to $G\alpha_s$ –mediated adenylyl cyclase activation and thereby promotes cAMP elevation, resulting in protein kinase A activation which exerts its effects via transcription factors, most notably cAMP responsive element binding protein (45). The effect on cAMP is shared with the EP4 receptor. Furthermore there is evidence of EP2 linkage to beta-arrestin1, which usually leads to receptor desensitization, but in EP2 receptors activates an additional pathway, resulting in PI3K stimulation (46, 47). Its physiological functions include repression of immune functions, but also significant vasodilation as shown in EP2-knockout mice (48, 49). In the lung, there is considerable evidence for the protective role of EP2 receptors under inflammatory and also fibrotic conditions (50-52). Furthermore, EP2 also mediates bronchodilation (53), although some of these effects might be mediated by EP4 receptors in humans (54).

EP3 receptors are mainly coupled to $G\alpha_i$ subunits and thus exert their actions via inhibition of adenylyl cyclase and its downstream effectors. They do in some ways have opposing roles as compared to EP2/4 signaling, leading for example to vasoconstriction (42) and platelet activation (55). Interestingly, variants exist of EP3 receptors that also couple to other G subunits such as G_q, activating the respective downstream signaling pathways (56). Furthermore, species-specific splice variants that differ in their subsequent G-protein signaling, rate of desensitization or constitutive activity have been described (57-60). In the airways, EP3 receptors induce bronchodilation and protect from allergic inflammation (61), but also lead to vasoconstriction in the pulmonary airways (42). Furthermore, they are responsible for the cough inducing effects of PGE_2 via sensory nerve depolarization (62).

EP4 receptors are also coupled to $G\alpha_s$ subunits and thus share a similar signaling pathway with EP2 receptors, which delayed its recognition as a receptor in its own right (63). It addition to the signaling pathways described for EP2 receptors, the EP4 receptor can also lead to PI3K and AKT (64) as well as extracellular signal regulated kinase (ERK) and protein kinase (PK)C

activation (65, 66). The EP4 receptor is partly responsible for the anti-inflammatory functions of PGE_2 in eosinophils and lymphocytes and prevents platelet activation (49, 55, 66). In the lungs, the EP4 receptor protects from inflammation and exerts antifibrotic functions (12, 67, 68).

Taken together, the PGE_2 –activated EP receptors mediate protective functions in the lungs which led to the notion that the lungs are "a privileged site for the beneficial actions of PGE_2" (69). However, PGE_2 has been recognized to play important roles in carcinogenesis and is the main reason why pharmacologic inhibition of COX-isoenzymes has been explored as a chemopreventive option (as recently reviewed in (70, 71)).

1.1.3.2 DP receptors

The DP1 receptor shows similar characteristics to EP2 and EP4, being also coupled to a $G\alpha_s$ subunit. Besides increasing cAMP levels, it can also function as a transcriptional regulator, for example in increasing serum response element (72). It is involved in immune cell function, especially in eosinophils, in addition to being a vasodilator (72, 73). In the lung, it has been shown that activation of DP1 exerts pro-inflammatory effects (74) and can induce cough via sensory nerve stimulation (75).

The DP2 receptor was first named Chemoattractant Receptor-homologous molecule expressed on T-Helper type 2 cells (CRTH2) or GPR44. It is coupled to $G\alpha_i$ subunit and decreases cellular cAMP levels, but DP2 can also signal via beta arrestin and PLC and IP3 (76). It is expressed on a wide variety of immune cells, including Th2 cells, eosinophils and basophils, and is involved in chemotactic responses (77). Consequently, antagonism of this receptor has been investigated as a target in asthma (78) and other inflammatory lung diseases (74). Of note, the antifibrotic effect of PGD_2 is probably also mediated via DP2 (79, 80).

Although PGD_2 is best known for its effects in allergy and especially asthma, it may also exert beneficial roles in the lungs, such as in models of fibrosis (80) or acute lung injury (81) although others show opposing effects (74).

1.1.3.3 IP receptors

Similar to the EP2/4 and DP1 receptor, the (human) IP receptor is predominantly coupled to a $G\alpha_s$ subunit (82). It exerts its effects via increased cAMP formation, thereby decreasing Ca^{2+} concentrations. The most prominent result of this cascade is the pronounced vasorelaxation especially in the pulmonary circulation that has found widespread therapeutic application in the treatment of pulmonary arterial hypertension (83). As PGI_2 - the primary ligand - is

notoriously unstable (84), agonists have been developed, most of which show some crossactivation of other prostanoid receptors (85). In addition to the vasodilatory effects, PGI_2 potently inhibits platelet aggregation (86) and acts in an anti-artherogenic manner (87).In addition, antifibrotic effects in a model of pulmonary fibrosis, where it also affects transcription via nuclear exclusion of transcription factors (88) have been described (89).

1.1.3.4 TP receptor

TP receptors are abundantly expressed on platelets and mediate the potent pro-thrombogenic effects of TXA_2 via coupling to $G_{\alpha q}$ and subsequent PLC activation, but $G_{12/13}$ coupling, followed by myosins light chain phosphorylation via RhoA is also involved and two splice variants have been described that differ in their affinity for G-protein coupling (90, 91). Similar to PGI_2, TXA_2 is unstable in solution, necessitating specific agonists for receptor studies (92). The therapeutic effect of acetylsalicylic acid on platelets depends upon the decrease in endogenous TXA_2 caused by irreversible COX-1-inhibition in platelets that results in reduced TP receptor activation (93). In addition, some studies describe effects of TP signaling in angiogenesis and cardiovascular disease, and in accordance with its role in haemostasis it is also a potent vasoconstrictor (93). In the lungs, TP activation was shown to lead to bronchoconstriction (94) and increased edema formation in acute lung injury (95).

1.1.3.5 FP receptor

FP receptors are coupled to $G_{\alpha q}$ in humans and activation leads to IP3 and diacylglycerol formation and Ca^{2+} mobilization. In humans, two splice forms have been described (96), with the main difference being the sensitivity to inactivation via phosphorylation by PKC (97). FP receptor activation via PGF_{2alpha} exerts pro-proliferative effects (98), and also shows great importance in parturition (99) as well as intraocular pressure regulation (100). In the lung, FP receptor activation has been associated with worsened fibrosis (101).

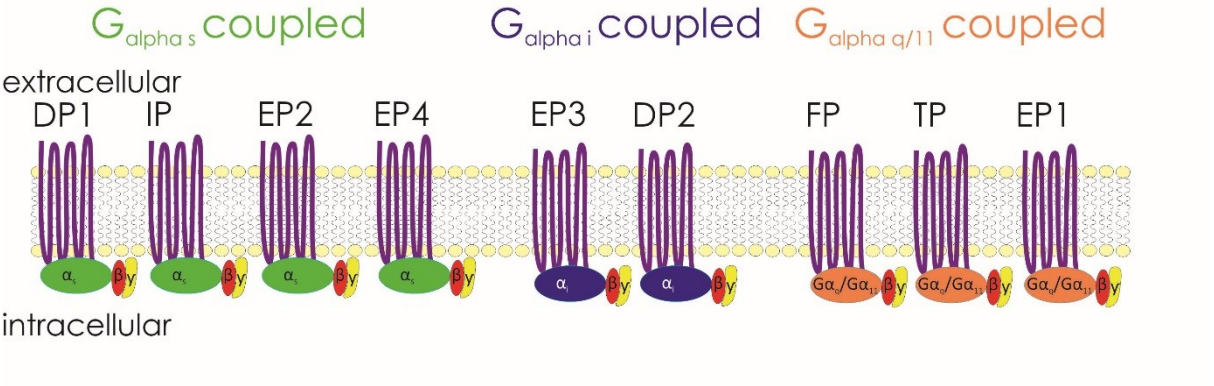

Figure 2. G_α subunit coupling of the prostaglandin receptors. *All PG-receptors are seven transmembrane, G-protein coupled receptors. While most of them couple to a adenylyl cyclase stimulatory subunit (α_s), some also*

show inhibitory properties (α_i) and others work via coupling to $G_{\alpha q}$/ G_{11}. This is one of the mechanisms that enables PGs to exert their widely differing functions.

1.1.4 Prostaglandin degradation/15-Prostaglandindehydrogenase

PGs are very potent molecules and the same mediator might exert different and even opposing effects, depending upon the spatial context and the expressed receptors (102). Therefore, termination of signaling via degradation is a crucial step in their metabolic pathways. In order to achieve this, different strategies have evolved. While PGI_2 and TXA_2 are rapidly degraded in plasma or aqueous solutions in a non-enzymatic fashion (half-lives 3 min and 30 seconds respectively) (84, 92), similar findings have been described for PGD_2 but at much lower rates (103). In contrast, PGE_2 is much more stable and PGF_{2alpha} withstands non-enzymatic degradation best (104).

In order to terminate their biological activity, they must first be transported into the cell, where their degradation takes place. As PGs do not readily cross cell membranes (105) they need to be transported. In 1995, a specific prostaglandin transporter (PGT) for eicosanoids was discovered (106), belonging to the family of solute carrier organic anion transporters (SLCO)/organic anion transporting polypeptides (OATP), and was later termed SLCO2A1/OATP2A1. These transporters work by exchanging intracellular with extracellular anions, being dependent upon local substrate gradients and pH (107). Interestingly, expression of this transporter is highest in the lung, where most degradation of PGE_2 takes place (108).

Consequently, PGE_2 and PGF_{2alpha} are predominantly metabolized by a specific enzyme, 15-prostaglandindehydrogenase (15-PGDH) (NAD+ dependent), which catalyzes the reaction of the 15-hydroxy group into a keto group, thereby greatly decreasing biological activity (109). The cofactor for this reaction is NAD/NADH and the reaction takes place in a stereospecific manner (110). The substrate with lowest K_m and highest V_{max} is PGE_1, closely followed by PGE_2 and PGE_3 (109). Besides PGE, PGF_{2alpha} (109) and LXA_4 (111) are metabolized at relatively high rates. Also PGI_2 and PGD_2 can be metabolized by 15-PGDH, but at much lower rates, thereby casting some doubt on the biological relevance of this process for these prostanoids (84, 92, 103, 112). However, there is also some evidence for a PGD_2 specific NADP-dependent 15-prostaglandin-D dehydrogenase (113). Another enzyme, carbonyl reductase type 1 (CBR1) also shows NAPD-dependent 15-PGDH activity in vitro, but is more efficient in reducing PGE_2 to PGF_{2alpha} (114). Thus, NAD-dependent 15-PGDH is considered the primary catabolic enzyme of PGE which is corroborated by the finding that loss of function mutations lead to increased PGE_2 levels in humans (115). Therefore, if not further identified, 15-PGDH refers to this isoform. The potency of this catabolic pathway is illustrated by the fact,

that after a single circulation through the liver or lung (where circulating PGE_2 is primarily metabolized) 70% and 95% are cleared, respectively (116). The notion that degradation of PGs is dependent upon a two-step model of initial cellular uptake via PGT and subsequent metabolization by 15-PGDH has been confirmed in an elegant set of experiments by Nomura et. al. (117).

Studies in 15-PGDH knockout-mice revealed multiple roles for this enzyme. The most prominent feature in homozygous mice is the persistent ductus arteriosus Botalli that ultimately leads to death in the first 48 hours after birth which can be prevented by the application of a single dose of a COX-inhibitor within 12 hours postnatally (118). This is due to the crucial role of PGE_2 in ductus arteriosus closure after birth, mirrored by the fact that also alterations in COX expression and EP4-receptors interfere with this important step of postnatal adaption (119, 120). The current hypothesis is that in the fetal circulation, PGE_2 suppresses smooth muscle activity in the ductus arteriosus via the EP4 receptor (120). Once the pup is born, the lungs unfold, resistance decreases, and blood circulates through the lungs, where high levels of 15-PGDH lead to degradation of PGE_2 and thereby terminate EP4 signalling in the ductus, resulting in its closure (118, 119). In addition, studies performed in 15-PGDH knockout -mice revealed reduced airway hyperresponsiveness in response to methacholine, further highlighting the importance of this enzyme in the lung (121). Furthermore there is considerable evidence that 15-PGDH knockdown leads to increased cancer susceptibility in mice and many types of tumors show downregulation of this enzyme, thereby presumably facilitating the pro-carcinogenic effects of PGE_2 (as reviewed in (122)).

However, in humans, loss of function of 15-PGDH has only been shown to lead to primary hypertrophic osteoarthropathy (PHO), characterized by digital clubbing (115). This has been elucidated by studying multiple families with increased incidences of PHO and the subsequent finding of mutations in the HPGD gene (115, 123-126). Although studies described downregulation of 15-PGDH in pancreatic, colon, breast and lung cancer, and identified it as a negative prognostic marker (122, 127-129), in all the investigations into these “knockdown” patients (~50), not a single one has been described to have had cancer, and no disposition towards malignancies of colon or lung were detected (115, 123-126, 130). Patent ductus arteriosus was present only in a few patients, being in stark contrast to the data from mice (115, 118, 126). However, ductus closure in human neonates can also be prevented by PGE_1 (7), meaning that reduction of EP receptor signaling is also a crucial step in humans. Thus, one explanation for the ductus closure in humans not possessing 15-PGDH might be that in the fetal circulation most PGE originates from the placenta, and that therefore, the decrease

in concentration achieved by cord clamping might be sufficient in the majority of cases (115). A recent work also showed a fundamental contribution of 15-PGDH on regulatory T-cell mediated suppression of conventional T-cells via PGE_2 metabolite 15-keto-PGE_2-dependent PPARγ-signaling (131).

Interestingly, mutations in the human SLCO2A1 gene revealed a different phenotype, which may consist, in addition to PHO, of hereditary enteropathy and patients also experience early onset colon adenomas (132, 133). Of note, digital clubbing is less common in these patients and seems to rather affect male individuals.

15-keto-PGE_2, the product of this katabolic steps is almost devoid of activity at EP receptors, but might still exert actions via PPARγ-signaling (131, 134). Therefore, also this compound is subject to subsequent degradation, resulting in the formation of 13,14-dihydro,15-keto-PGE_2 via Δ^{13}-15-ketoprostaglandin reductase (135) and ultimately PGE-major urinary metabolite (136). However, the rate-limiting steps of degradation seem to be internalization by SLCO2A1 and inactivation via 15-PGDH (117, 135). The processes leading to PGE_2 degradation are illustrated in Figure 3.

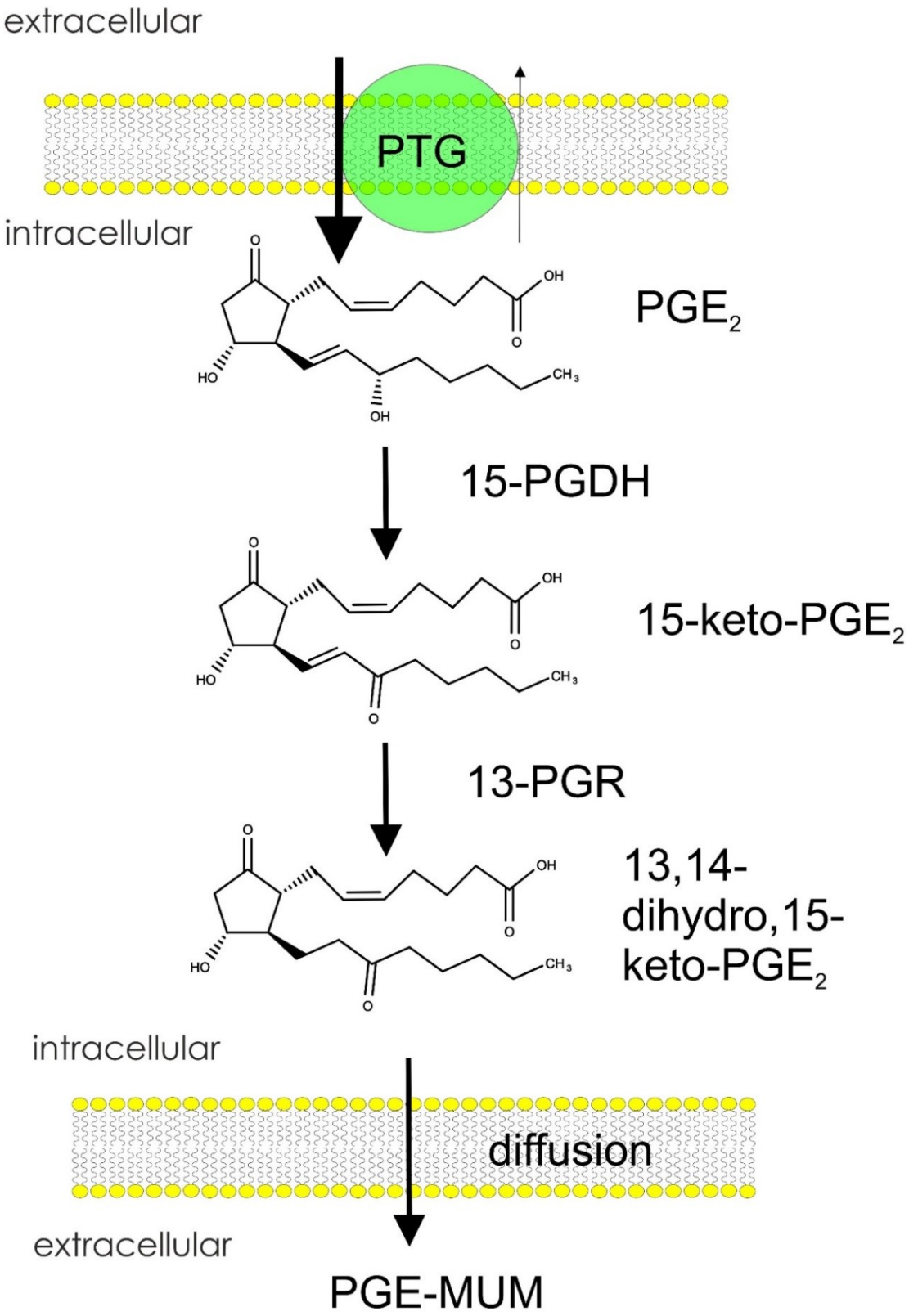

Figure 3. Degradation of prostaglandins as shown by the example of PGE_2. *After uptake into the cell from plasma or extracellular space via the prostaglandin transporter (PTG, aka SLCO2A1/OATP2A1), PGE_2 is oxidized by 15-prostaglandindehydrogenase (15-PGDH). The resulting metabolite (15-keto-PGE_2) is then further broken down by Δ13-15-ketoprostaglandin reductase (13-PGR) to 13,14-dihydro,15-keto-PGE_2 that leaves the cell via diffusion. The final metabolite, PGE-major urinary metabolite (MUM) can be detected in the urine.*

1.2 Idiopathic pulmonary fibrosis

1.2.1 Definition

Idiopathic pulmonary fibrosis (IPF) belongs to the family of interstitial lung diseases (ILD). These are defined by interstitial fibrosis, inflammation, and increased cellular proliferation; these features are neither caused by cancer nor infection, with fibrosis being the predominant finding in most cases (137). While IPF is probably the single most common ILD, the majority of patients ultimately receive a different diagnosis, with chronic hypersensitivity pneumonia, autoimmune disease and pulmonary sarcoidosis being the most likely. The defining features of IPF are its chronic progressive nature, the lack of causative agents, and the presence of specific histologic and radiologic findings. In general, Hamman and Rich are considered to first have described IPF, especially in view of its clinical presentation, but reports from autopsies and patient histories being consistent with this disease date back until 1887 (138).

1.2.2 Epidemiology

In general, IPF has been considered a rare disease, but epidemiological data are often hard to interpret, mainly due to unclear definitions (139). Nevertheless, a systematic review gives an incidence of fewer than 4 (South America and East Asia) and 3-9 (Europe and North America) per 100 000 inhabitants(140), although much higher rates, depending on the stringency of diagnostics, ranging up to 17.4 per 100 000 have been reported (139). The incidence of IPF seems to increase in recent years; however, whether that is due to an actual increase or rather to better diagnostic procedures and heightened scrutiny in the face of specific therapies remains unclear (140). Most studies show that more man than women are affected (140). Of note, untreated IPF has a serious prognosis, with a median survival of only 3.8 years (141). New treatment options (as will be discussed below) have been shown to significantly increase survival.

1.2.3 Clinical presentation / Diagnosis

The most prominent symptoms in ILD are chronic dry cough and dyspnea (especially under exercise). Clinical examination might reveal crackles upon auscultation of the lungs. Early recognition is crucial, as current antifibrotic drugs are able to significantly slow disease progression but do not regenerate fibrotic tissue (142). However, time from onset of symptoms to diagnosis can be long, in a single digit percentage of patients probably exceeding 5 years (143). This is due to the similarities of IPF symptoms to other diseases, such as heart failure or chronic obstructive pulmonary disease, which can both present with exertional dyspnea but are 100-1000-fold more common (143-145).

For diagnosis, there are certain criteria that must be met, as detailed in the specific guidelines (146):

1. Known causes of other interstitial lung disease should be excluded (especially but not limited to exposure to occupational hazards (e.g. birds, mold), autoimmune disease or medications (e.g. amiodaron or nitrofurantoin))
2. High resolution computed tomography (HRCT) should reveal presence of lesions specific for IPF
3. If lung biopsy is performed, the combination of histologic evaluation and HRCT should match specific findings

HRCT is now considered to be sufficient for final diagnosis without the need for lung biopsy if it is consistent with a usual interstitial pneumonia (UIP, the name for the histological and radiographic findings indicative of IPF) pattern as studies have shown a positive predictive value in 90-100% of cases (146). This includes three hallmarks: i) subpleural, basal predominance, ii) reticular abnormality, iii) honeycombing with or without traction bronchiectasis, while the absence of these hallmarks or the presence of features that are inconsistent with IPF hints towards other pathologies. In other cases, a lung biopsy is necessary for further evaluation and might still provide a final diagnosis of IPF. Histology is remarkable for the patchy involvement, evidence of marked fibrosis with our without honeycombing and the presence of fibroblastic foci (146).

1.2.4 Pathogenesis and pathophysiology

Although the ultimate cause for IPF has not been established so far, there is considerable evidence for an involvement of both alveolar epithelial cells as well as fibroblasts in the pathogenesis and progression of this disease. Furthermore, there are indications that cells of the immune system might play a crucial role and that relations to the microbiome might also exist (as recently reviewed in (147) and (148)). In general it is believed that via mechanisms that are not completely understood, repeated injury to alveolar epithelium leads to denuding of this area and to a subsequent increase in fibroblast proliferation and extracellular matrix (ECM) production. This in turn not only hinders inflation/expansion of the lung, but also increases the distance between blood and airspace, thereby impairing diffusion of oxygen and CO_2 that strongly depends upon this very distance. Ultimately this causes respiratory failure, and necessitates lung transplantation or eventually leads to death. Pathophysiological findings are summarized in Figure 4.

1.2.4.1 Alveolar epithelial cells

Alveolar epithelial cells (AEC) are the cells that line the alveoli, the terminal airspace of mammalian lungs, where gas exchange takes place. They form one part of the blood-air barrier facing the inhaled gases. There are two different types of AECs, type I (ATI) and type II (ATII) cells, with tremendously different morphology and function.

ATI cells line 95% to 99% of the alveoli, although they only account for about 10% of alveolar cell counts. This illustrates the vast surface covered by a single cell, as recently modeled in an elegant approach by Schneider et al. (149). They share a single basal membrane with endothelial cells of the pulmonary capillaries and are thin and flat in order to keep diffusion distance low (150, 151). While maintaining barrier integrity might be one of their key functions, these cells are also involved in fluid clearance from the alveoli and produce cytokines upon stimulation (152, 153).

ATII cells are cuboidal cells that contain lamellar bodies, rich in phospholipids. This reflects its most well-known function namely the production of surfactant, the protein/lipid layer that lowers surface tension in the lungs in order to prevent collapse and adhesion (150). Besides, they also play a role in host defense and function as “defenders of the alveolus”(154). One of their functions that has also received attention in IPF is that they can act as stem cells for alveolar regeneration under certain conditions (155).

The initiating event in pulmonary fibrosis seems to be the loss of epithelial barrier integrity via exogenous or endogenous injury, and this is substantiated by the facts that familial interstitial fibrosis (FIF) shows genetic alterations in epithelial (barrier) related genes, such as surfactant proteins or desmoplakins (as reviewed in (148)). Subsequently, impaired regeneration of the epithelial cell layer leads to the initiation of a pro-inflammatory, and - depending upon other risk factors - pro-fibrotic response. This view is corroborated by findings that shortened telomeres can be found in ATII cells in IPF patients and telomeres are significantly shorter in more affected areas and decreased telomere-length is associated with bad prognosis (156). Furthermore, mice with selective telomere dysfunction in ATII cells develop pulmonary fibrosis (157), and telomerase mutations were present in FIF (148). In addition, mitochondrial dysfunction (158) and endoplasmatic reticulum stress (159) are factors that contribute to the damage of epithelial cells and also increased apoptosis has been noted (102). In conclusion, it is well accepted that increased loss of epithelial cells and decreased regeneration are factors that significantly contribute to pulmonary fibrosis. Although the resulting processes are still incompletely understood, one factor seems to be the decrease in antifibrotic factors synthesized by AECs (e.g.PGE_2), thereby leading to aberrant fibroblast activation and ECM

deposition (18, 51, 160). Interestingly, also hyperplasia of ATII cells, probably a sign of compensatory proliferation, has been described (161).

1.2.4.2 Fibroblasts

Fibroblasts are interstitial cells in the lungs that show considerable heterogeneity (162) and contribute to its diverse functions depending on their subtype.

Interstitial fibroblasts are responsible for maintaining the complex structure of the lungs, in part via formation of ECM (162). Furthermore, these cells have been strongly implicated in wound healing processes, such as post-pneumonectomy lung growth (163). They are localized in the alveolar septa.

Lipofibroblasts are a different population of mesenchymal cells and can be found in close proximity to ATII cells and are characterized by containing lipid droplets. These cells seem to serve as helper cells under physiologic conditions and take up triglycerides and subsequently transfer them to ATII cells, thereby promoting surfactant production (164, 165).

In fibrosis, both types of fibroblasts can undergo transdifferentiation towards a third identity, called myofibroblast (166, 167). Myofibroblasts express alpha-smooth muscle actin (aSMA), and thus acquire a contractile phenotype as for example needed in wound closure (168) .The physiologic response of fibroblasts to tissue injury consists of activation (including ECM synthesis), proliferation and transdifferentiation towards myofibroblasts. This process is dysregulated in IPF, thereby leading to excessive fibroblast proliferation and myofibroblast formation. The current paradigm is that injured epithelial cells produce soluble factors, such as transforming growth factor β1 (TGFβ1), platelet derived growth factor (PDGF) or connective tissue growth factor (CTGF) and thereby activate fibroblasts in an attempt to heal damaged tissue. In contrast to physiologic wound healing, for reasons described above, epithelial cells are not able to inhibit this process anymore and thus, activation of fibroblasts prevails, their apoptosis is inhibited and this ultimately leads to the development of pulmonary fibrosis. In addition, alterations in signaling confer increased resistance to these inhibitory signals (e.g. PGE_2) (169). These are the reasons why fibroblasts are considered the main effector cell in IPF (167). The histopathologic correlation of this process is the fibrotic focus.

Indeed, there is evidence that myofibroblast transdifferentiation can be reversed by some agents that ameliorate fibrosis in mouse models (166, 170).

In addition to the described roles, there is also evidence that activated or fibrotic fibroblasts can induce alveolar epithelial cell apoptosis, thereby further promoting the described *circulus vitiosus* (171).

1.2.4.3 Fibrocytes

Since the first identification of fibrocytes (172), their role in fibrosis has been investigated. Fibrocytes represent a population of bone marrow derived cells that also express mesenchymal markers, first and foremost collagen I (resulting in positivity for both CD45 and collagen I among others (173)). Under physiologic conditions, similar to fibroblasts, fibrocytes seem to be involved in tissue repair and wound healing, as suggested by their ability to quickly migrate to sites of injury and enhancement of wound healing (174, 175). In IPF, fibrocytes have been identified as a potential biomarker and prognostic tool, and increased fibrocyte counts in the peripheral blood of patients are associated with a worsened prognosis and decreased survival (176, 177). Interestingly, in mouse models, these cells do not rely on collagen I to promote fibrosis, but rather do so via paracrine effects. This was shown in an elegant set of experiments, where bone marrow specific deletion of collagen I did not ameliorate fibrosis, but prevention of fibrocyte accumulation in the lungs via deletion of their chemokine receptors did (174, 178-180). Furthermore, fibrocytes do not seem to contribute to the myofibroblast population described above but do accumulate in IPF lungs (167, 176).

1.2.4.4 Other cells involved in IPF

In addition to the cell types described above, also other populations are involved in this disease. There is evidence for the emergence of myofibroblasts from pericytes, but the differentiation of epithelial and endothelial cells to myofibroblasts (termed epithelial- or endothelial-to-mesenchymal transdifferentiation) probably does not play a role (167, 181). In addition, IPF pericytes show increased migratory and invasive behavior as compared to pericytes from healthy controls (182). As for endothelial cells there is some evidence that increased endothelial nitric oxide synthase in a mouse model is protective, but overall, their role in IPF is less clear (183). Also macrophages/monocytes show involvement in the pathogenesis of IPF and are able to drive or prevent fibrosis, depending on their phenotype and the secreted mediators (as recently reviewed in (184)).

1.2.4.5 Pathophysiologic changes

The above mentioned processes ultimately lead to the aberrant ECM formation, corresponding thickening of alveolar wall, and, subsequently, replacement of healthy alveoli with fibrotic tissue in IPF patients. Initially, this process is reflected in a decrease in total lung capacity and forced vital capacity as well as forced expiratory volume/1s in lung function testing, factors that are caused by the increasing restriction of lung tissue. Finally, this leads to a worsening of gas exchange and results in death due to respiratory failure, although comorbidities such as

ischemic heart disease are not uncommon (185). Of note, a decrease in forced vital capacity more than 10% as compared to previous values is significantly associated with bad prognosis.

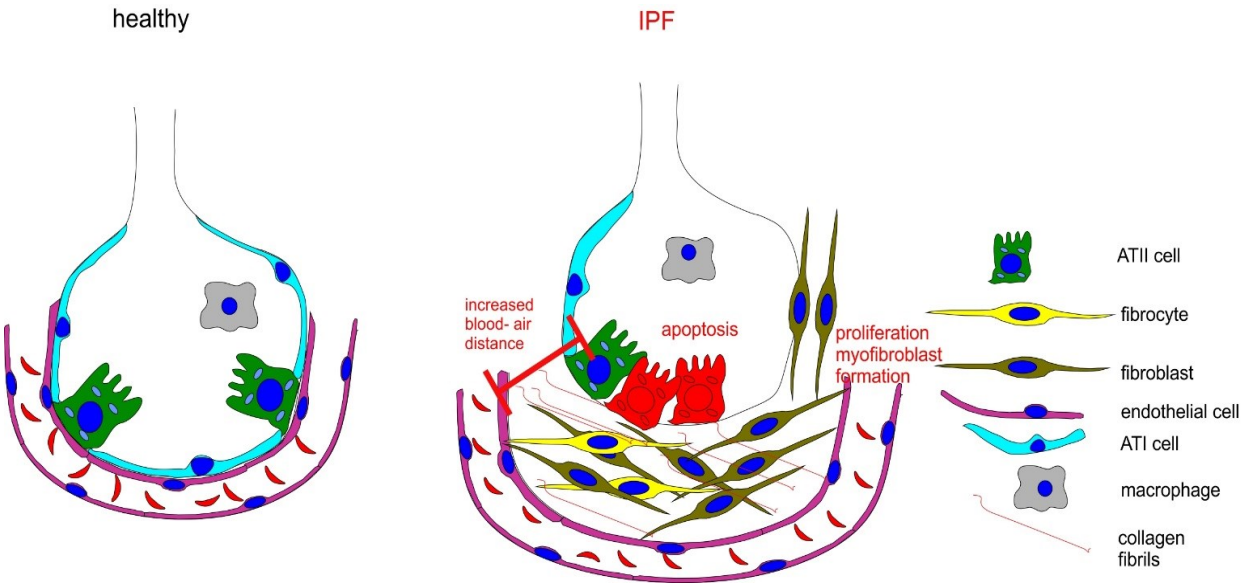

Figure 4. Changes in alveolar structure in IPF. *(Left) In the healthy alveolus, endothelial cells of the capillaries are directly adjacent to the alveolar epithelium, only separated by one shared basal membrane, and this enable a very short diffusion distance for both oxygen and carbon dioxide. Most of the alveolar surface is covered by ATI cells while occasional ATII cells are present for surfactant production. (Right) in IPF, apoptosis of ATII and I cells leads to partially denuded alveoli that epithelial cells try to repair. In this process, fibroblast proliferation and myofibroblast formation is increased and aberrant collagen synthesis occurs, leading to the phenomenon described as fibrotic foci. Furthermore, fibrocytes migrate into the tissue. This ultimately results in increased blood air distance and thereby hinders gas exchange to the point of respiratory failure.*

1.2.5 IPF Therapy

1.2.5.1 Pharmacotherapy

Treatment of IPF has been complicated by the fact that this disease is incompletely understood. One of the most tragic examples of erroneous pharmacotherapy was the standard use of steroids and azathioprine until the 2010s that was later revealed to actually decrease survival as compared to placebo (186). This therapeutic approach was due to the fact that inflammation has been overestimated as a contributing factor to IPF and the immunosuppressive therapies further led to decreased resistance in the patients (186-188). Consequently, the improved understanding of this disease has paved the way for further developments and there are now two specific anti-fibrotic drugs for the treatment of IPF (188).

Pirfenidone is considered a first-line treatment for IPF, although its mode of action is still not completely understood (189). The breakthrough for this therapy came with the publication of

the CAPCITY results from two phase 3 trials that showed beneficial effects on decline of lung function and pulmonary fibrosis associated mortality, which were confirmed later (190, 191). The mode of action of pirfenidone is predominantly focused on fibroblast biology, reflecting its central role in IPF. Pirfenidone has been shown to inhibit fibroblast to myofibroblast transdifferentiation, fibroblast proliferation and collagen secretion, hallmarks of IPF. Furthermore, it interferes with TGFβ1 signaling as shown by decreased phosphorylation of its effector proteins (192). In addition, data from mouse models show profound effects on pulmonary cytokines, suggesting that a decrease in pro-fibrotic (e.g. TGFβ1) and an increase in anti-fibrotic (e.g. interferon γ) mediators might be partly responsible for the beneficial effects of pirfenidone (193). Of note, pirfenidone is also an antioxidant (194) and exerts anti-inflammatory functions (195). In addition, pirfenidone was also shown to decrease fibrocyte chemotaxis and fibrocyte counts in mouse models of IPF (196).

Nintedanib (formerly known as BIBF1120) is a small molecule tyrosine kinase inhibitor that, in the nanomolar range, inhibits vascular endothelial growth factor receptors (VEGFR) 1-3, fibroblast growth factor receptor (FGFR) 1-4 and PDGF receptors α and β (197). It was introduced into clinical practice after the INPULSIS trials as it slowed the decline in forced vital capacity (198). Also this compound predominantly exerts its effects via inhibition of fibroblast functions. It has been shown to reduce growth factor-induced proliferation and collagen secretion in both healthy and IPF lung fibroblasts (199). Furthermore it prevents fibroblast to myofibroblast transdifferentiation and has preventive and therapeutic actions in mouse models of lung fibrosis. It also has anti-inflammatory properties, reducing pro-inflammatory cytokine levels in lung tissue and influx of immune cells into the bronchoalveolar lavage (BAL) in mice (200). In contrast to pirfenidone, nintedanib also seems to positively regulate ATII cell gene expression, although whether this mechanism is of relevance for its effects is unknown (201). Similar to pirfenidone, nintedanib acts on fibrocytes by hindering their synthesis of pro-fibrotic factors, migration and differentiation and also reduces their accumulation in a mouse model of pulmonary fibrosis (202).

Although there are other options, such as for example acetylcysteine, the evidence for these treatments is scarce and pirfenidone and nintedanib are the only treatments so far that are used in clinical practice (203). As these drugs only slow disease progression but are neither curative, nor regenerative, other treatment options are urgently needed (142). In addition, the focus of current therapeutics on fibroblasts is of concern, as especially rescue of epithelial cells might significantly add to the therapeutic efficacy of a treatment (142, 204).

1.2.5.2 Non-pharmacologic approaches

Besides drugs, increasing disease burden might necessitate the initiation of oxygen supplementation in order to ameliorate exercise capacity and dyspnea (205) and there is also evidence for pulmonary rehabilitation through exercise (206). Ultimately, lung transplantation is considered as a valid therapy that improves survival. However, the selection of patients who benefit from this therapy, and more importantly, choosing the right time for transplantation can prove to be challenging. 5 year post-transplant survival is close to 50% (207, 208). Of note, IPF has so far not been reported to reoccur after transplantation (147).

1.2.6 Eicosanoids in IPF

Most of the research on eicosanoids in IPF has focused on the role of $PGE_{(2)}$ since it was found that PGE_2 has potent inhibitory effects on fibroblasts, and that its levels are decreased in the BAL of IPF patients as compared to healthy controls (209, 210). Subsequently, a host of studies described antifibrotic effects in mouse models (211-213) or *in vitro* (51, 169, 170, 214). Interestingly, PGE_2 was shown to be one of the mediators that could regulate the crucial cross talk of epithelial cells and fibroblasts, being synthetized by alveolar epithelial cells in sufficient extent to suppress fibroblasts proliferation and collagen secretion (12, 18, 160, 215). Importantly, it is one of the few molecules that can not only prevent, but also reverse myofibroblast differentiation (51, 170). Furthermore it has been shown that PGE_2 affects the apoptosis paradox in IPF. This term refers to the fact that ATII cell apoptosis is increased, while fibroblasts become resistant to apoptosis. PGE_2 is able to both prevent apoptosis in ATII cells but induce it in IPF fibroblasts, thereby exerting its beneficial actions via a two-pronged approach (102, 204). However, there are observations that EP receptor signaling in IPF might be dysregulated in fibroblasts, potentially hindering the therapeutic usage of PGE_2 (169, 216). Besides PGE_2, also other eicosanoids have been investigated and there is considerable evidence for beneficial effects of PGI_2 (89, 217), PGD_2 (79, 80) and LXA_4 (218, 219). However, other members of this family were shown to aggravate fibrosis in mouse models such as LTB_4 (18) or PGF_{2alpha} (101). In the lungs, PGI_2 and PGE_2 are the prostanoids present at the highest concentrations (220).

Following the insight that PGE_2 is decreased in IPF patients, investigations into the mechanism for this finding have been initiated. Most of this work focused on the anabolic enzymes, predominantly COX-1 and COX-2. Investigations revealed that fibroblasts from both IPF patients and bleomycin treated animals are deficient in COX-2 upregulation/PGE_2 synthetic capacities (160, 221, 222) and this is partly mediated via epigenetic changes (223), but other studies revealed increased COX-2 expression in fibrotic foci in IPF lungs (19). Others also

examined COX-1 expression and found a decrease in some cells, but the evidence is more scarce (224). Interestingly, TGFβ1 has been shown to be able to induce 15-PGDH in lung epithelial cells and microRNAs that suppress 15-PGDH translation are downregulated in IPF (225-228). Furthermore, while PGE_2 levels in the BAL are decreased, the PGE-MUM concentrations are increased in IPF patients (209, 229).

1.3 Hypothesis

We therefore hypothesized

- **(I)** that 15-PGDH is upregulated in IPF and
- **(II)** that its regulation contributes to the decreased PGE_2 levels and thereby antagonizes the antifibrotic effects of PGE_2 (as illustrated in Figure 5).

Furthermore we proposed

- **(III)** that inhibition of this enzyme increases eicosanoid levels in IPF and
- **(IV)** this in turn exerts protective and therapeutic effects in mouse models of pulmonary fibrosis.

Consequently the aim of this thesis was to investigate the contribution of 15-PGDH in IPF. Besides the exploration of expression and distribution of 15-PGDH in healthy and in IPF lungs, we were especially interested, whether small molecule inhibition of this enzyme will show increased eicosanoid levels, and thereby amelioration of the features associated with IPF, and might therefore represent a target in this disease.

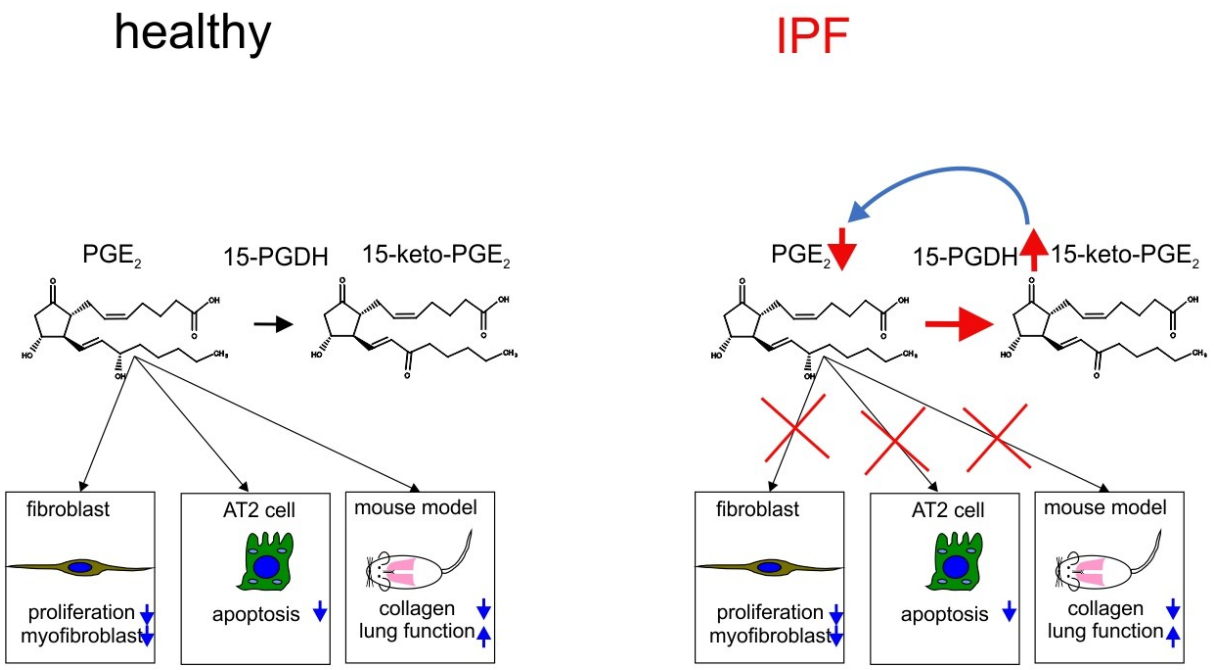

Figure 5. Hypothesis. *We proposed that increased 15-PGDH expression in IPF lungs leads to inhibition of PGE_2 signaling via its degradation and this in term contributes to the phenotypic features of IPF.*

2 Methods

Most of the methods of this thesis have already been published by the author (12, 230).

2.1 Reagents

If not indicated otherwise, all reagents were ordered from Sigma Aldrich (Vienna, Austria). PGE_2 and prostanoid receptor antagonists were purchased from Cayman Chemicals (Ann Arbor, MI, USA). Vectashield/DAPI mounting medium as well as secondary antibodies and

	antibody	host species	company	number	IF/IHC dilution	WB dilution
primary AB	15-PGDH	rabbit	Abcam	187161	1:500	-
	15-PGDH	rabbit	Abcam	178682	-	1:1000
	pro-SP-C	rabbit	millipore	AB3786	1:500	-
	CD68	mouse	Abcam	955	1:100	-
	GAPDH	rabbit	Cell signaling	2118S	-	1:5000
	VE-cadherin	mouse	Santa Cruz	sc-9989	1:200	-
	aSMA	rabbit	Abcam	5694	1:1000	-
	Vimentin	rat	R & D systems	MAB2105	1:100	-
	vWF	rabbit	Dako	A0082	1:500	-
	cleaved caspase 3	rabbit	Gentaur	MAB835-SP	1:50	-
	Ki67	rabbit	Cell signaling	12202S	1:100	-
	COX2	rabbit	abcam	15191	1:500	1:1000
	COX1	goat	santa cruz	sc-1754	1:250	1:200
	AQP5	rabbit	alomone labs	AQP-005	1:500	-
	beta-actin	mouse	Sigma	A2228	-	1:7500
	FSP	rabbit	millipore	07-2274	1:500	-
	F'ab fragments	goat	Jackson	111-007-003	1:50	-
	CD45	rat	Sigma	SAB4700578	1:100	-
secondary AB	anti rabbit Cy3	goat	Invitrogen	A-10520	1:500	-
	anti rabbit AF488	goat	Invitrogen	A-11008	1:500	-
	anti rabbit AF647	goat	Invitrogen	A-21244	1:500	-
	anti goat AF488	rabbit	Invitrogen	A-11078	1:500	-
	anti rat AF647	goat	Invitrogen	A-21247	1:500	-
	anti rat AF488	goat	Invitrogen	A-11006	1:500	-
	anti mouse AF488	goat	Invitrogen	A-11001	1:500	-
	anti goat HRP	rabbit	Jackson	305-035-003	-	1:1000
	anti mouse HRP	goat	Jackson	115-036-062	-	1:1000
	anti rabbit HRP	goat	Cell signaling	70745	-	1:10000

Table 1. Antibodies (AB) used in Western blots (WB) and immunofluorescence/immunohistochemistry (IF/IHC) microscopy.

HRP/AP conjugated streptavidin was obtained from Vector Laboratories (Burlingam, CA, USA). MirVana miRNA mimics and inhibitors as well as transfection reagents were purchased from Thermo Fisher Scientific (Waltham, MA, USA) as were buffers and cell culture media and

reagents. Primary antibodies were purchased from Merck Millipore (Burlington, MA, USA), Cell Signaling (Cambridge, UK) Santa Cruz (Santa Cruz, CA, USA), Abcam (Cambridge, UK), Jackson ImmunoResearch (Baltimore Pike, PA, USA) and Sigma. The recently discovered and patented 15-PGDH inhibitor SW033291 (231) was purchased from THP Medical Products (Vienna, Austria). A list of antibodies used and their dilutions is shown in Table 1. Lycopersicon esculentum lectin (fluorescein labeled, 1:50) was from Jackson ImmunoResearch.

2.2 Patients/ ethical approvals

All experiments using human tissue or cells were approved by the Ethical Committee of the Medical University of Graz. Blood was drawn from healthy volunteers (17-291 ex 05/06) and IPF patients (30-537 ex 17/18, defined by typical UIP pattern on HRCT or HRCT and lung biopsy) after obtaining informed consent (230). For histology, tissue dating back at least 7 years was used, thus not requiring informed consent (29-014 ex 16/17). The applied protocol and the usage of the IPF tissue (defined by histology of the explants) for precision cut lung slices were approved by the institutional ethics committee (976/2010) of the Medical University of Vienna and patients' informed consent was obtained before lung transplantation.

2.3 Histology

For all histologic methods involving tissue, paraformaldehyde fixation, followed by paraffin-embedding was used and 5µm sections were prepared on a microtome (Diapath Galileo Auto Series 2). In brief, 4% paraformaldehyde (20g) was prepared in Millipore water (350 ml) by heating to 55°C while stirring. Afterwards 10 N NaOH was added until the suspension cleared, followed by 10x concentrated PBS (50 ml). pH was adjusted to 7.00 with HCl and solution was filled up to final volume (500 ml) with Millipore water and kept at 4°C for a maximum of two weeks. Before fixation with paraformaldehyde, mice were euthanized with a pentobarbital overdose (150 mg/kg i.p.), exsanguinated and mouse lungs were perfused with PBS. Paraformaldehyde (1ml) was injected via the trachea and trapped by tying a thread. After 48 h in paraformaldehyde, tissue was dissected and lobes were separated, washed in tap water and dehydrated in ascending EtOH concentrations and subsequently transferred to butyl acetate and finally paraffin. After cutting 5µm sections, these sections were stretched in a water bath (38°C), adhered to Superfrost+ slides and left to dry at 40°C. For all following stainings, sections were transferred to xylene, followed by descending EtOH concentrations and a final wash step in Millipore water. A similar protocol was used for human lung tissue and precision cut lung slices.

Cultured cells were grown on chamber slides (Thermo Fisher Scientific), fixed using neutral buffered formaline, and then subjected to stainings without further antigen retrieval.

2.3.1 Immunohistochemistry (IHC)

After rehydration, slides were transferred to preheated citrate buffer (10mM sodium tri-citrate in Millipore water, pH=6) and left in the microwave for 2 x 5 min (750 W) for antigen retrieval. Afterwards, slides were allowed to cool down for 1 h before they were washed in PBS (which was used for all washing steps) and subjected to 0.3% H_2O_2 incubation to block endogenous enzyme activity. Subsequently, slides were blocked with PBS containing 0.3% Triton X, 10% serum of secondary antibody host and 4% bovine serum albumin for 2 h to prevent nonspecific antibody binding. This was followed by addition of primary antibody overnight at room temperature. Vectastain horseradish peroxidase (HRP) or alkaline phosphatase (AP) kits (Vectorlabs) were used to detect the signal, according to the manufacturer's instructions. In brief, after thorough washing, incubation with the biotinylated secondary antibody was performed for 3 h and was followed by two washing steps and incubation with streptavidin bound HRP/AP. Afterwards the signal was detected by incubation with a 3,3'-diaminobenzidin (DAB) or fast red detection kit (Vectorlabs). If double labelling was performed, DAB procedure was completed first, followed by microwaving, blocking, and incubation with second primary antibody and AP kit (12). Methyl green was used as a counterstain.

2.3.2 Immunfluorescence (IF)

Staining procedure was essentially the same as for IHC until primary antibody incubation. After this, slides were incubated with fluorochrome conjugated secondary antibodies for 2 h and finally counterstained with 4′,6-diamidino-2-phenylindole (DAPI) and embedded (Vectastain mounting medium) and sealed with nail polish. For human lung tissue, autofluorescence quenching was performed according to the manufacturer's protocol for 3 min (Truestain, Vectorlabs). If same species antibodies were used, F'ab fragment blocking steps and intermediary microwaving were performed. Cleaved caspase 3 staining was performed by first following the IHC procedure for AP staining (as Fast red is also a fluorescent substrate) and afterwards microwaving and other antibodies were applied, followed by detection with fluorochrome conjugated secondary antibodies. Appropriate isotype controls and omission of primary antibody were used as controls in both IF and IHC (12).

2.3.3 *In situ* hybridization (ISH)

In situ hybridization (ISH) was performed using RNAscope kit for 15-PGDH/HPGD and BaseScope for pre-miRNA-218 (both ACD, Newark, CA, USA) according to the manufacturer's

protocol. In brief, slides were baked in the oven at 60°C for 1 h to improve adherence. After cooling overnight, rehydration was performed, H_2O_2 enzyme blocking was done followed by antigen retrieval via steaming at 99°C for 30 min and proteinase digestion for 20 min. Probe incubation and amplification steps were executed in accordance with the manufacturer's instructions. Detection was performed with an AP system and fast red substrate for 15-PGDH single ISH and for pre-miRNA-218, while HRP detection followed by TSA 488 reagent (Thermo Fisher Scientific) was used for 15-PGDH in double ISH experiments. If immunofluorescence staining for cell markers was also performed, ISH was finished first and this was followed by the blocking step and subsequent primary antibody incubation, in accordance with the Method described for IF. For fluorescence application, Truestain reagents were used as described above, followed by DAPI mounting medium and embedding. For light microscopy, methyl green was used as a counterstain.

2.3.4 Masson's trichrome staining

For the histologic evaluation of pulmonary fibrosis in the bleomycin mouse model, sections of each lobe were used. After rehydration, sections were incubated in Bouin's solution (75 ml aqueous saturated picric acid solution, 25 ml neutral formaline, 5 ml glacial acetic acid) for 60 min at 56°C. Afterwards, slides were washed under running tap water until the yellowish hue disappeared (typically ~ 10 min) and Masson Goldner Trichrome kit (Carl Roth, Vienna, Austria) was used according to the manufacturer's instructions with some modifications. In brief, sections were stained in Weigert's iron hematoxyline for 4 min and differentiated under running tap water for 8 ½ min to visualize nuclei. Subsequently, slides were transferred to Goldner's stain I (Ponceau-Fuchsin) for 7 min, rinsed in acetic acid solution (1% in Millipore water) for 30 seconds and connective tissue was decolorized in Goldner's stain II. This was verified by checking decolorization of peri-bronchial connective tissue under the microscope and, if deemed sufficient (usually after ~6 min), a second acetic acid wash was started. Connective tissue was counterstained using aniline blue (2.5% in 2% acetic acid solution) for 5 min, followed by a washing step in distilled water and incubation in acetic acid solution (6 min). Afterwards, slides were dehydrated and cover slipped.

2.4 Cell culture

All cell culture experiments were performed in a cell culture facility equipped with a laminar flow bench in an S2 lab and cell lines were routinely tested for the presence of mycoplasma contamination. Passaging in 75 cm^2 flasks was done by adding 5 ml of trypsin/EDTA, for 5 min at 37°C or until cells were detached and 10 ml medium with 10% fetal bovine serum (FBS)

were added for neutralization. Cells were then cultured further/used for experiments. Cell lines (MRC-5 and A549 cells) were acquired from the ZMF core facility.

2.4.1 MRC-5 cell culture

MRC-5 cells were kept in DMEM supplemented with 10% FBS, 1% penicillin/streptomycin. For experiments, cells were seeded at 2 x 10^5 in 6 well plates and grown to confluence for 3 days. Cells were then starved with OPTI-MEM for 24h and afterwards treated with indicated concentrations of TGFβ1 for three days.

2.4.2 A549 cell transfection/culture

A549 cells were kept in DMEM supplemented with 10% FBS plus 2mM L-glutamine. For microRNA transfection in 24 well plates, 6x concentrated miRNA was added to 100 µl Opti-MEM followed by 1 µl of Lipofectamine RNAiMAX reagent. After mixing, followed by incubation for 20 minutes at room temperature, 30 000 passaged A549 cells were added in 500 µl of medium and the plate was rocked back and forth. Final concentration of miRNA-mimic, -inhibitor and -negative control was 30 nM. Cells were harvested at indicated time points, in TRIZOL for quantification of mRNA and in RIPA buffer for Western blot analysis.

2.4.3 Primary human lung fibroblast isolation and culture

Both healthy and IPF fibroblasts were a kind gift from the Ludwig Boltzmann Institute for Lung Vascular Research and were isolated from 5 healthy controls and 4 confirmed IPF patients as described elsewhere (232). In brief, lung tissue was minced with scissors to pieces <1mm^3 and left in 100 mm petri dishes in in DMEM supplemented with 10% heat inactivated FBS, 1% penicillin/streptomycin until fibroblasts grew out. These cells were used until passage 9. For experiments involving myofibroblast formation, 70 000 cells were seeded in 24 well plates, cultured in medium for 1 day and then starved without FBS for 1 additional day. Afterwards veh/TGFβ1 was added (2ng/ml) in the presence of vehicle or SW033291 (1µM). After 3 days, cells were harvested.

2.4.4 Fibrocyte isolation and culture

For the isolation of fibrocytes, blood was collected with citrate as an anticoagulant. Peripheral blood mononuclear cells (PBMCs) were then isolated as previously described (230). In brief, collected blood was centrifuged for 20 min at 300 x g to obtain the cellular fraction while plasma was discarded. Afterwards, dextran sedimentation was performed for 30 min and resulting supernatant was transferred on a Histopaque 1077 density gradient, followed by centrifugation for 20 min at 300 x g. Cells on the interface were considered PBMC, counted and assessed

for purity in a hemocytometer. Fibrocytes were further isolated as described (233). In order to remove remaining platelets, PBMCs were washed 6 times, by resuspending them in 1 ml PBS and adding 9 ml of PBS. After the final wash step, cells were counted again, and seeded in 8 well chamber slides (300 000 per well) in the presence of indicated treatments or respective vehicle. After 5 days of treatment (media changed and substance added every other day), cells were stained with Hemacolor rapid staining for blood smears (Merck, Vienna, Austria). Six photomicrographs of the corners of the chamber slide wells of each treatment were taken at a 200 x magnification, and the percentage of fibrocytes of total cells was assessed by a blinded observer.

2.4.5 Alveolar epithelial cell isolation and culture

Mouse alveolar epithelial cells were isolated and cultured as previously described from male Balb/c mice, 6-8 weeks old (12). After mice were euthanized (150mg/kg pentobarbital i.p.), an 18G cannula was inserted in the trachea, tied in place, and mice were exsanguinated via severing the abdominal aorta and vena cava and lungs were perfused with HEPES buffered saline solution until they appeared whitish (~10 ml). Subsequently, lung and heart were removed en bloc and 1 ml of dispase (50 U/ml) followed by 0.5 ml of low-melt agarose was injected into the tracheal cannula and left to harden on ice. Lung lobes were separated and incubated in a falcon containing dispase solution (50 U/ml) for 40 min at room temperature. Thereafter, tissue was minced thoroughly, aspirated through an 18 G for further homogenization and filtered through 100 µm and 40 µm cell strainers. Resulting single cells were washed and counted using a hemocytometer and were further processed using the EasySep-kit (StemCell, Vancouver, CA) for negative magnetic isolation of epithelial cells according to the manufacturer's instructions. Cells were adjusted to a concentration of 1 x 10^8 cells/ml and epithelial cell enrichment cocktail containing antibodies against leukocytes, erythrocytes and endothelial cells was added (50 µl/ml single cell suspension). After washing and centrifugation (10 min 8° C at 130 x g) biotin selection cocktail (100 µl/ml single cell suspension, containing biotinylated secondary antibody complexes) was added, followed by washing and centrifuging, and incubation with magnetic nanoparticles (50 µl/ml single cell suspension). After the terminal washing step, cells were incubated in a magnet for 5 min, and unlabeled cells in the supernatant were poured into a new falcon, washed and incubated in the magnet again. Afterwards, the supernatant was poured off, cells were washed, enumerated and seeded at a density of 1 x 10^6 cells/cm² in laminin pre-coated plastic ware. Cells were left to become adherent until day three whereupon medium (epithelial cell medium, Cell Biologics, Chicago, IL, USA) was changed every day. Treatments were performed on day 6 after isolation

and lasted for 8 h. We also performed experiments in specific-pathogen free mice, in order to exclude possible interferences by subclinical infection.

2.4.6 Human lung microvascular endothelial cell cultures

Human lung microvascular endothelial cells (HMVEC-L) were cultured as previously described (234). Cells and EGM-2 MV medium were purchased from Lonza (Basel, Switzerland) and cells were used until passage 8. All plates used were pre-coated with 1% gelatin to promote adhesion and passaging was done according to the manufacturer's instructions. For measurements of barrier function, cells were seeded at a density of 80 000 cells/cm^2.

2.5 Mouse bleomycin experiments

10-12 weeks old female C57/Bl6 J mice were used for all animal experiments. All animal care complied with national and international guidelines. The experimental protocols used in this study were approved by the Austrian Federal Ministry of Science, Research and Economy (BMWFW-66.010/0142-WF/V/3b/2016) and performed in accordance with the European Communities Council Directive of 24 November 1986 (86/609/EEC). Mice were housed in individually ventilated cages (4-5 per cage) under controlled conditions of temperature (set point 21°C), air humidity (set point 50%) and a 12 h light/dark cycle (lights on at 6:00 a.m.) and habituated to the environment for at least one week. Standard chow and water was provided ad libitum. Mice were randomly assigned before treatment.

2.5.1 Experimental design

1.25 U/kg of bleomycine in 0.9% NaCl or vehicle only were instilled into the lungs via intratracheal (i.t.) administration (235) using a Hamilton syringe in a total volume of 50 µl, in two equal dosings of 25 µl each, set 10 min apart. For this procedure, mice were anesthetized using ketamine (75 mg/kg) and xylazine (7.5 mg/kg) via intraperitoneal injection. After absence of pain reactions, mice were suspended in an 80° angle on their incisors on a wooden board and, through a stereomicroscope, the larynx was visualized using a forceps. A blunted and curved 21 G needle was inserted into the trachea to instill bleomycin/vehicle. Mice were put on a heating pad (37°C) and their eyes were covered with pre-wetted dabbers to prevent drying. When mice sufficiently recovered from anesthesia, they were put back into their cages. For pharmacologic studies, mice received the 15-PGDH inhibitor SW033291, 10 mg/kg in cremophor/EtOH/ 5% glucose solution or vehicle intraperitoneally (i.p.) twice daily. Accordingly, mice were separated into 4 groups.

-Group 1 vehicle (0.9%NaCl i.t.)/ vehicle (cremophor/EtOH/ 5% glucose solution i.p. twice daily)

-Group 2 vehicle (0.9%NaCl i.t.)/ SW033291, (10 mg/kg i.p. twice daily)

-Group 3: bleomycin 1,25 U kg (i.t.) / vehicle (cremophor/EtOH/ 5% glucose solution i.p. twice daily)

-Group 4: bleomycin 1,25 U kg (i.t.)/ SW033291, (10 mg/kg i.p. twice daily).

Two different sets of experiments were conducted, and each was at least done twice.

2.5.1.1 Preventive model

For the preventive approach, inhibitor (SW003291) treatment was started on the same day when mice received bleomycin (Figure 6). After 21 days, mice were euthanized, and BAL was performed via an 18G cannula. 1 ml of PBS containing 0.1 mM EDTA was instilled into the lung and collected (236) and thereafter, lungs were perfused with 10 ml PBS until free of blood. Lungs were dissected, snap frozen in liquid nitrogen, pulverized using a sonicator (Bandelin Sonopuls, HD2070; 30 x 4, 70%) and subsequent analyses were performed. From some mice, bone marrow was obtained as described previously (237) to determine PGE_2 levels. To this end, the isolated femur was cut open at the ends and was perfused with 1 ml of BAL buffer, followed by centrifugation. Processing for histological assessments is described in detail in subchapter “Histology”.

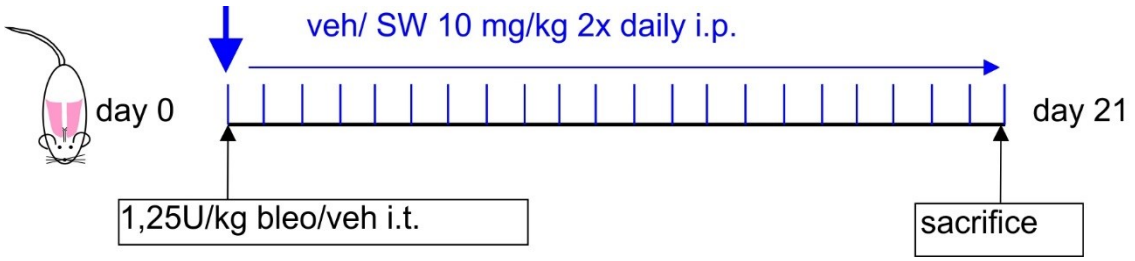

Figure 6. Treatment regimen for the protective bleomycine model. *Starting on day 0, bleomycin (bleo) or vehicle (veh) was given intratracheally (i.t.) and at the same time, twice daily treatment with the 15-PGDH inhibitor SW033291 (SW) or matching vehicle was started intraperitoneally (i.p.). Mice were sacrificed on day 21.*

2.5.1.2 Therapeutic model

For the therapeutic approach, treatment with SW033291 or vehicle was started on day 11 after bleomycin instillation (Figure 7). This represents a time point, where the inflammatory phase is over and is thus thought to better resemble the human disease of IPF (188, 238, 239). Processing of lungs was done in a similar manner as described for the preventive model,

except that mice were in addition subjected to lung function measurements before BAL.

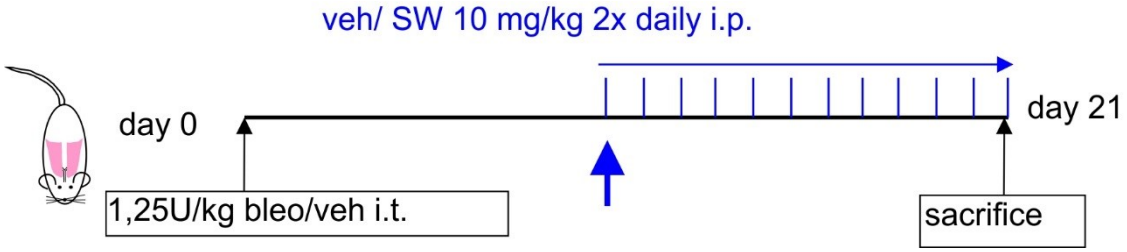

Figure 7. Treatment regimen for the therapeutic bleomycine model. *Starting on day 0, bleomycin (bleo) or vehicle (veh) was given intratracheally(i.t.) and beginning on day 11,mice were treated twice daily with the 15-PGDH inhibitor SW033291 (SW) or matching vehicle intraperitoneally (i.p.). Mice were sacrificed on day 21.*

2.5.2 Histologic evaluation

All histologic evaluations were performed in a double-blinded manner, meaning that both the person taking the photomicrographs and the person(s) evaluating these were unaware of the experimental condition. For fibrosis grading, Masson's trichrome stained whole lung sections were photographed (60-70 photomicrographs per lung at a 200 x magnification) and graded according to the Modified Ashcroft Scale (240). For all other evaluations (fibrocytes, proliferating/apoptotic ATII cells and proliferating fibroblasts), 10 photomicrographs per lung were taken at a 400 x magnification and double stained cells were counted manually using ImageJ (241).

2.5.3 Hydroxyproline measurements

As a measurement for collagen accumulation in mouse lungs, hydroxyproline measurements were performed. ~10 mg of pulverized lung tissue was dissolved in the 10 x volume ddH_2O and an equal volume of 12N HCl was added and incubated for 3 hours at 120° C. Afterwards, samples were centrifuged (10 000 x g for 3 min) and 5 - 10 µl of the resulting supernatants were pipetted onto a 96-well plate. Thereafter, samples were left to dry and the subsequent steps were performed using the Biovision (San Francisco,CA, USA) hydroxyproline kit, according to the manufacturer's instructions. In brief, 100 µl of Chloramin T reagent were added to the samples and standards, incubated for 5 min at room temperature and subsequently, 100 µl of p-dimethylaminobenzaldehyde (DMAB) reagent were put into each well, incubated for 90 min at 60°C, and thereafter, samples were measured using a microplate reader at a wavelength of 560 nm. Hydroxyproline concentrations were calculated after background subtraction related to a linear standard curve.

2.5.4 Lung function measurements

Lung function was assessed by using the FlexiVent system (SCIREQ, Montreal, PQ, Canada), as described previously (74), with some modifications (211, 242). After anesthesia (ketamine

(150 mg/kg) and xylazine (15 mg/kg)), mice were tested for the absence of pain reactions and received rocuronium bromide (5 mg/kg i.p.) after connection to the respirator unit and initiation of mechanical ventilation (89). After a total lung inflation maneuver, three snapshot-150 v5.1 perturbations (resulting in data for resistance, dynamic compliance and elastance), two quick prime-3 and two prime-8 perturbations (resulting in data for airway resistance, tissue dampening, tissue elasticity and total lung capacity) and two volume-guided, ramp-form pressure volume curve maneuvers (resulting in form of deflating pressure volume loop, static compliance, static elastance and hysteresis/area) were performed and this whole process was repeated twice. Only measurements with a coefficient of dispersion higher than 0,95 were accepted.

2.6 In vivo transfection

Mice were anesthetized for *in vivo* transfection using ketamine (75 mg/kg) and xylazine (7.5 mg/kg) via intraperitoneal injection as described above. Invivofectamine 3.0 reagent kit was used according to the manufacturer's instruction with some modifications (243). For a single dose 2.5 µl of negative control stock (50 µM) /miRNA mimic stock (50 µM) was mixed with 2.5 µl of complexation buffer and 5 µl of Invivofectamine was added, the solution was vortexed and incubated at 50°C for 30 minutes. Subsequently, 50 µl of sterile PBS were added, resulting in a final concentration of 2.08 µM. Mice received 50 µl by intratracheal instillation separated in two equal volumes as described above, resulting in a delivery of 58 ng mimic/mg body weight (243). After 24 h, mice were euthanized as described above, lungs were perfused, snap frozen and subsequently pulverized in liquid nitrogen. 10 mg of powder were dissolved in RIPA buffer and subjected to Western blotting.

2.7 15-PGDH activity assay

For assessment of 15-PGDH activity, tissue pulverized in liquid nitrogen was dissolved in the 10 x volume of 0.1 M potassium phosphate buffer pH 7.5 and homogenized by a sonicator as previously described (244). All centrifugation steps were done at 4°C, and sonication was done on ice. One centrifugation step was performed to remove remaining tissue pieces and debris (20 min, 10 000 x g) and the supernatant was transferred to an ultracentrifuge (60 min, 105 000 x g). The resulting pellet was discarded and supernatant was used for activity measurements.

100 µl were added to a reaction mixture, containing 5 mM NH_4Cl, 1 mM NAD+,100 µM ketoglutarate monosodium salt, 0,1mM dithiothreitol and 5 Units glutamate dehydrogenase in 50 mM Tris/HCl, pH 7.5. The reaction was started by the addition of heptatritiated PGE_2

(PerkinElmer, Waltham, MA, USA) to the samples and to the according standards of recombinant 15-PGDH (Cayman Chemicals). The reaction was performed at 37°C for 30 min and 300 µl of activated charcoal (10%) and dextran T70 (1%) were added. After 15 min, vials were centrifuged at 3000 x g (15 min) and the supernatant was transferred to scintillation vials, scintillation cocktail (1 ml, Perkin Elmer) was added, vials were vortexed and samples were measured on a beta counter. Specific activity was inferred from the standard curve and normalized to the protein content as determined by the bichinonic acid method.

2.8 PGE_2 radioimmunoassay

The radioimmunoassay (RIA) was performed as previously described (245). Serum from rabbits immunized against PGE_2 was used for this assay. GelPhos (0,1% gelatin in PBS) was used as a diluent for all steps. Samples or standards of unlabeled PGE_2 were incubated overnight at 4°C with heptatritiated PGE_2 (activity being in the range of 10 000 to 14 000 cpm), and 100 µl antiserum (diluted 1:1350) in a working volume of 2 ml. The next day, 300µl of activated charcoal (10%) were added, vials were incubated for 15 min at 4°C to allow adherence of unbound PGE_2 to charcoal and vials were centrifuged at 3000 x g for 15 min at 4°C. Supernatants were transferred to scintillation vials, scintillation cocktail was added, vials were vortexed and samples were measured on a beta counter. Blanks were subtracted from all values, and concentration was calculated from % inhibition of binding as compared to binding in the absence of unlabeled PGE_2. The IC_{50} was 91.1 ± 8.95 pg/ml (n=14) and detection limit, defined as 10% inhibition of binding was at 9.85 ± 1.15 pg/ml (n=14). For cell culture experiments, standard curves were also done in the presence of medium in order to exclude nonspecific binding.

2.9 Western blot

Western blots were performed as described with some modifications (12, 230). Cells or tissues were lysed in RIPA buffer or extraction buffer (50 mM TRIS, 10 mM EDTA, 1% v/v Triton X), containing protease inhibitor cocktail (Roche, Basel, Switzerland) and 1 mM phenylmethylsulfonyl fluoride. For cells, buffer was pipetted into the wells, incubated until cells were visibly dissolved and additional detachment was achieved by scratching and pipetting up and down. Powdered tissue was further homogenized by sonication on ice (2x 10x, 40%). Subsequently, samples were centrifuged at 14 000 x g for 20 min at 4°C and pellets were discarded while supernatants were frozen at -20°C. The supernatants were analyzed for their protein content by using the Pierce BCA-kit (Thermo Fisher Scientific, Waltham, MA, USA), and 15 µg protein per sample were separated by SDS-PAGE on a 4-20% TRIS-glycine

gradient gel (Thermo Fisher Scientific) with voltage and time according to the manufacturer's instructions. The protein was blotted onto a polyvinylidene fluoride membrane (Bio-Rad, Vienna, Austria) using the iBlot dry transfer system (Thermo Fisher Scientific). Membranes were blocked with 5% non-fat dry milk for one hour at room temperature and target proteins were immunochemically detected using specific antibodies (Table 1) dissolved in the blocking solution overnight. These were visualized with the respective horseradish peroxidase (HRP)-conjugated antibodies and HRP detection substrate (Bio-Rad). Chemoluminescence was recorded by a ChemiDoc Touch Imaging system (Bio-Rad). After stripping the membranes with stripping buffer (Restore PLUS, Thermo Fisher Scientific), membranes were reprobed with housekeeping protein antibodies and further processed as described above. Densitometric analysis of the protein bands was performed by using the Imagelab Software (Bio-Rad).

2.10 Real-time quantitative polymerase chain reaction

For relative quantification of mRNA expression, real-time PCR was performed as described previously (12). Powdered tissue or cells were dissolved in 1 ml RNAzol RT or 500µl of TRIZOL (Thermo Fisher Scientific) and RNA was isolated according to the manufacturer's instructions. These steps were followed by DNA removal with a kit (Ambion DNA removal kit, Thermo Fisher Scientific). 1 µg of total RNA was reverse transcribed using the iScript cDNA Synthesis Kit (Biorad, Hercules, CA, USA) according to the manufacturer's instruction; real-time PCR was performed using SsoAdvanced™ Universal SYBR® Green Supermix with PrimePCR™ SYBR® Green Assay primers for human HPGD and GAPDH and mouse Hpgd, Sftpc, Gapdh, Col1a1 and Hprt1(all Biorad). For all primers, initial test runs were performed with dilutions of pooled cDNA to establish the linear range of the reaction, and final experiments were performed accordingly. Reaction was performed in a CDX Connect™ Real-Time PCR detection system with CFX Manager™ software 3.1(Biorad). The quantification of mRNA expression relative to vehicle was calculated with the $2^{-\Delta\Delta CT}$ method (cells) and as housekeeping gene minus gene of interest (mouse lung).

2.11 Precision-cut lung slices

Precision-cut lung slices (PCLS) were obtained from IPF patients undergoing lung transplantation and were prepared as previously described with some modifications by the Ludwig Boltzmann Institute for Lung Vascular Research (246). Fresh lung tissue was cut to pieces and cylindrical cones, similar to punch biopsies, with a diameter of 8 mm were obtained. These were then sliced (200 µm ± 20 µm sections) with a Krumdieck live tissue microtome in

Earle's balanced salt solution (EBSS), enriched with 25 mM HEPES and 17 mM glucose. Incubation medium, that furthermore contained MEM aminoacids MEM vitamins, Na-Pyruvate, L-Glutamin) and penicillin (100 U/ml)/streptomycin (100 µg/ml) was used to wash slides 7 times for 30 min at 37°C. After overnight incubation, indicated treatments were added for 3 days (Figure 8). Afterwards, supernatants were collected and tissue was fixed with neutral buffered formalin and further processed as described in the histology section.

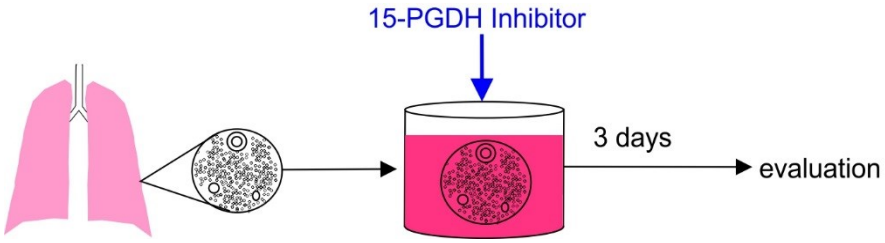

Figure 8. Schematic representation of the culture of precision cut lung slices.

2.12 Enzyme linked immunosorbent assay

Enzyme linked immunosorbent assay (ELISA) for the determination of Collagen 1 alpha 1 (COL1A1)/pro collagen 1 alpha 1 was done using the Duo set kit from bio-techne (Minneapolis, MN, USA) according to the manufacturer's instructions. Supernatants from PCLS were used and standard curve preparation was done in the presence of medium and values were obtained by subtracting absorption at 540 nm from that at 450 nm on a microplate reader. For calculating concentrations of collagen in supernatants, Log Log standard curves were used and data were normalized to protein concentrations in the supernatants.

2.13 High performance liquid chromatography tandem mass spectrometry

It should be noted that none of the mass spectrometry procedures were performed by the author himself, but in collaboration with Dominique Thomas, Pharmazentrum Zafes, Frankfurt. However, for the completeness of this dissertation, mass spectrometry data are integral, and will thus be included as previously published (12, 230).

2.13.1 Prostanoids

In brief, 200 µl supernatant were spiked with the isotopically labeled internal standards and extracted using ethyl acetate. The chromatographic separation of the analytes was carried out

using a chiral column Lux Amylose-2 (150 x 2 mm I.D., 3 µm) coupled to a Synergi Hydro-RP column (150 x 2 mm I.D., 4-µm; both from Phenomenex, Aschaffenburg, Germany) under gradient conditions. Water and acetonitrile, both containing 0.1% formic acid were used as mobile phases and sample run time was 22 minutes. The MS/MS system consisted of a hybrid triple quadrupole-ion trap mass spectrometer QTrap 5500 (Sciex, Darmstadt, Germany) equipped with a Turbo-V-source operating in negative ESI mode. Analysis was done in MRM mode with a dwell time of 50 ms for all analytes.

For both sphingolipids and prostanoids, data was acquired using Analyst Software V 1.6 and quantification was performed with MultiQuant Software V 3.0 (both Sciex, Darmstadt, Germany), employing the internal standard method (isotope dilution mass spectrometry). The coefficient of correlation was at least 0.99. Variations in accuracy were less than 15% over the whole range of calibration, except for the lower limit of quantification, where a variation in accuracy of 20% was accepted.

2.13.2 Combined specialized pro-resolving mediators and prostanoids

Prostanoids and specialized pro-resolving mediators were quantified by UHPLC coupled to tandem mass spectrometry after solid-phase extraction (SPE). 80 µl supernatant from IPF PCLS were spiked with 20 µl of the isotopically labeled internal standards (Cayman Chemical, Ann Arbor, USA), 200 µL PBS, 400 µL citric acid buffer (pH = 5.7) and 90 µL BHT (0.1% in methanol). Sample was loaded on Biotage Express ABN cartridges (Biotage, Uppsala, Sweden) and eluted with methanol (+2% ammonia solution) after washing with methanol/water 1:1 (v/v, + 2% formic acid) followed by water. Samples were evaporated to dryness in amber glass vials and reconstituted in 50 µL acetonitrile/water 2:8 (v/v, +0.0025% formic acid).

The chromatographic separation of the analytes was carried out using an Acquity UPLC BEH C18 2.1x100mm column, 1.7 µm (Waters, Eschborn, Germany) equipped with a precolumn VanGuard 2.1 x 5 mm, 1.7 µm (Waters, Eschborn, Germany) under gradient conditions. Water and acetonitrile, both containing 0.0025% formic acid were used as mobile phases and sample run time was 15 minutes. The LC-MS/MS analysis was carried out using an Agilent 1290 Infinity LC system (Agilent, Waldbronn, Germany) coupled to a hybrid triple quadrupole linear ion trap mass spectrometer QTRAP 6500+ (Sciex, Darmstadt, Germany) equipped with a Turbo-V-source operating in negative ESI mode. Analysis was done in MRM mode with a dwell time of 5 ms for all analytes.

Data were acquired using Analyst Software V 1.6.2 and quantification was performed with MultiQuant Software V 3.0 (both Sciex, Darmstadt, Germany), employing the internal standard method (isotope dilution mass spectrometry). The coefficient of correlation was at least 0.99. Variations in accuracy were less than 15% over the whole range of calibration, except for the lower limit of quantification, where a variation in accuracy of 20% was accepted.

2.14 Electric cell substrate impedance sensing

Mouse alveolar epithelial cells (MAEC) or human lung microvascular endothelial cells (HMVEC-L) were seeded on precoated (laminin 1 oder gelatin) biochips with golden electrodes and grown to confluence (Applied Biophysics, Troy, NY, USA) (12). For MAEC, 96 well plates (interdigitated finger design, 20) and for HMVEC-L 8W10E+ chips were used. On the day of experiments, cells were starved with respective media, containing 2% FBS, for at least one hour. The electrical resistance of the cell monolayers was measured at a frequency of 4000 Hz by using Electrical Cell-Substrate Impendance Sensing (ECIS; Applied Biosphysics). All measurements were conducted for at least 8 hours and values were normalized to a starting point of the experiments.

2.15 Statistical analysis

All statistical analysis was performed using Graph Pad Prism® 6 (GraphPad Software, Inc. CA, USA). Comparisons of two groups were performed using paired or unpaired two tailed Student's t-test; if values were calculated as percent of vehicle and compared against vehicle, a one sample t-test was performed. For multiple comparisons one-way ANOVA followed by Tukey's post hoc test for comparing all groups was used for more than three groups. For exactly three groups, a Newman-Keuls post hoc test was used (247). A two-way ANOVA for repeated measurements with Bonferroni's post hoc test to compensate for multiple comparisons was used for time courses and Gehan-Breslow test was applied to compare survival curves. Mann-Whitney test was employed for non-parametric data such as scores, or if normality of data was not confirmed. Significance was set at $p< 0.05$. All data are given as mean ± SEM. Where applicable, normality was confirmed by using Kolmogorov-Smirnov testing.

3 Results

3.1 Preparatory chapter: Alveolar epithelial cells

Before we set out to investigate the effects of 15-PGDH inhibition in IPF, we elucidated whether prostanoid synthesis was present in alveolar epithelial cells, as these had been reported to express 15-PGDH in mice (248) and in a human cell line (A549 cells) prostaglandin concentrations were increased upon inhibition of this enzyme (231). The direct comparison of murine primary alveolar epithelial cells and A549 cells with regard to prostaglandin metabolism was performed in order to reveal whether we could apply this cell line for subsequent experiments. . Furthermore, we also investigated whether the described barrier-enhancing effects of alveolar epithelial cell supernatants (249) were due to PGE_2 synthesis and subsequent EP4 receptor activation. In addition, we assessed which COX isoforms are expressed in mouse lungs *in vivo*, as an approach to correlate our *in vitro* findings with mechanisms in epithelial-to-endothelial crosstalk *in vivo*.

Importantly, most of the results of this chapter have already been published in

Bärnthaler, T; Maric, J; Platzer, W; Konya, V; Theiler, A; Hasenöhrl, C; Gottschalk, B; Trautmann, S; Schreiber, Y; Graier, WF; Schicho, R; Marsche, G; Olschewski, A; Thomas, D; Schuligoi, R; Heinemann, A.

The Role of PGE_2 in Alveolar Epithelial and Lung Microvascular Endothelial Crosstalk.

Scientific Reports (2017) 7 (1): 7923. doi: 10.1038/s41598-017-08228-y,(12).

3.1.1 Isolated alveolar epithelial cells express according markers and form a monolayer

After isolation of alveolar epithelial cells from mice, we investigated the phenotype of these cells in order to confirm their identity. We differentiated them for 6 days on laminin I coating in order to induce monolayer formation, as has been described (250). We observed marked staining of cell junctions and whole cells using an aquaporin 5 (AQP5) antibody, a marker of alveolar epithelial cells and this was prevented by pre-incubation with the appropriate blocking

peptide (Figure 9 A,C). When measuring transepithelial resistance on the ECIS device, we found values between 600 and 700 ohm, which was much higher than blanks (Figure 9 E). Because the culture conditions described in this study induce differentiation of alveolar epithelial cells towards an ATI-like phenotype (as witnessed by barrier formation and AQP5 expression), cells will be referenced as “ATI-like” cells.

3.1.2 Murine ATI-like cells and the human alveolar epithelial cell line A549, produce prostaglandins

After we knew that our cells were indeed alveolar epithelial cells, we set out to investigate the production of prostanoids in these cells and which COX isoform is responsible. To this end, we treated the cells with LPS, a known stimulator of PG production (230) in the absence and presence of COX inhibitors. We found that murine ATI-like cells produce vast amounts of PGE_2 already at baseline and this was further increased by LPS stimulation. However, both at baseline and in response to LPS, a pan-COX (diclofenac, 10 µM) and a specific COX-2 inhibitor (NS398, 1 µM) markedly reduced PGE_2 levels to the same extent (Figure 10 A). As COX-2 is in general considered to be upregulated upon stimuli, we wanted to exclude the possibility that our culture conditions are responsible for COX-2 induction. To prevent upregulation of COX-2, we pre-treated cells for 3 days with the corticosteroid dexamethasone (251). Interestingly, dexamethasone pretreatment prevented the upregulation of PGE_2 production by LPS, but showed only a minor and non-significant effect on baseline production (Figure 10 B). Mass spectrometry revealed – besides PGE_2 - high production of 6-keto-PGF_{1alpha} and much lower levels of other prostanoids; all of them showed a trend towards increased levels after LPS stimulation (Figure 10 C,D). Also in A549 cells, a human alveolar epithelial cell line, PGE_2 production was dependent upon COX-2, but overall levels were much lower. Interestingly, dexamethasone pretreatment completely abrogated PGE_2 in A549 cells (Figure 11).

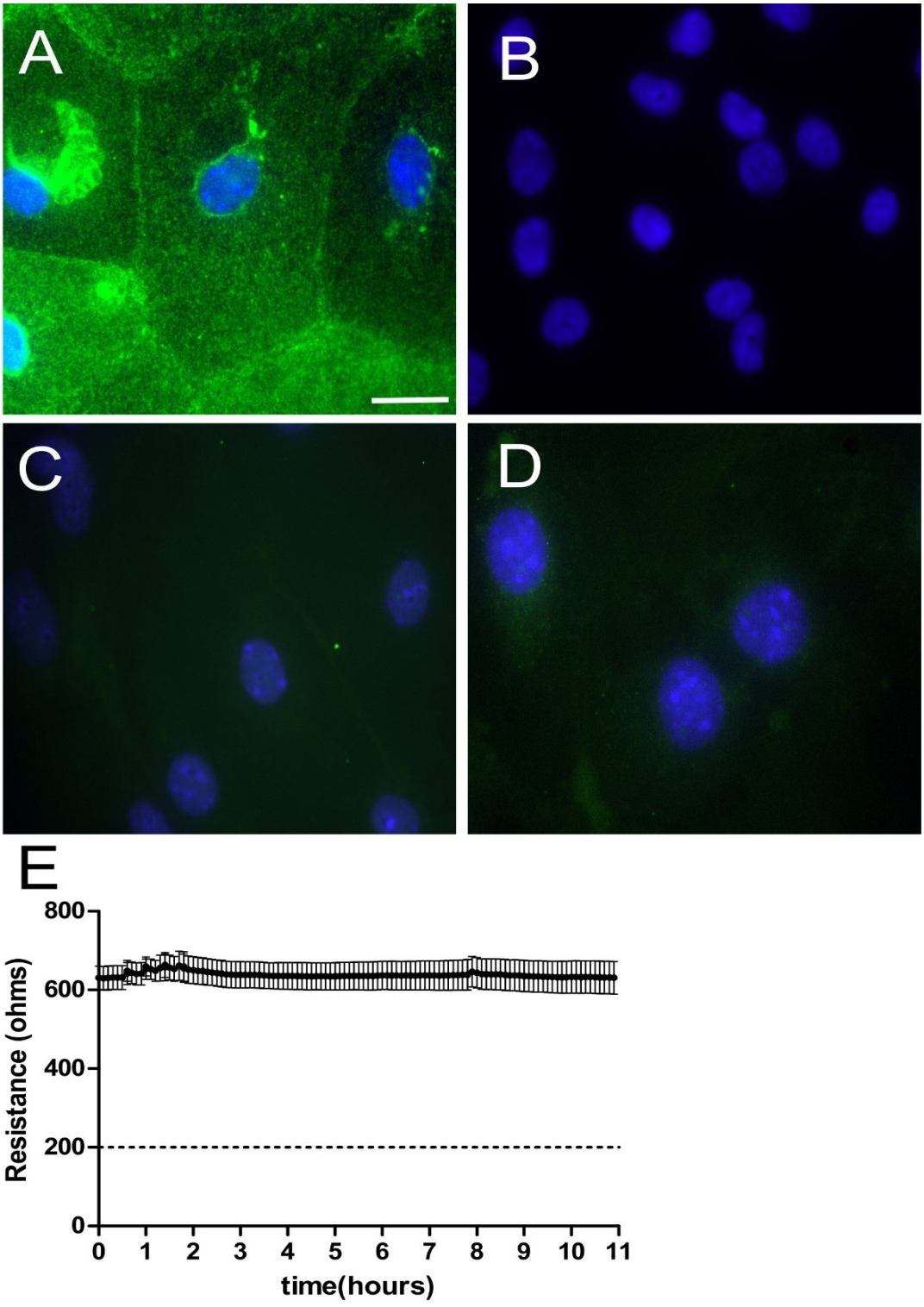

Figure 9. Isolated alveolar epithelial cells express aquaporin 5 and form a monolayer. *(A,C,D) 6 days cultured alveolar epithelial cells or (B) endothelial cells were incubated with (A,B) anti- AQP5 antibody, (C) matching isotype control or (D) anti- AQP5 antibody pre-incubated with blocking peptide. (E) Electrical resistance of 6 days cultured alveolar epithelial cells is shown. Dotted line shows the value of blank wells. n=3-5 scale bar is 10 μm, modified from (12).*

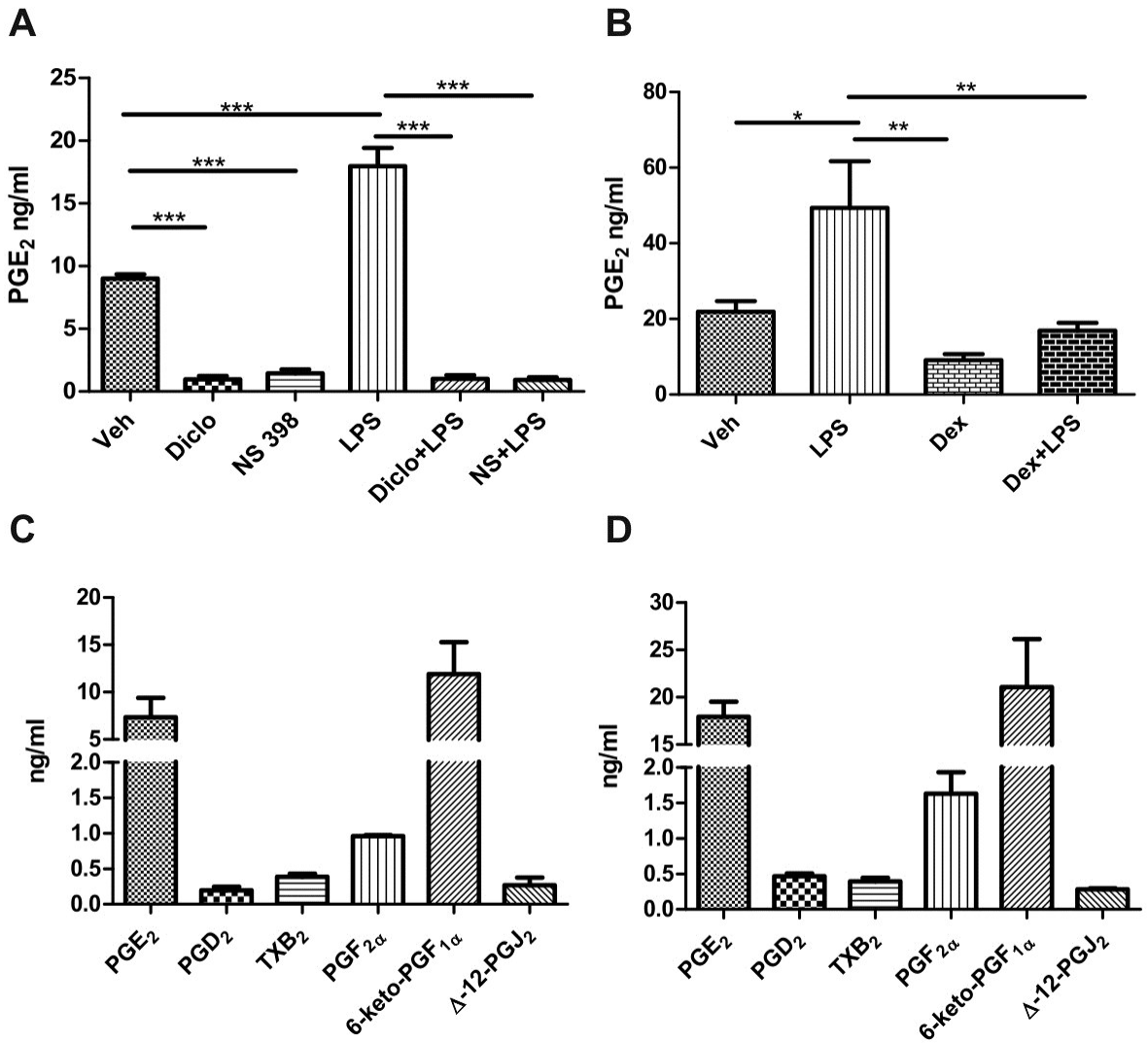

Figure 10. Murine ATI-like cells release PGE_2. *(**A,B,C,D**)Primary ATI-like cells were isolated and kept in culture for 6 days. After 6 days, medium was changed and cells were pretreated with (**A**) either diclofenac (diclo, 10 µM), NS398 (1 µM), or vehicle (Veh) for 20 min; (**B**) dexamethasone-pretreatment (dexa 1 µM) was performed for three days. Thereafter, cells were stimulated with LPS (10µg/ml) or vehicle (Veh). (**C,D**) ATI-like cells were treated with (**C**) vehicle or (**D**) LPS for 8 h and prostanoid levels were determined in the supernatants by mass spectrometry (n=3). Statistical analysis was performed using (**A,B**) One Way ANOVA and Bonferroni's post-hoc (n=5), *=p<0.05; **=p<0.01; ***=p<0.001, modified from (12).*

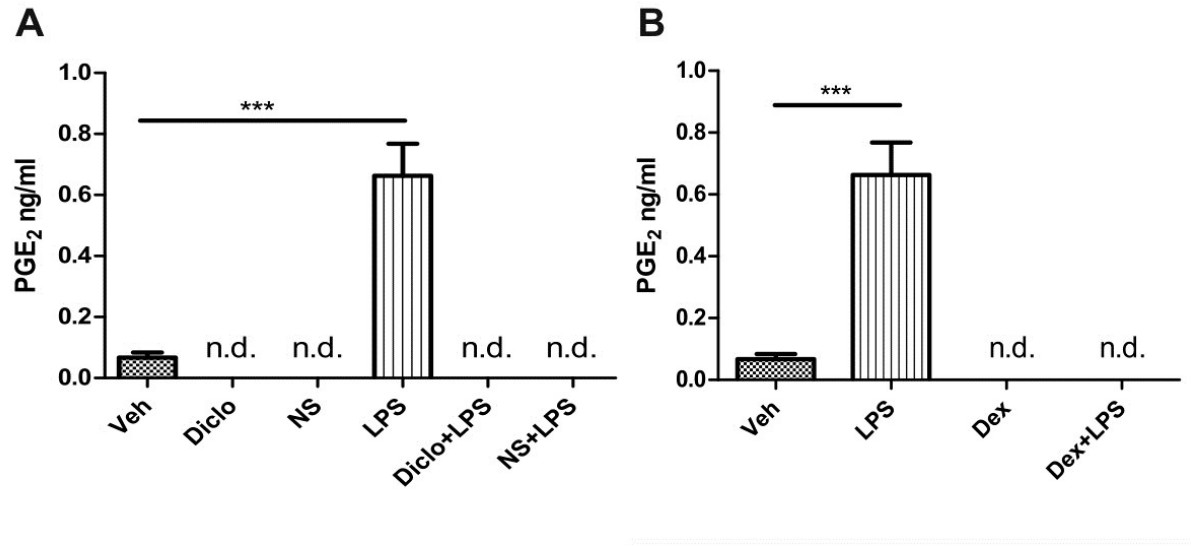

Figure 11. A549 cells release PGE$_2$. ***(A,B)*** *A549 cells were kept in culture for 3 days. On the third day, cells were pretreated (**A**) with either diclofenac (Diclo, 10 µM), NS398 (NS 1 µM), or vehicle (Veh) for 20 min; (**B**) dexamethasone-pretreatment (Dexa 1 µM) was performed for two days. Thereafter, cells were stimulated with LPS (10µg/ml) or vehicle (Veh). Statistical analysis was performed using **(A, B)** two-tailed t-test for A549, n=6, ***=p<0.001 n.d…not detected, modified from (12).*

3.1.3 Murine ATI-like cells and the human alveolar epithelial cell line A549, express key enzymes of prostaglandin production

As we could see that PGE_2 is produced by both human and mouse alveolar epithelial cells which is in accordance with the literature (18), we wanted to investigate the expression of the COX isoenzymes. In order to control for changes under inflammatory conditions, we also treated cells with LPS, an agent that has been shown to upregulate COX-2 expression and increase prostaglandin synthesis (251, 252). Western blotting data revealed the expression of both isoforms in mouse cells, but only COX-2 could be detected in A549 cells (Figure 12 and 13, respectively). As expected, LPS stimulation upregulated COX-2, but did not alter COX-1 expression. In ATI-like cells, dexamethasone inhibited LPS-induced COX-2 upregulation but had no detectable impact on baseline levels, which is in accordance with the findings for PGE_2 synthesis. In contrast, in A549 cells, dexamethasone caused a downregulation of COX-2 already in the absence of LPS. The expression of COX isoenzymes for ATI-like cells was also confirmed by immunofluorescence staining. Furthermore these cells also express 15-PGDH (Figure 14).

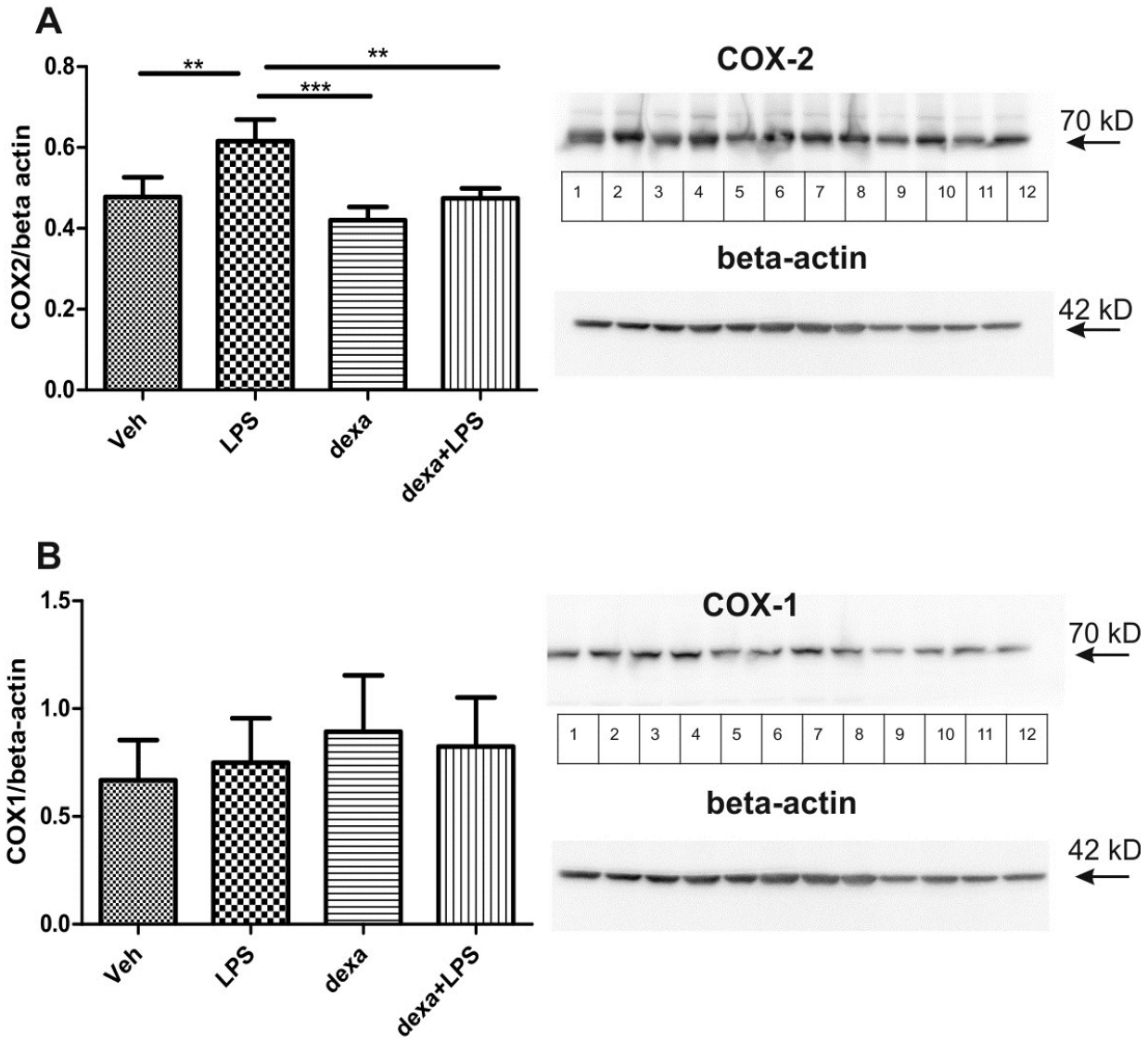

Figure 12. ATI-like cells express COX-1 and COX-2. *Mouse primary ATI-like cells were treated with vehicle (Veh), LPS (10 µg/ml) and/or dexamethasone (dexa; 1 µM) and (A) COX-2 or (B) COX-1 expression was determined by Western blot. Inserts on the right show typical blots (lanes vehicle: 1,5,9; LPS: 2,6,10; dexamethasone: 3,7,11; LPS + dexamethasone: 4,8,12). Beta actin blot was probed on the same blot after stripping of the membrane. Statistical analysis was performed using One-Way ANOVA and Bonferroni's post-hoc test, n=5.; **=p<0.01; ***=p<0.001, modified from (12).*

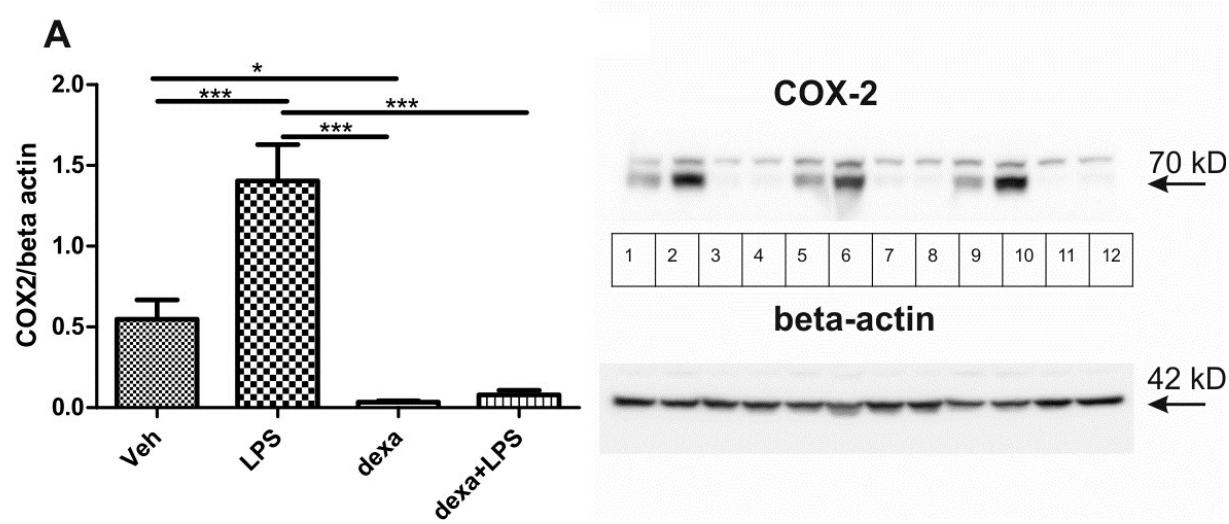

Figure 13. A549 cells express COX-2. *A549 cells were treated with vehicle (Veh), LPS (10 µg/ml) and/or dexamethasone (dexa; 1 µM) and COX-2 expression was determined by Western blot. Inserts on the right show typical blots (lanes vehicle: 1,5,9; LPS: 2,6,10; dexamethasone: 3,7,11; LPS + dexamethasone: 4,8,12). Statistical analysis was performed using One-Way ANOVA and Bonferroni's post-hoc test, n=6.; *=p<0.05 **=p<0.01; ***=p<0.001, modified from (12).*

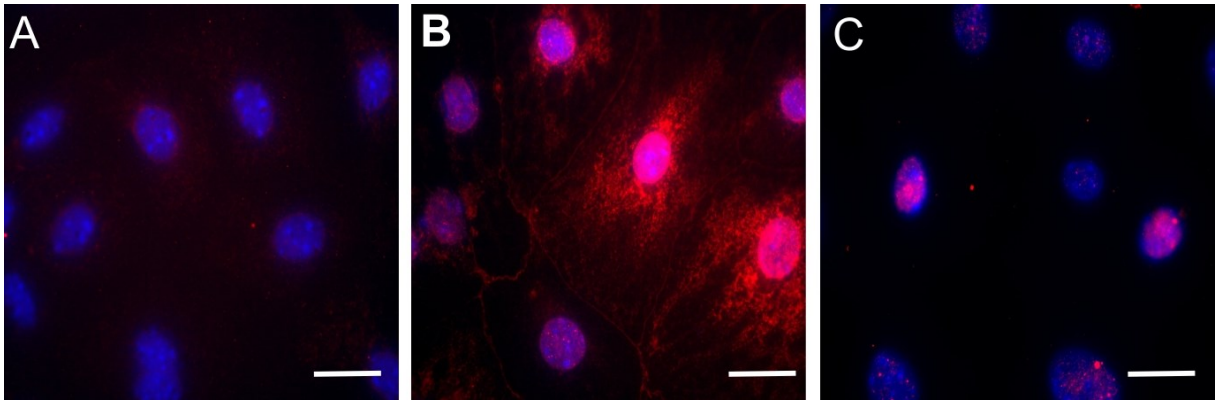

Figure 14. ATI-like cells express key enzymes of prostaglandin metabolism*. (**A,B,C**) 6 days cultured alveolar epithelial cells were incubated with (**A**) anti COX-1 antibody, (**B**) anti COX-2 antibody and (**C**) anti 15-PGDH antibody. n=3-5, scale bar is 10 µm, modified from (12).*

3.1.4 ATII cells express COX *in situ*

As expression of COX-2 could still be an isolation artefact, we stained lungs of specific pathogen free mice for COX isoenzyme expression. We found colocalization of both COX-1 and COX-2 in ATII cells (as determined by pro-surfactant protein (SP)C immunoreactivity). COX-2 in the lungs was predominantly localized to pro-SP-C positive cells, while COX-1 was also expressed in other cell types, as would be expected (Figure 15). This was reflected by the fact that pro-SP-C positive cells accounted for 84 ± 7.6% of all COX-2 positive cells but only for 18.2 ± 2.8% of COX-1 positive cells. In addition, we also found evidence of 15-PGDH

expression in these mouse lungs, in a pattern consistent with alveolar epithelial cell expression (Figure 16).

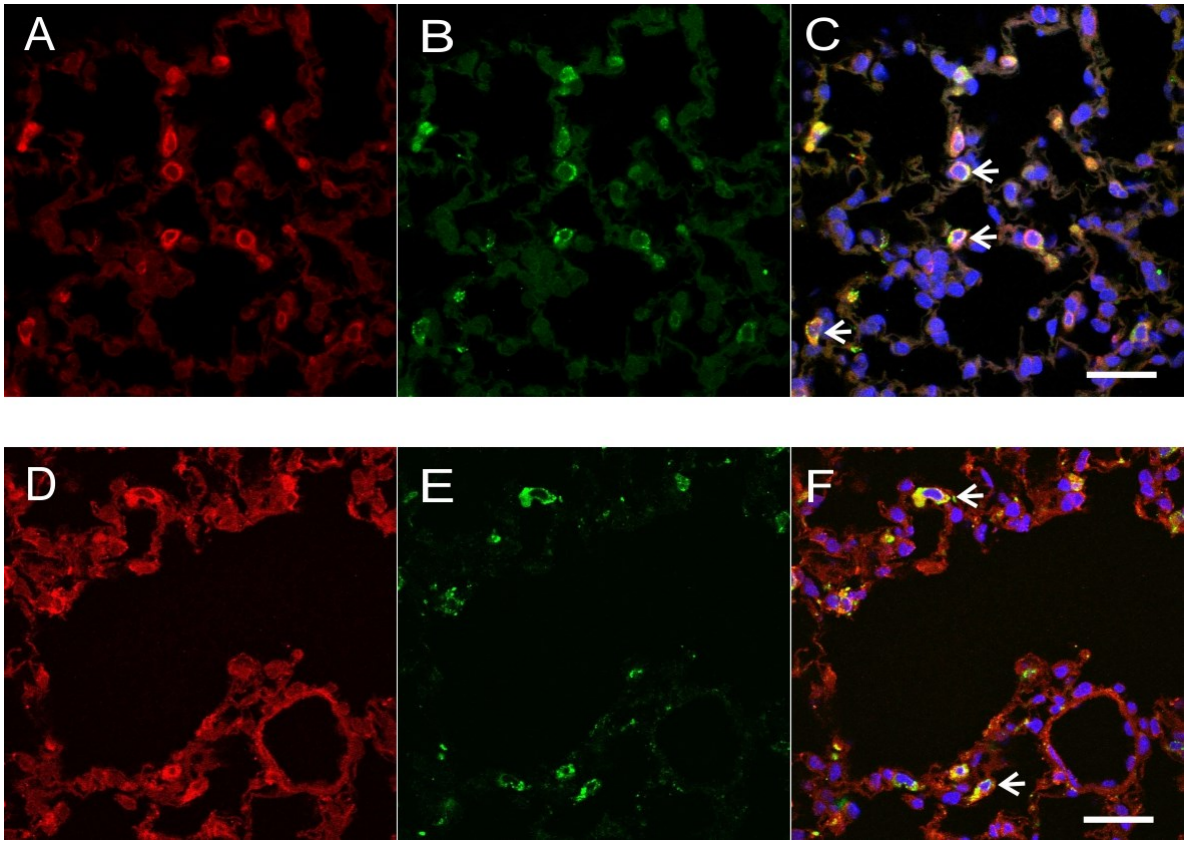

Figure 15. Murine ATII cells express COX-1 and COX-2 in situ. *Lungs of specific pathogen free mice were stained with antibodies directed against (A) COX-2, (D) COX-1 and (B,E) pro-SP-C. (C,F) Overlays were created using DAPI as nuclear counterstain. Arrows show double positive cells. Photomicrographs are representative for 4 independent experiments. Scale bar is 20 µm, modified from (12).*

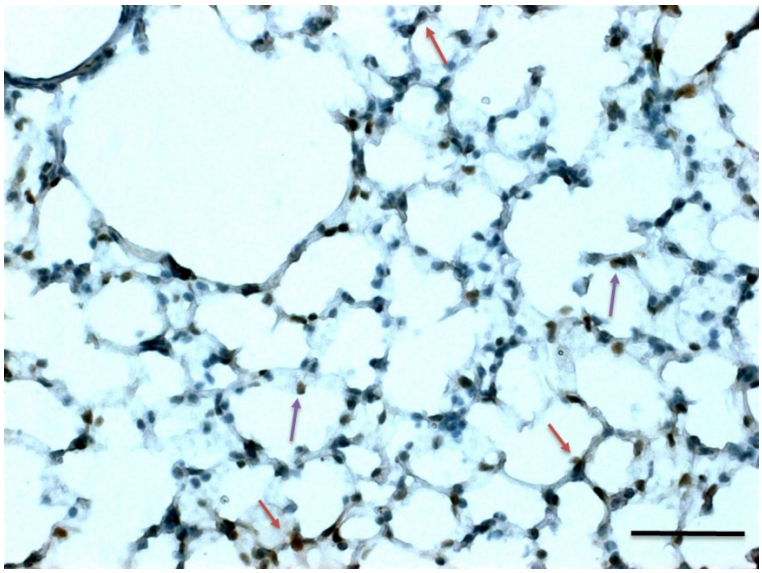

Figure 16. 15-PGDH is expressed in mouse lungs. *Lung sections from healthy specific pathogen-free BALB/c mice were stained with a 15-PGDH-antibody (brown). Counterstaining for nuclei was done using methyl green. Red*

arrows show positive cuboidal cells in alveolar walls, most likely corresponding to alveolar type II cells. Pink arrows show positive cells in alveolar spaces, most likely corresponding to alveolar macrophages. Scale bar: 20 µm. Images are representative for 3 independent experiments.

3.1.5 Murine ATI-like cell supernatants promote lung endothelial barrier function via EP4 receptor activation and PGE_2

It has been shown that PGE_2 from alveolar epithelial cells inhibits fibroblast proliferation and is involved in crosstalk with alveolar macrophages (18, 253). As we could also observe that alveolar epithelial cells secrete high amounts of PGE_2 and that its biosynthetic enzymes are present in healthy lungs, we wanted to investigate, whether alveolar epithelial cell-derived prostaglandins might exert effects on other, directly adjacent cells, the microvascular endothelium. To this end, we measured transendothelial resistance of HMVEC-L in the ECIS device and added supernatants (also referred to as conditioned medium) from isolated alveolar epithelial cells. Interestingly, we found a significant increase upon addition of these supernatants that was partially blocked if ATI like cells were pretreated with COX inhibitors (Figure 17 A,B). As this proved that the barrier function-modulating effects depend on PGs, we next set out to investigate the responsible prostanoid receptor subtype. As we could already show that EP4 receptor activation leads to increased endothelial barrier function (254), we added a specific antagonist for this receptor, ONO AE3-208. We found that EP4 receptor antagonism led to an even greater inhibition than COX inhibitors, which could be explained by the fact that residual PGE_2 synthesis took place (Figure 17 C,D). As IP-agonism has also been shown to increase endothelial barrier function(255), and 6-keto-PGF_{1alpha} was present in high concentrations, we wanted to know whether PGI_2 might also play a role. However, we could not observe any changes in the barrier promoting effects of supernatants using a specific IP antagonist (Figure 17 E,F). Therefore, the effect of alveolar epithelial cell-derived PGE_2 on barrier function might contribute to protective effects of these cells in acute lung injury models (256).

3.1.6 Inhibition of 15-PGDH increases PG levels

Given the beneficial effects of PGE_2 in our investigations and the expression of 15-PGDH in ATII cells, we wanted to investigate whether inhibition of this enzyme might further increase prostaglandin release. Although this had been shown for whole lungs, there were no data concerning isolated epithelial cells (231). Our results show that inhibition of 15-PGDH with SW033291 (500 nM) increases PGE_2 as well as Δ 12-PGJ_2 and 6-keto-PGF_{1alpha} levels in those cells (Figure 18), which are considered a major source of PGs in the lungs [45]. Neither TXB_2, nor PGF_{2alpha} showed significant differences, probably due to low levels of basal secretion (0.3 ± 0.02 ng/ml and 0.9 ± 0.013 ng/ml respectively).

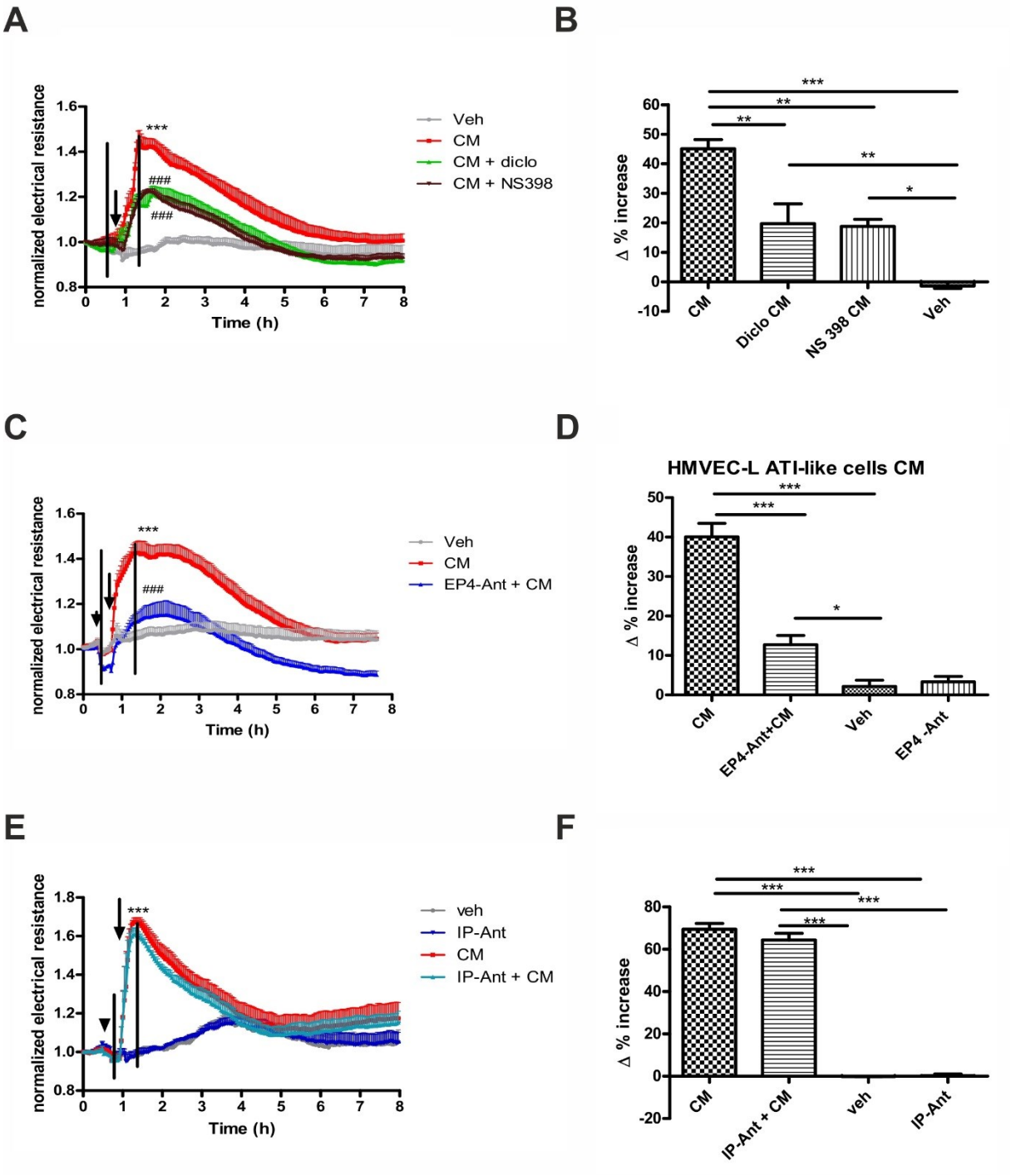

Figure 17. Conditioned medium (CM) from ATI-like cells promotes endothelial barrier function via PGE_2 induced EP4 receptor activation. *HMVEC-L were grown on gold microelectrodes and were pretreated (arrowhead) with vehicle, (**C,D**) EP4 antagonist ONO AE3-208 (EP4 Ant; 300 nM) or (**E,F**) IP antagonist Cay10441 (IP-Ant; 1µM). CM from ATI like cells treated with (**A-F**) vehicle or (**A,B**) diclofenac (diclo 10µM) and NS398 (1µM) was added (indicated by arrows). To detect differences in barrier function (measured as change in resistance), Δ% values were calculated. The normalized electrical resistance values of the first black line were subtracted from those of the second and are given in **B**, **D**, **F**. Statistical analysis was performed using two-way ANOVA and Tukey's multiple comparison test for **A, C,** and **E** and one-way ANOVA followed by Bonferroni's post hoc test for **B, D,** and **F**; n=5, * p<0.05; ** p<0.01; *** p<0.001; * vs vehicle; # vs CM alone, modified from (12).*

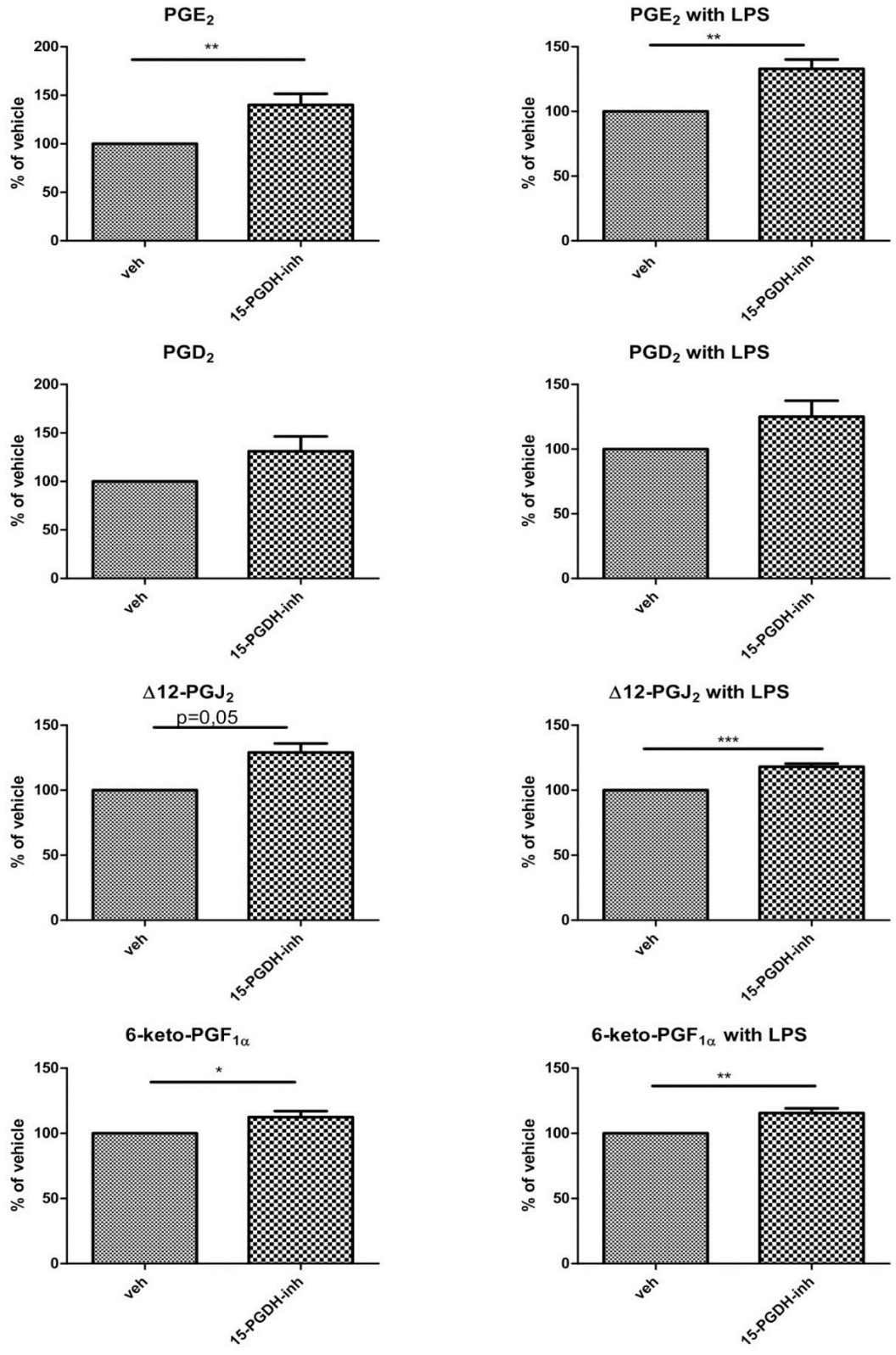

Figure 18. Inhibition of 15-PGDH increases eicosanoid levels in isolated alveolar epithelial cells. *Cells were grown to confluence for 6 days and treated with vehicle or SW033291 (500 nM). After incubation for 20 minutes, vehicle (left) or LPS (10 µg/ml) (right) was added. Two-tailed one-sample t-test against 100% was performed. n=3-4, *=p<0,05, **=p<0,01, ***=p<0,001*

3.2 Main chapter: 15-PGDH in IPF

The data contained in this chapter are currently under review for publication.

3.2.1 IPF patients show differing expression of 15-PGDH

In order to investigate the expression of 15-PGDH in human lungs, we stained tissue from both IPF patients and donor lungs by means of IHC (Figure 19). Using a specific antibody we found pronounced staining in certain areas of IPF lungs, predominantly where alveoli were still preserved. In healthy donor lungs, the pattern was quite evenly distributed throughout the whole lungs. Interestingly, severely fibrotic tissue in IPF showed almost no staining in all investigated patients. Subsequently, we wanted to determine which cells express 15-PGDH and further corroborate our findings. To this end, we detected 15-PGDH by in situ hybridization and co-stained specific cell types with according markers. In these experiments we found that in IPF lungs, 15-PGDH was predominantly expressed in endothelial cells, alveolar macrophages and alveolar epithelial cells (Figure 20). However, in healthy lungs, 15-PGDH predominantly co-localized with von Willebrand Factor (vWF), a marker for endothelial cells (Figure 21). Also in ISH experiments, alveolar structures in IPF showed an increase in 15-PGDH expression as compared to donor lungs, but fibroblastic foci, as defined by dense accumulations of vimentin-positive cells were almost devoid of staining.

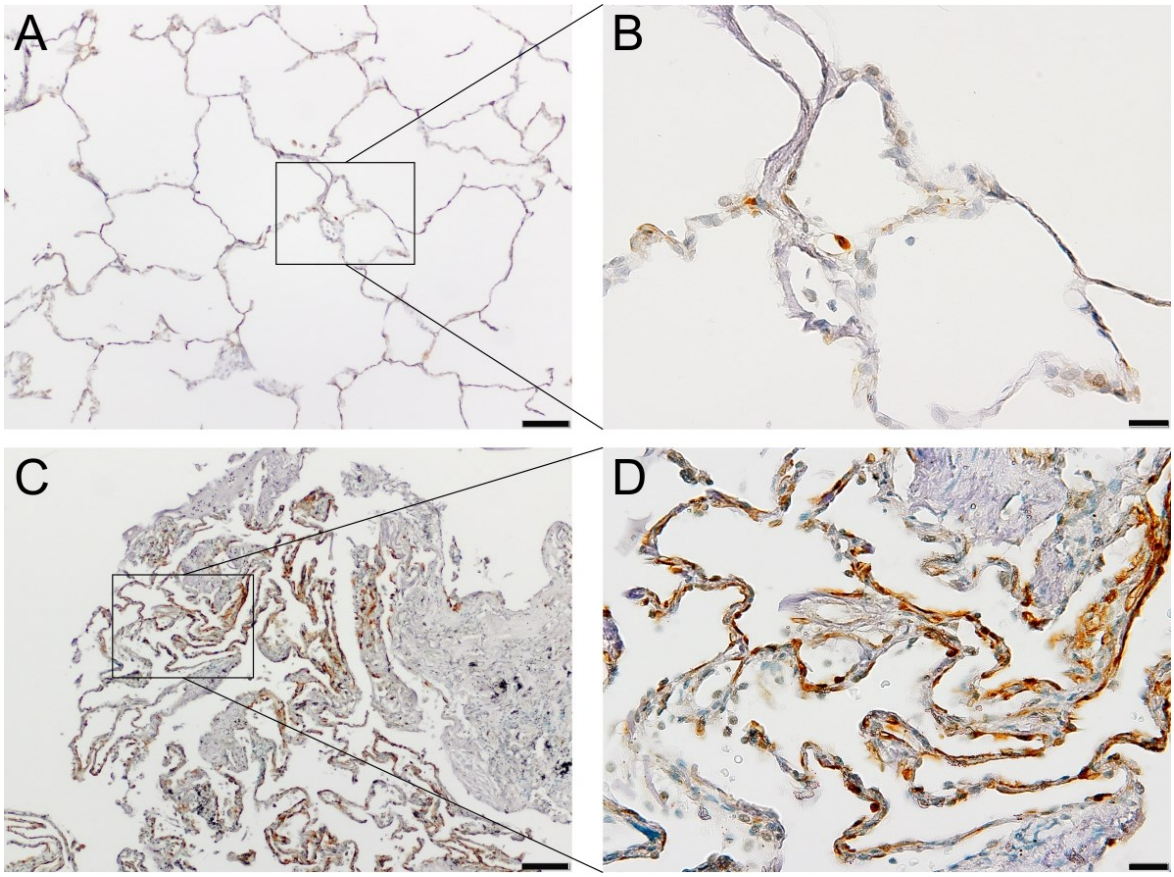

Figure 19. Staining patterns for 15-PGDH differ between healthy donors and IPF patients. *(**A-D**) Immunohistochemistry with an antibody against 15-PGDH (brown) was performed on biopsy samples from IPF patients and control lung sections from organ donors. Nuclei were counterstained with methyl green. (**A,B**) 15-PGDH is expressed in lungs from healthy donors, mainly in the alveolar walls. (**C,D**) IPF patients showed foci of more intensive staining. Images are representative for 5 controls and 5 IPF patients. (**A,C**) Scale bars indicate 200 µm and (**B,D**) 20 µm, respectively*

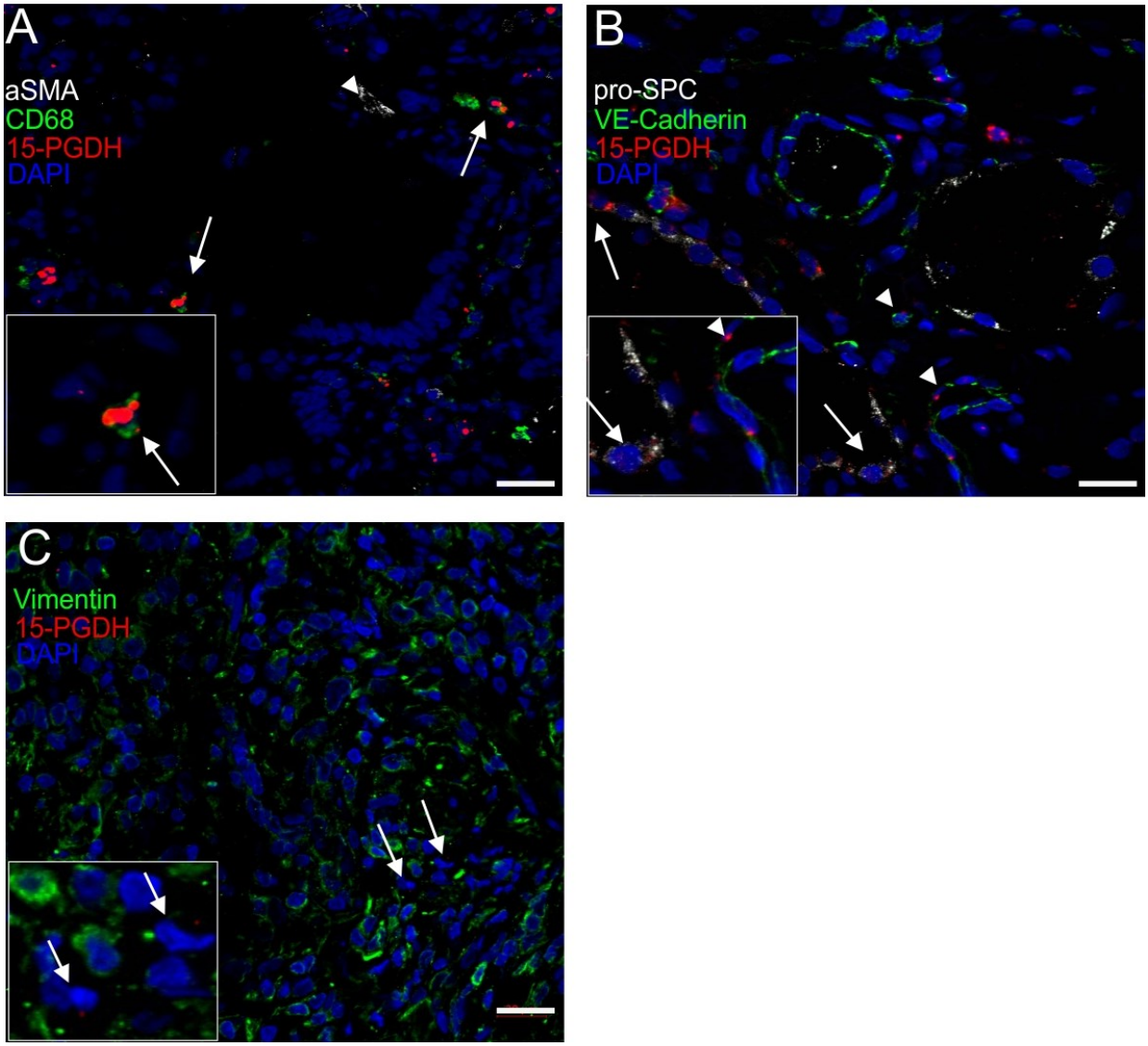

Figure 20. 15-PGDH mRNA is expressed in IPF lungs in alveolar epithelial and endothelial cells, as well as macrophages, but neither in vimentin- nor smooth muscle actin- positive cells. *In situ hybridization for 15-PGDH mRNA and immunostaining for indicated antibodies was performed. (**A**) Arrows indicate 15-PGDH/ CD68 double positive cells, arrowhead indicates a 15-PGDH negative, aSMA positive cell. (**B**) Arrows indicate 15-PGDH/ pro-SP-C double positive cells, arrowheads indicate 15-PGDH/ VE-cadherin double positive cells. (**C**) Arrows indicate 15-PGDH positive/ vimentin negative cells, Images are representative for 5 IPF patients. Scale bar indicate 20 µm, insets show 15-PGDH positive cells.*

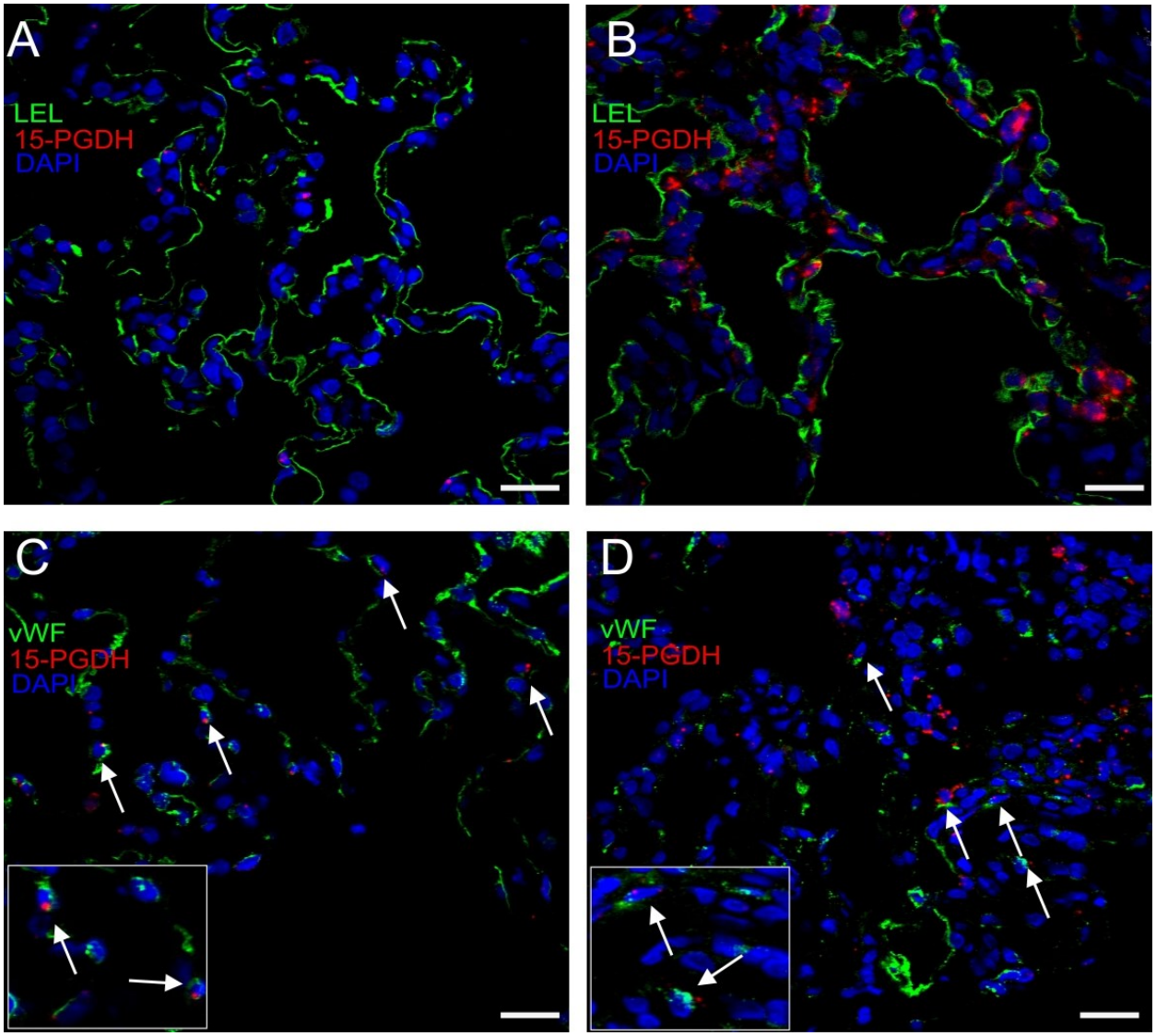

Figure 21. 15-PGDH mRNA is expressed in endothelial cells in healthy lungs. *ISH for 15-PGDH was performed on (**A,C**) healthy and (**B,D**) IPF lungs, and section were stained with (**A,B**) lycopersicon esculentum lectin (LEL) to visualize ATI cell surface or (**C,D**) von Willebrand Factor (vWF) to visualize endothelial cells.(C,D) Arrows indicate 15-PGDH/ vWF double positive cells. Insets show 15-PGDH positive cells. Images are representative for 5 IPF patients and 5 controls. Scale bar indicates 20 µm.*

3.2.2 15-PGDH activity in total lung tissue is not significantly different in IPF patients and healthy controls

Considering these results, we were interested, whether we could detect differences in the activity of 15-PGDH in total lung tissue. To this end, we obtained samples from explanted IPF and non-used donor lungs, pulverized them in liquid nitrogen and thereafter performed the 15-PGDH activity assay. Although we could detect activity in both samples, we could not measure significant differences between patients and healthy controls. There was even a slight but non-

significant trend towards increased activity in donor lungs that might be explained by the fact that IPF samples were from end stage disease where fibrotic tissue is even more prevalent (Figure 22).

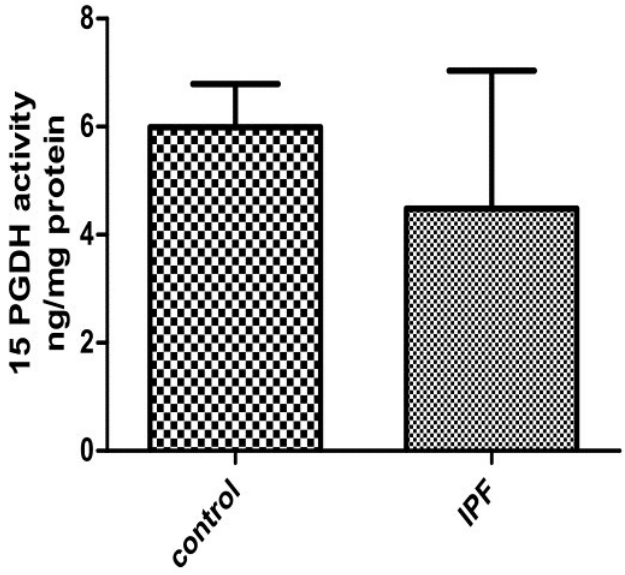

Figure 22. 15-PGDH activity does not differ between healthy donors and IPF patients. *Homogenized lung tissue activity of 15-PGDH was not significantly different between controls and IPF patients (n=5, Student's t-test).*

3.2.3 Mouse lungs show 15 PGDH activity and mRNA expression

As 15-PGDH expression patterns differed in control and IPF lung tissue, thereby corroborating our initial hypothesis, we wanted to investigate the effects of 15-PGDH inhibition on hallmarks of pulmonary fibrosis in a mouse model. To this end, we had to confirm the preliminary findings concerning murine 15-PGDH expression obtained by isolation of ATII cells and IHC. To achieve this, we performed ISH and an activity assay for 15-PGDH on murine lungs. We found considerable expression at the mRNA level and even higher values for activity than obtained from human samples (Figure 23). For comparison, we used kidney samples from the same mouse strain, where we could also measure 15-PGDH activity, albeit at lower levels. Thus, we deemed it feasible to start with mouse experiments.

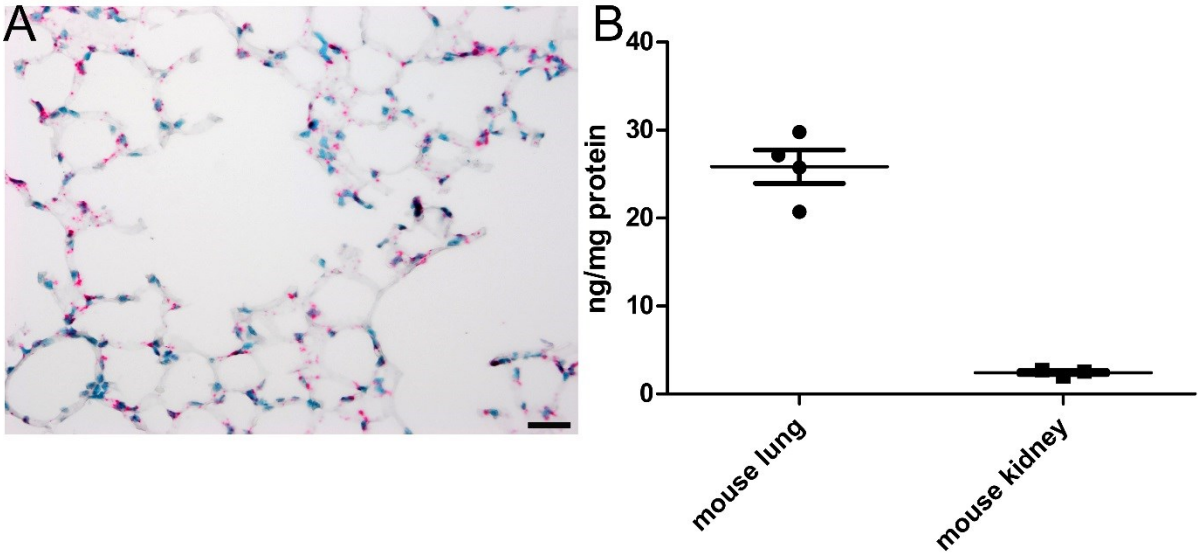

Figure 23. Murine lungs show high levels of 15-PGDH mRNA and enzyme activity*. (A) ISH for 15-PGDH mRNA (red) and counterstaining with methyl green were performed on C57/Bl6 mouse lungs. This image is representative for 5 lungs. (B) 15-PGDH activity was measured in lung and kidney homogenates of C57/Bl6 mice. n=3-4.*

3.2.4 Inhibition of 15-PGDH protects mice from pulmonary fibrosis

In order to investigate the protective effects of 15-PGDH inhibition in IPF, we used the bleomycin model, an established model of pulmonary fibrosis in mice. Bleomycin is a chemotherapeutic agent with the main side effect of pulmonary fibrosis in humans (7). It is usually applied into mouse lungs via intratracheal application. In the protective setting, used here, and indicated by schemes on the top of the graphs, treatment was started concomitantly with induction of fibrosis by bleomycin. The histologic evaluation, via modified Ashcroft scaling of Masson-trichrome stained lung sections, revealed marked attenuation of fibrosis in the 15-PGDH inhibitor treated group (Figure 24). To account for the heterogeneous distribution of fibrosis in this model, which is reminiscent of the appearance in humans (147), we evaluated sections from every lung lobe in a double-blinded fashion. For the same reason, we also pulverized whole lung tissue and aliquots were used in the further experiments. We performed measurements of hydroxyproline content in the lungs, which is a surrogate for collagen levels as this is its predominant source. This analysis also showed that 15-PGDH inhibition prevented the bleomycin-induced increases in total lung collagen (Figure 25 A). In addition, 15-PGDH inhibition protected mice from bleomycin-induced weight loss and death (Figure 25 A,B).

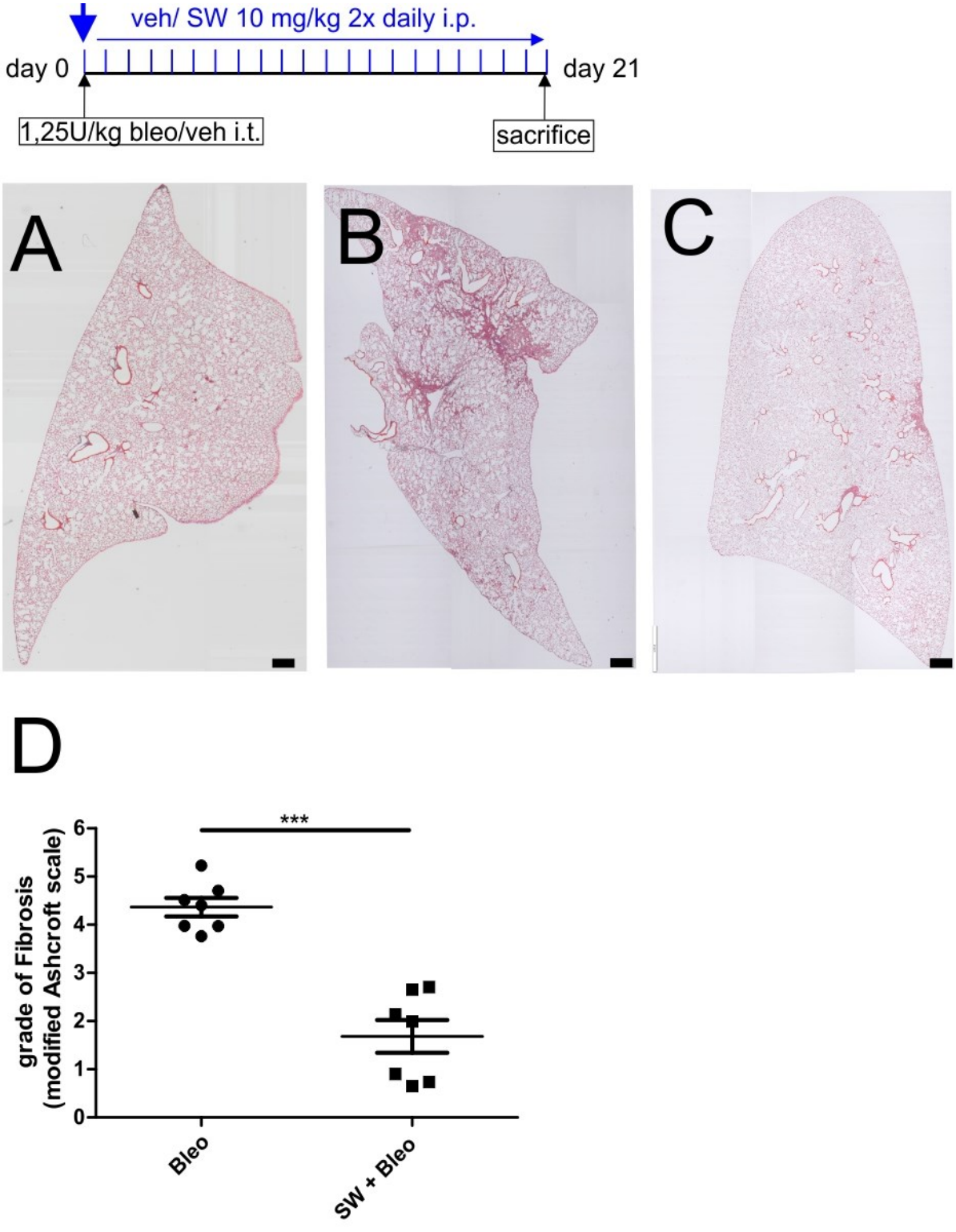

Figure 24. Inhibition of 15-PGDH protects mice from histological features of fibrosis*. Lobes from mice treated with (**A**) vehicle (veh), (**B**) bleomycin (1,25 U/kg, Bleo) and (**C**) 15-PGDH inhibitor ((SW+Bleo; SW033291 10 mg/kg twice daily, start at day 1) were stained with Masson's trichrome staining and (**D**) 60-70 photomicrographs were scored using modified Ashcroft scale. Mann Whitney test was performed (n=7-8). ***=p<0.001 (**A-C**) Scale bar is 1mm.*

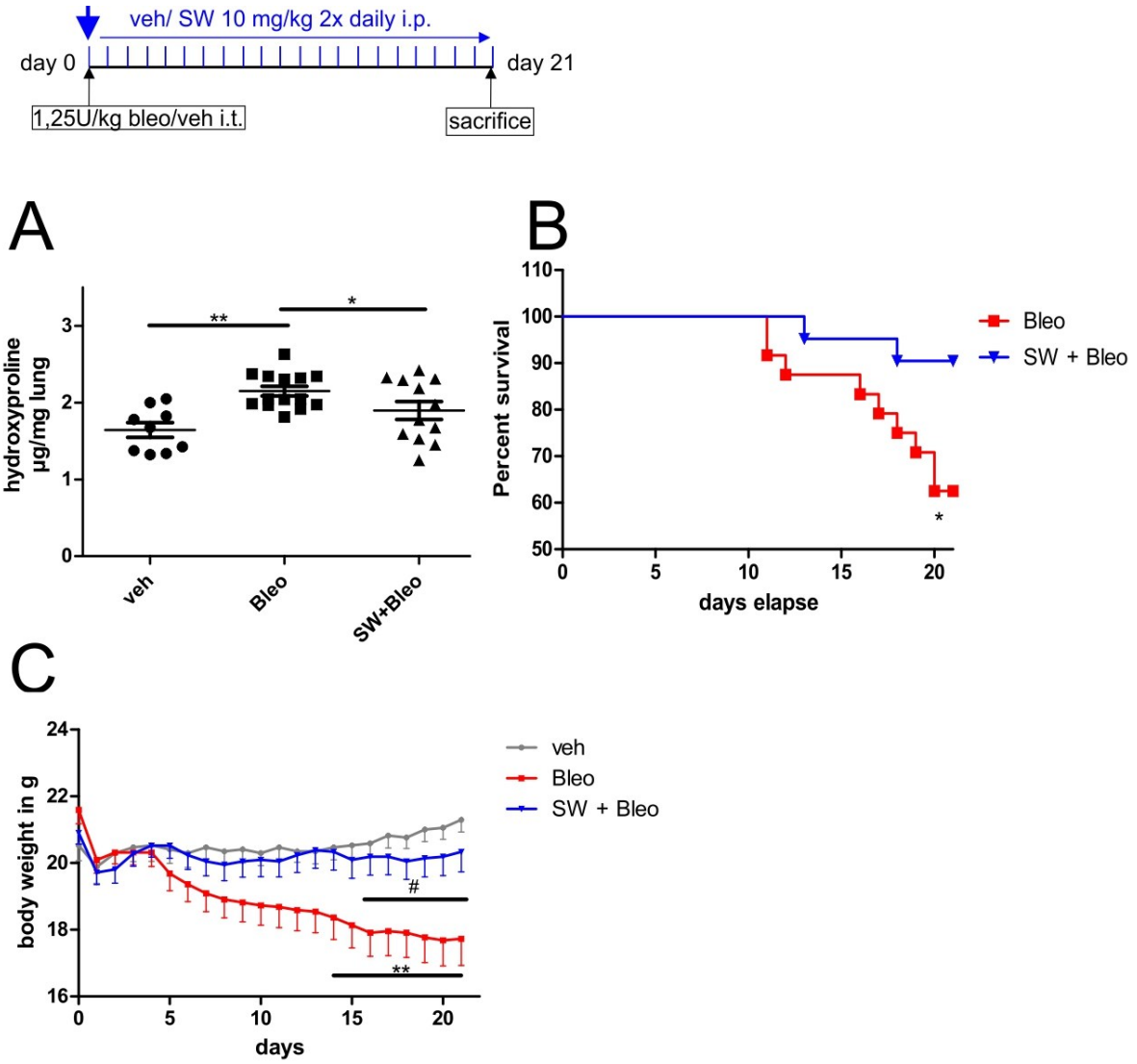

Figure 25. Inhibition of 15-PGDH protects mice from bleomycin induced fibrosis. *(A) Mice treated with Vehicle (veh), bleomycin (1,25 U/kg, Bleo) and 15-PGDH inhibitor ((SW+Bleo; SW033291 10 mg/kg twice daily, start at day 1) were sacrificed on day 21 and lung tissue was used for hydroxyproline measurements. (B) Survival over time during the experiment was recorded. (C) Weight was measured once daily and the last observation was carried forward for deceased mice. One-way ANOVA, followed by Newman-Keuls-test was used in **A** (n=8-12). For **C**, two-way ANOVA for repeated measurements followed by Bonferroni's post-hoc test was applied. For **B**, Gehan-Breslow test was used (n=8-20). *=p<0.05, **=p<0.01, for (**C**) #=p<0.05 SW+ Bleo vs Bleo*

3.2.5 Inhibition of 15-PGDH increases PGE_2 levels in murine lungs and bone marrow

In order to confirm the effects of our treatment on PGE_2 levels, we measured them in both bone marrow and lung tissue from mice in the protective model. We could observe that in the lungs, bleomycin alone led to a significant increase in PGE_2 levels and this was further elevated by 15-PGDH inhibition (Figure 26). In the bone marrow, however, bleomycin alone did not increase PGE_2 levels, but 15-PGDH inhibition did (Figure 27).

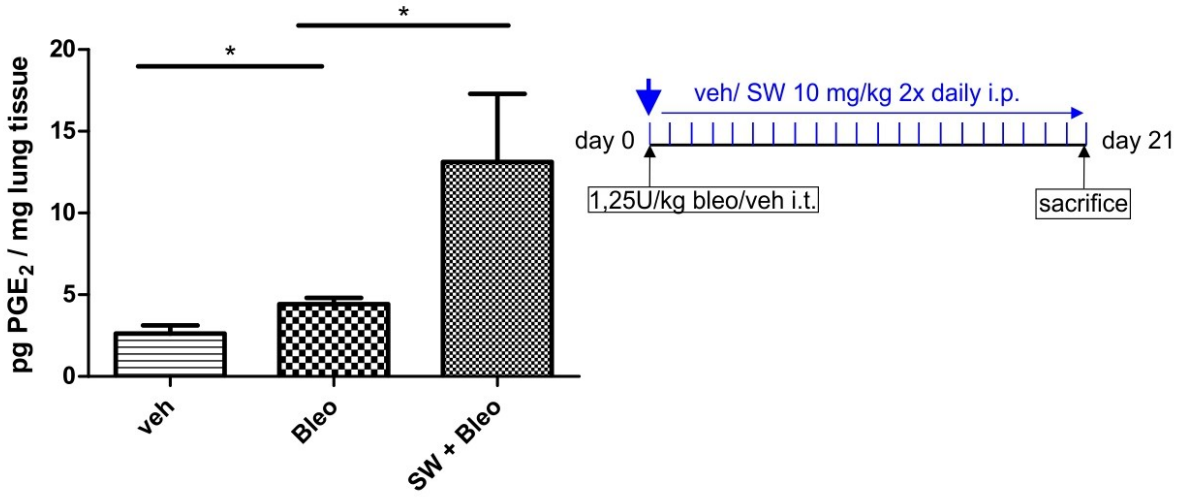

Figure 26. Inhibition of 15-PGDH further increases pulmonary PGE_2 levels in the bleomycin model. *Pulverized lung tissue was used for mass spectrometry measurements. Mann-Whitney test was performed, n=5-10 *p<0.05*

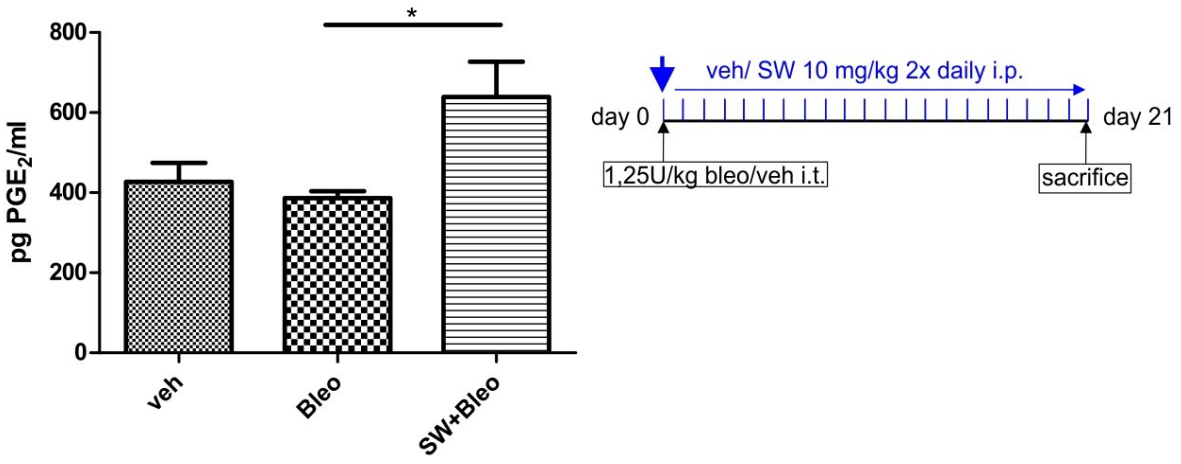

Figure 27. Inhibition of 15-PGDH increases bone marrow PGE_2 levels in the bleomycin model. *Femur was perfused with 1 ml of PBS and PGE_2 concentration was measured by radioimmunoassay. Mann-Whitney test was performed, n=5, *=p<0.05*

3.2.6 Inhibition of 15-PGDH protects ATII cells from apoptosis and promotes their proliferation in bleomycin-treated mice

As exaggerated apoptosis and subsequent loss of ATII cells is a hallmark of IPF, strategies to prevent this phenomenon might exert beneficial effects (102). As PGE_2 was increased in the lungs in our experiments and has been shown to protect ATII cells from apoptosis (102), we wanted to know, whether 15-PGDH inhibition might show similar effects. We therefore stained mouse lungs with antibodies against caspase 3 and pro-SP-C to detect apoptotic ATII cells.

As has been described, we found greatly increased apoptosis of ATII cells upon bleomycin treatment (257). The percentage of apoptotic cells in the bleomycin treated mice was in good agreement with earlier observations (257). Treatment with the 15-PGDH inhibitor decreased apoptosis to almost baseline levels showing pronounced protection (Figure 28). In addition, we wanted to establish whether our treatment might also increase ATII cell proliferation. To this end we used immunohistochemical staining for Ki-67, a proliferation marker, and pro-SP-C. We found that while bleomycin alone led to a small increase in proliferation as has been described (258), additional treatment with the 15-PGDH inhibitor led to a further significant increase (Figure 29).

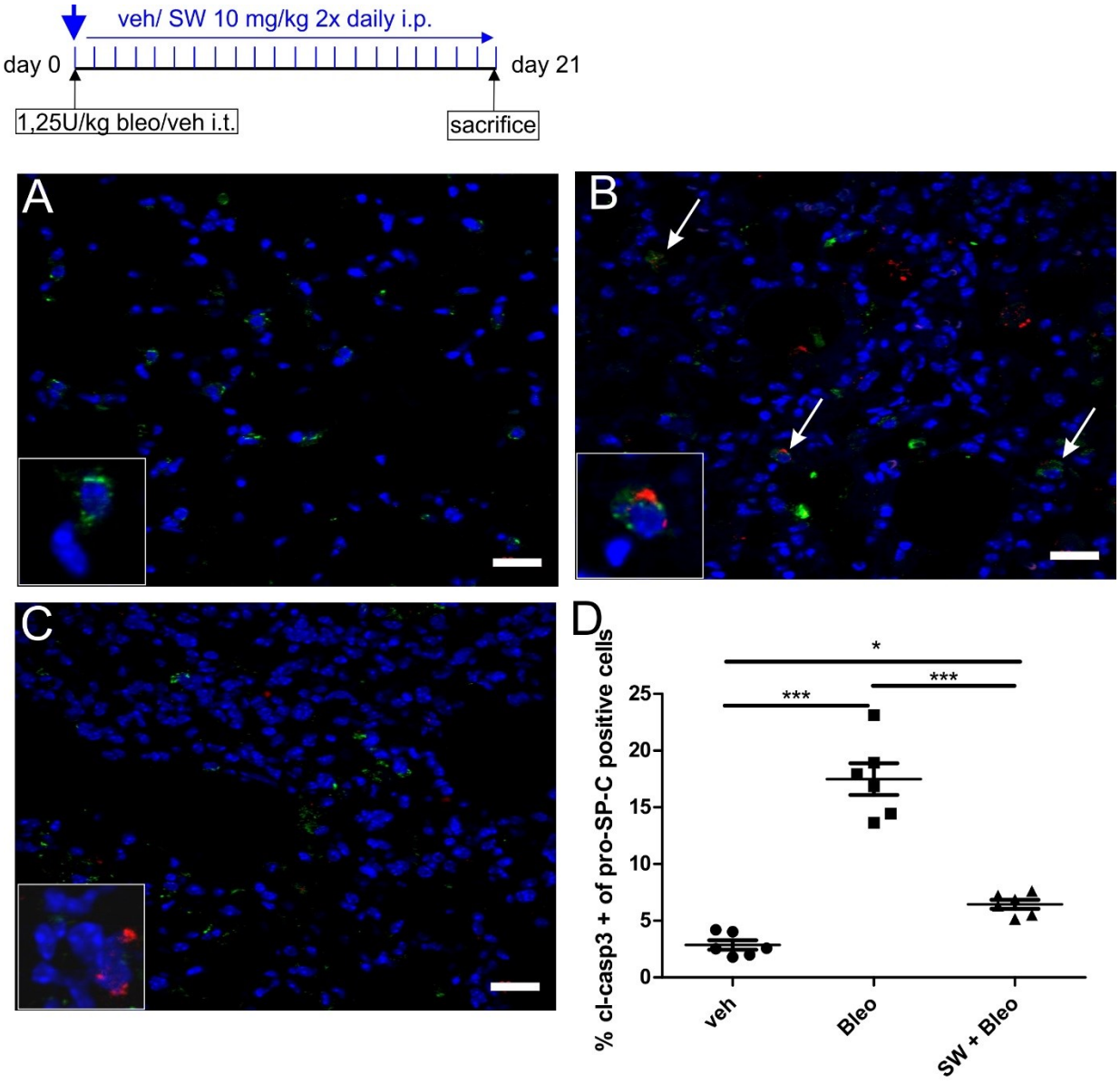

Figure 28. ATII cells are protected from apoptosis by inhibition of 15-PGDH in the bleomycin model. *(**A-C**) Apoptotic cells (red) and ATII cells (green) were stained with antibodies for cleaved caspase (cl-casp) 3 and pro-*

*SP-C, respectively; **A, B** and **C** show photomicrographs of lungs from animals treated with vehicle (veh), bleomycin (Bleo) and bleomycin/15-PGDH inhibitor (SW + Bleo), respectively and arrows indicate double positive cells. Insets show (**A**) a cell positively stained for pro-SP-C / but negative for cleaved caspase 3, (**B**) positive for both pro-SP-C /cleaved caspase 3 and (**C**) a cell negative for pro-SP-C but positive for cleaved caspase 3. (**D**) Double positive cells were counted in a double-blinded fashion (in 10 high-power field images per lung) and the percentage of apoptotic cells was calculated. One-way ANOVA, followed by Newman-Keuls-test was used for **D.** Scale bars show 20 µm *=p<0.05, ***=p<0.001*

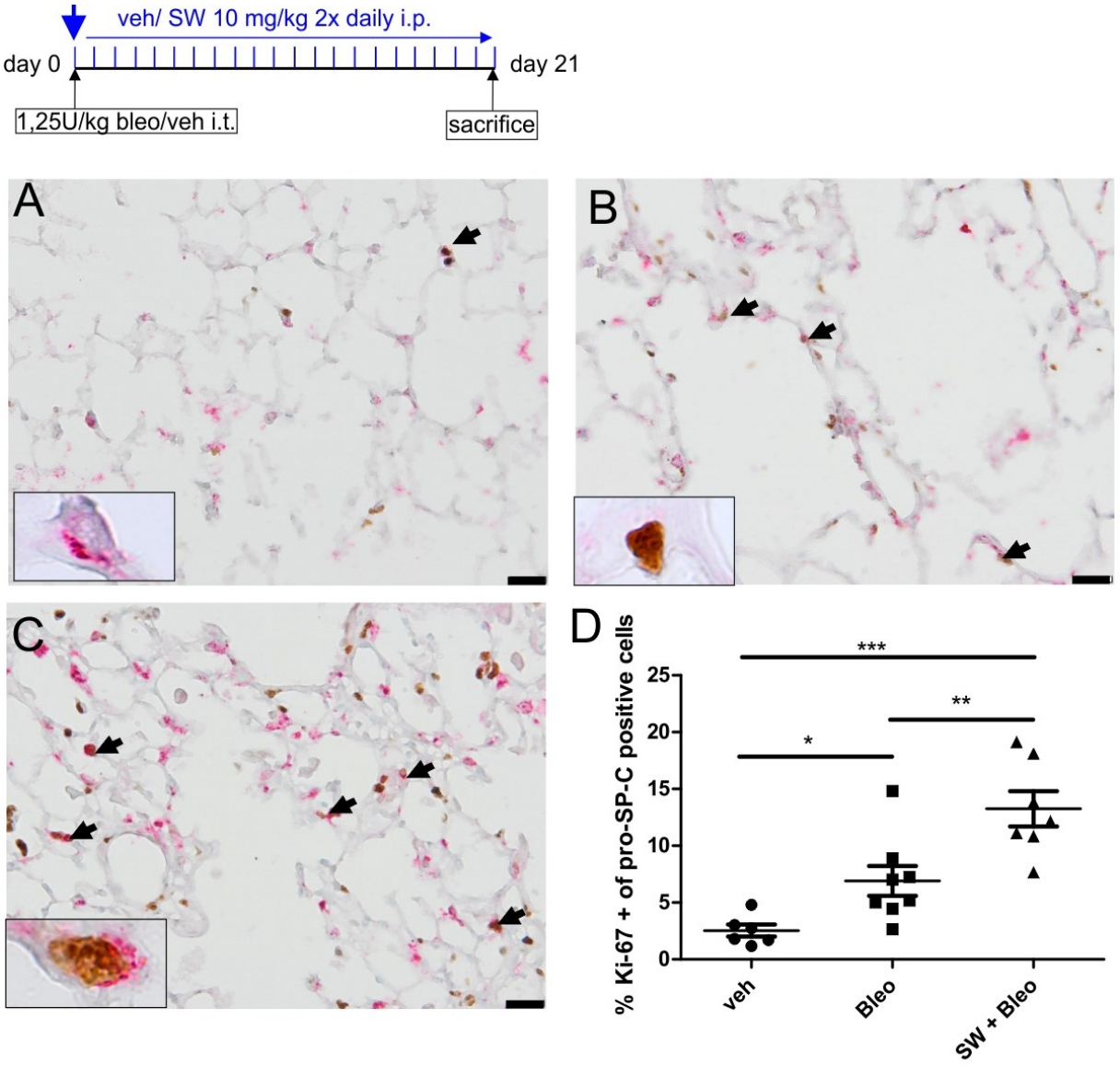

Figure 29. ATII cell proliferation is stimulated by inhibition of 15-PGDH. *(**A-C**) Proliferating cells (brown) and ATII cells (red) were stained with antibodies for Ki-67 and pro-SP-C, respectively; **A, B** and **C** show photomicrographs of lungs from animals treated with vehicle (veh), bleomycin (Bleo) and bleomycin/15-PGDH inhibitor (SW + Bleo), respectively and arrows indicate double positive cells. Insets show (**A**) a cell positively stained for pro-SP-C / but negative for Ki-67, (**B**) cell negative for pro-SP-C but positive for Ki-67and (**C**) positive for both pro-SP-C / Ki-67. (**D**) Double positive cells were counted in a double-blinded fashion (in 10 high-power field images per lung) and the percentage of proliferating cells was calculated. One-way ANOVA, followed by Newman-Keuls-test was used for **D.** Scale bars show 20 µm *=p<0.05, **=p<0.01, ***=p<0.001*

3.2.7 Inhibition of 15-PGDH prevents fibroblast proliferation in bleomycin-treated mice

Excessive proliferation of fibroblasts is one of the main characteristics in IPF and is also increased in isolated fibroblasts as compared to healthy controls as well as in the bleomycin mouse model (259, 260). As PGE_2 is a known suppressor of fibroblast proliferation (18), we wanted to know whether this effect could also be detected in our approach. We performed immunohistochemistry for Ki-67, and vimentin, a marker of mesenchymal cells/fibroblasts. This revealed a pronounced increase of fibroblast proliferation in the bleomycin treated mice as compared to vehicle. Additional treatment with the 15-PGDH inhibitor decreased numbers of proliferating fibroblasts (Figure 30).

3.2.8 Pulmonary fibrocyte accumulation is reduced upon 15-PGDH inhibition in bleomycin-treated mice

As both pirfenidone and nintedanib –among other targets– inhibit pulmonary fibrocyte accumulation, we wanted to assess whether these cells are also influenced by 15-PGDH inhibition. Furthermore, the expression of EP2 and EP4 receptors on these cells has been described and we found increased PGE_2 levels in the lungs and bone marrow of bleomycin treated mice that were treated with 15-PGDH inhibitor (261). We visualized these cells by co-staining for CD45 and fibroblast specific protein (FSP) (202) and could show that bleomycin indeed increases fibrocyte counts in the lungs as has been described (196, 202). This was prevented by treating animals receiving bleomycin with the 15-PGDH inhibitor (Figure 31).

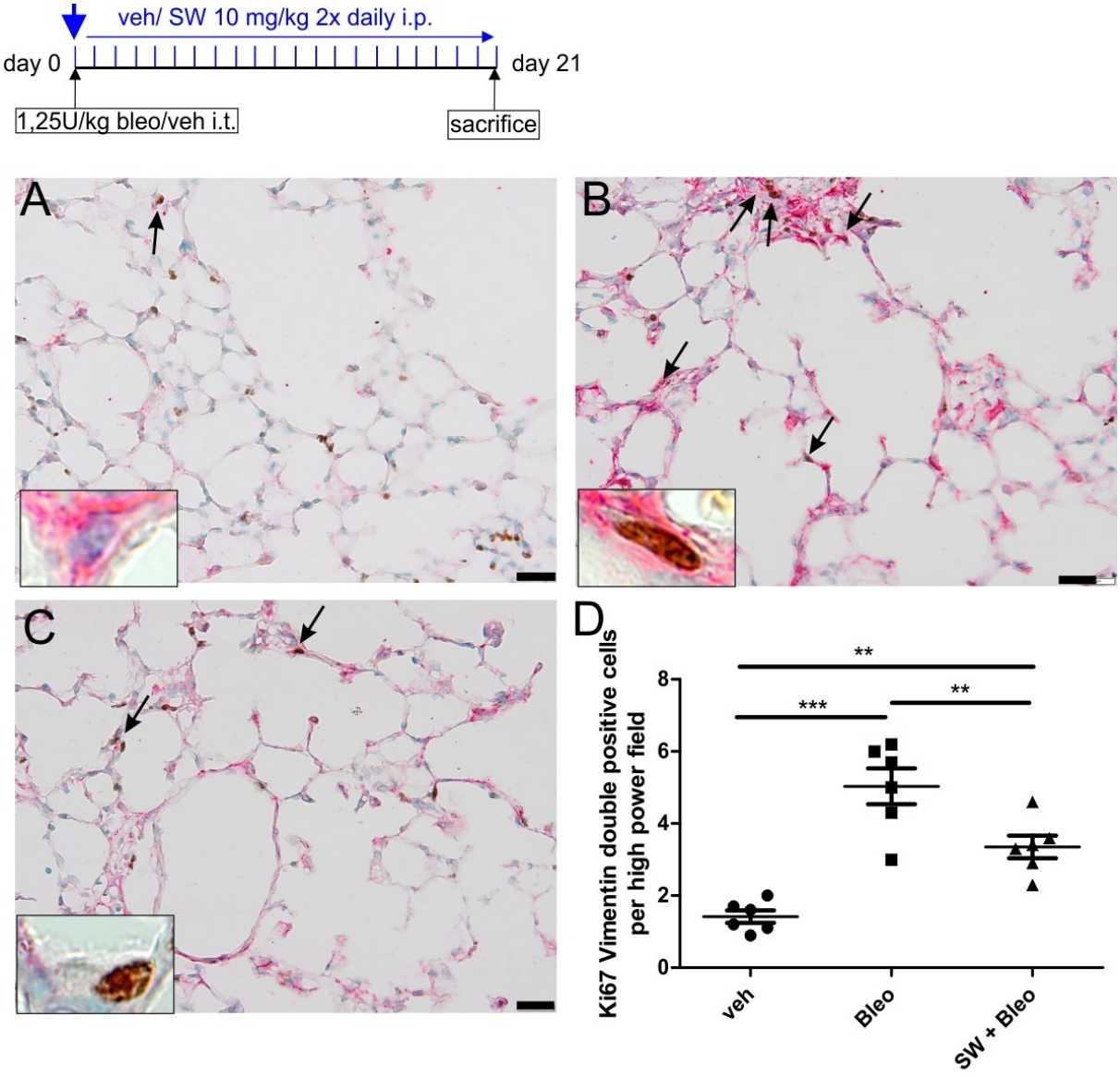

Figure 30. Fibroblast proliferation is decreased by inhibition of 15-PGDH. *(**A-C**) Proliferating cells (brown) and fibroblasts (red) were stained with antibodies for Ki-67 and vimentin, respectively; **A, B** and **C** show photomicrographs of lungs from animals treated with vehicle (veh), bleomycin (Bleo) and bleomycin/15-PGDH inhibitor (SW + Bleo), respectively and arrows indicate double positive cells. Insets show (**A**) a cell positively stained for vimentin / but negative for Ki-67, (**B**) cell positive for both vimentin / Ki-67 and (**C**) a cell negative for vimentin but positive for Ki-67 (**D**) Double positive cells were counted in a double-blinded fashion (in 10 high-power field images per lung). One-way ANOVA, followed by Newman-Keuls-test was used for **D.** Scale bars show 20 µm, **=p<0.01, ***=p<0.001*

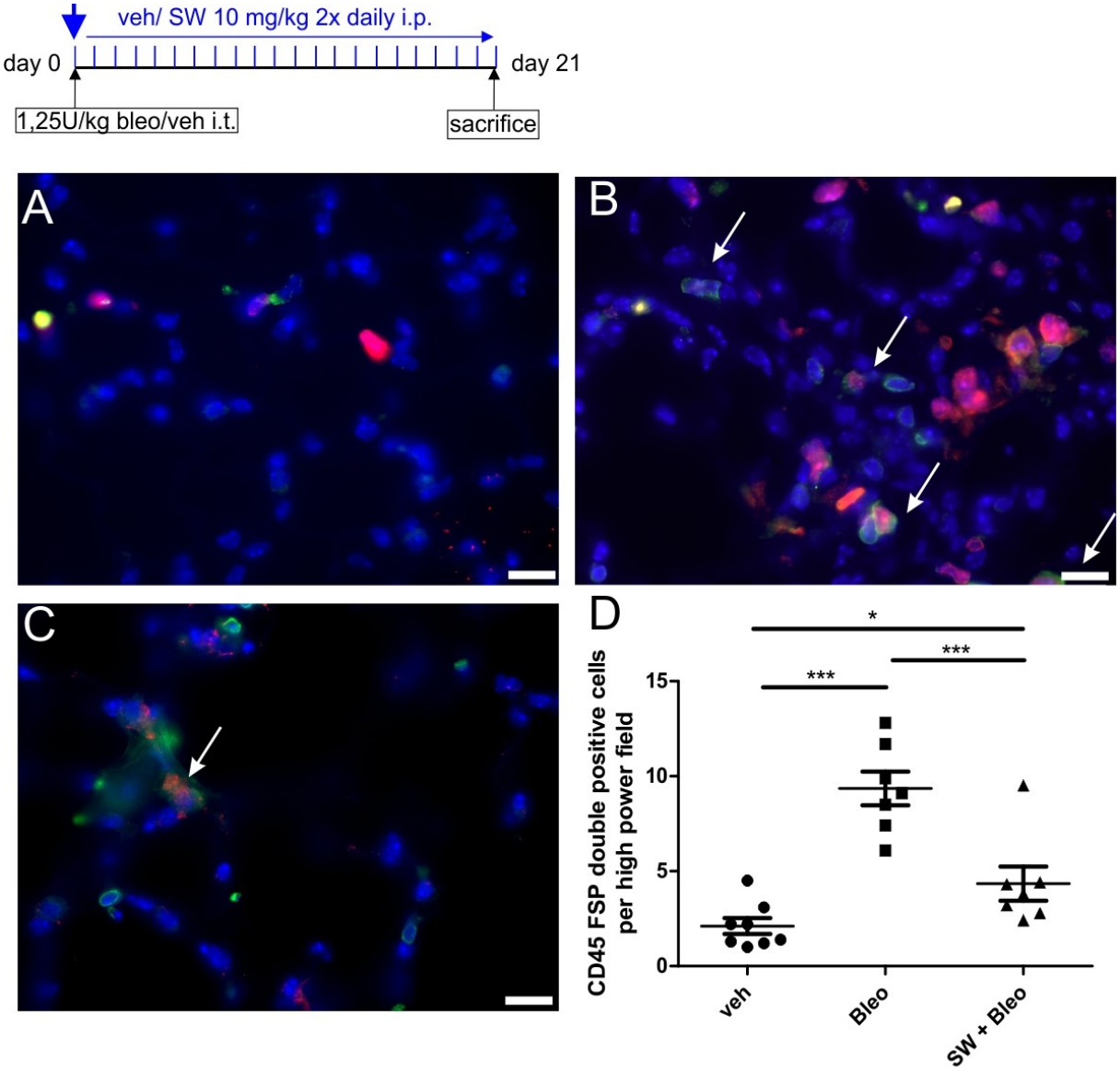

Figure 31. Inhibition of 15-PGDH reduces fibrocyte counts in the bleomycin model. (A-C) *Fibrocytes were visualized by immunostaining sections for CD45 (green) and fibroblast specific protein (FSP, red);* ***A, B*** *and* ***C*** *show photomicrographs of lungs from animals treated with vehicle (veh), bleomycin (Bleo) and bleomycin/15-PGDH inhibitor (SW + Bleo), respectively and arrows indicate double positive cells. Double positive cells were counted in a double-blinded fashion (in 10 high-power field images per lung). One-way ANOVA, followed by Newman-Keuls-test was used for* ***D.*** *Scale bars show 20 µm, *=p<0.01, ***=p<0.001*

3.2.9 Human fibrocyte differentiation is inhibited by PGE_2

The effects of PGE_2 on fibrocytes have not been investigated so far. Therefore, we used an established assay for fibrocyte differentiation from peripheral blood and found that PGE_2 decreased fibrocyte differentiation in a concentration-dependent manner and that this was mediated via EP2 and EP4 receptor activation, as both antagonists could block parts of the PGE_2 effect (Figure 32 B,C). Furthermore, we also wanted to determine whether PGE_2 only

blocks differentiation or whether it also acts on already differentiated fibrocytes. To this end, we allowed cells to differentiate in the presence of vehicle and PGE_2 treatment was started after the first 5 days, and thereafter for 5 more days. We found that even under these circumstances, fibrocytes were significantly decreased by PGE_2 (Figure 32 D). In order to evaluate our model we also used nintedanib and pirfenidone and both compounds significantly inhibited fibrocyte differentiation to a similar extent as PGE_2 but much higher concentrations were needed (Figure 32 E).

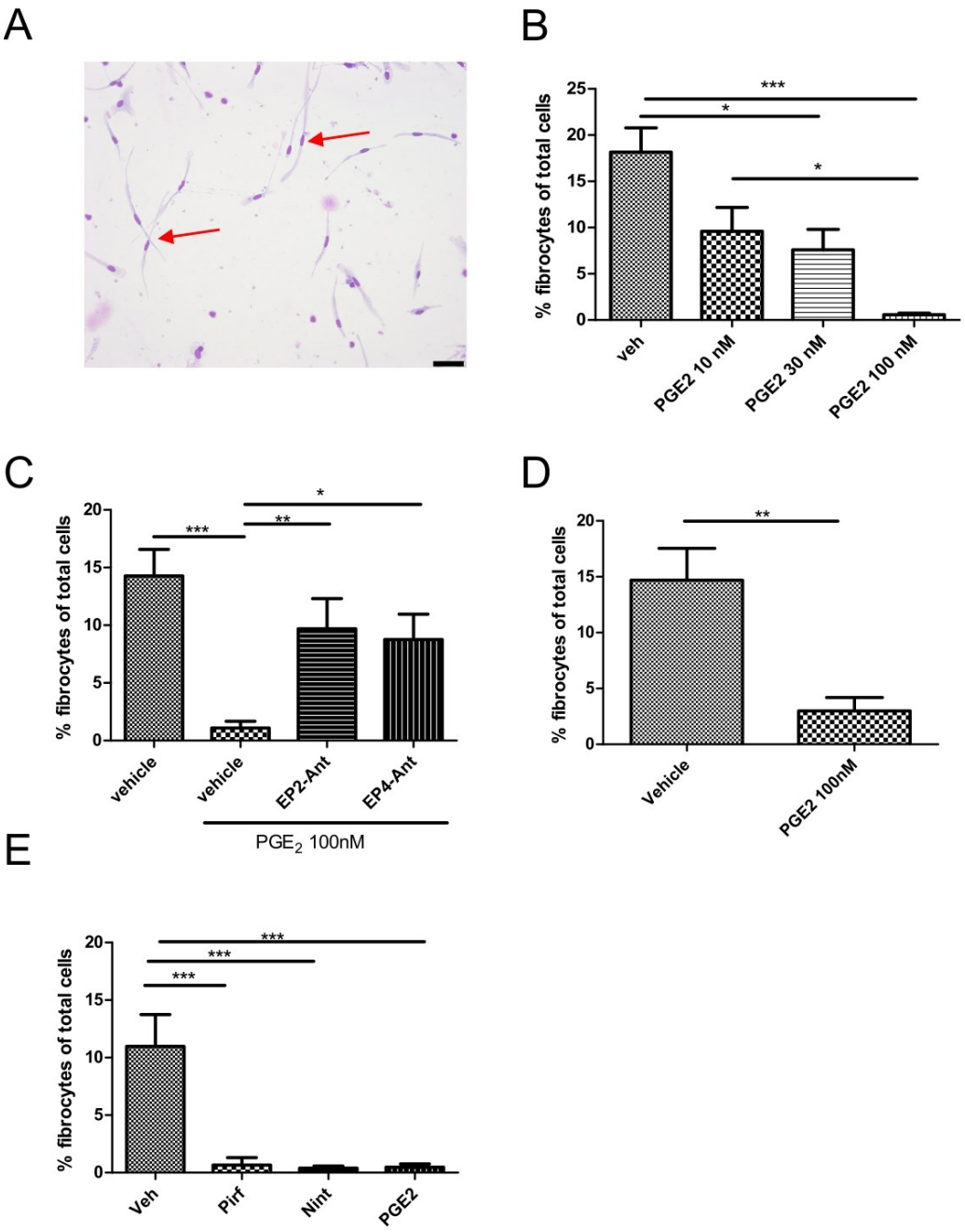

Figure 32. PGE_2 inhibits fibrocyte differentiation in vitro. *(**A-C,E**) Peripheral blood mononuclear cells from healthy donors were differentiated and after 5 days cells were stained with DiffQuick. Scale bar shows 50 µM. (**B,C**)*

*Fibrocytes from healthy donors were counted and the effects of (**B**) PGE_2, in the absence and presence of the (**C**) EP2 antagonist (PF04418948 1 µM) and the EP4 antagonist (ONO AE3 208 1µM) were determined. (**D**) Fibrocytes were differentiated for 5 days and afterwards treatment with vehicle or PGE_2 was initiated for additional 5 days. (**E**)Fibrocytes were cultured for 5 days in the presence of vehicle (veh), pirfenidone (Pirf,500 µM) nintedanib (Nint, 1 µM) or PGE_2 (100 nM). One-way ANOVA for repeated measurements, followed by Tukey's test was used for (**B,C,E**) and Student's t-test for (**D**) (n=7-9). *=p<0.05, **=p<0.01, ***=p<0.001*

3.2.10 Fibrocyte differentiation in IPF patient-derived blood is inhibited by PGE_2

As there are findings describing reduced expression and aberrant signaling of the EP2 receptor in IPF fibroblasts (169, 216), we wanted to know whether this might also be true in fibrocytes. To this end we differentiated fibrocytes from peripheral blood of IPF patients and treated them with PGE_2. However, also in IPF patients, fibrocyte differentiation was abrogated by PGE_2 (Figure 33). This seems to be irrespective of the obtained treatment, but n-numbers were too low for statistical analysis.

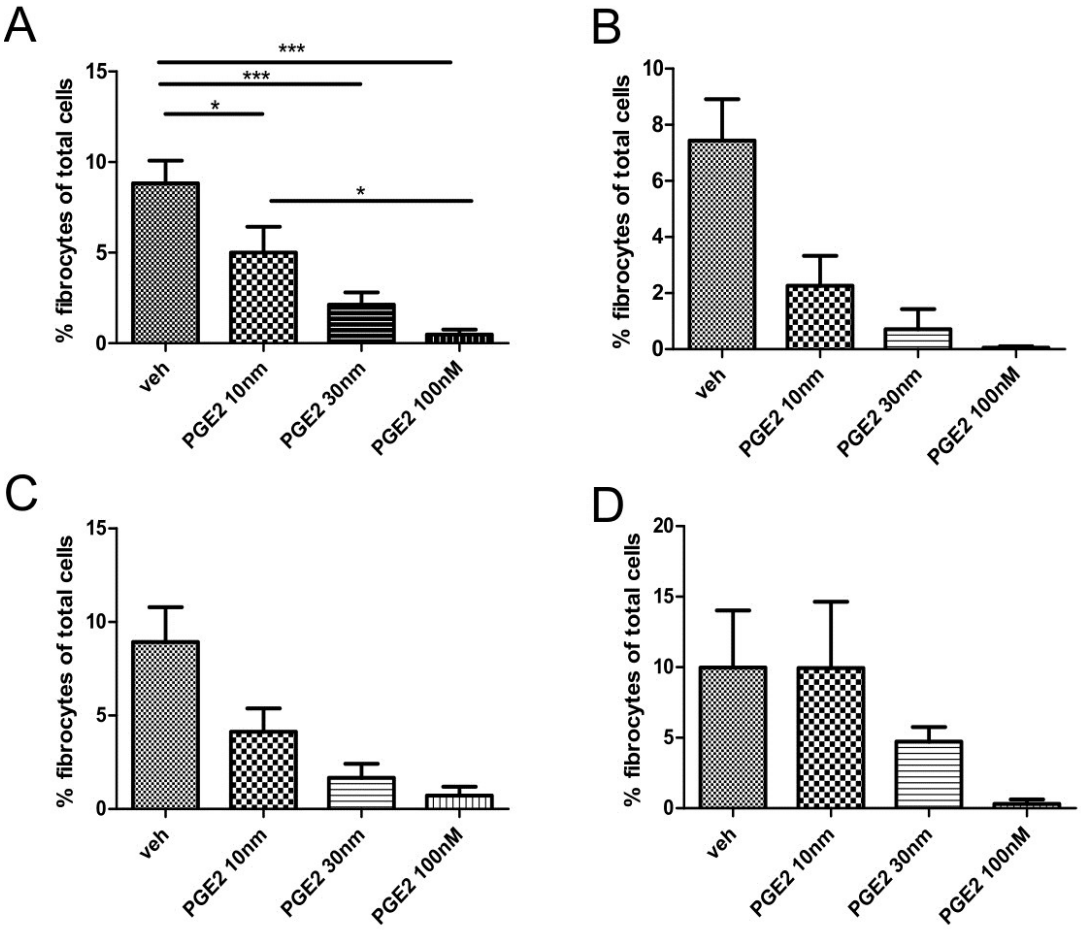

Figure 33. PGE_2 inhibits fibrocyte differentiation in vitro. *(**A-D**) Peripheral blood mononuclear cells from (A) IPF patients treated with either (**B**) nintedanib, or (**C**) pirfenidone or (**D**) untreated patients, were differentiated in the presence of increasing concentrations of PGE_2 and after 5 days, cells were stained with DiffQuick and counted.*

*One-way ANOVA for repeated measurements, followed by Tukey's test was used for A, while statistics were not calculated for other panels due to low n-numbers (n=9 for A and 5, 2 and 2 for B, C and D respectively). *=p<0.05,, ***=p<0.001*

3.2.11 Fibrocytes express EP receptors

As earlier reports investigated EP receptor expression in lysates of differentiated fibrocytes with the potential of contamination of other cell types (261) we decided to use a more direct method. To this end, we differentiated fibrocytes for 5 days and afterwards performed in situ hybridization for EP2 and EP4 receptors, as these were the ones that mediated the effects of PGE_2. Using this approach, we found that cells showing fibrocyte morphology (i.e. elongated, spindle shaped appearance) expressed both of these receptors, while they were negative for 15-PGDH mRNA. As EP2 receptor expression has been shown to be impaired in IPF patients, we also performed the same experiment on fibrocytes from IPF patients. However, also there, both EP receptor mRNAs were still expressed which provided an explanation for the finding that PGE_2 was still able to reduce fibrocyte differentiation. In contrast, 15-PGDH mRNA was also not expressed in IPF patient-derived fibrocytes (Figure 34).

3.2.12 Pulmonary fibroblasts do not express 15-PGDH

As reports show expression of 15-PGDH in various fibroblast cell lines (262), we wanted to investigate, whether inhibition of this enzyme might alter fibroblast phenotypes. Most importantly, we wanted to know, whether inhibiting 15-PGDH might, by acting via increased PGE_2 levels, prevent and/or reverse myofibroblast formation, as has been described for PGE_2 (51, 170). To this end, we used MRC5 cells, a lung fibroblasts cell line, as well as primary fibroblasts from donor and IPF lungs. Surprisingly, we found no effect 15-PGDH inhibition whatsoever, although TGFβ1 treatment induced myofibroblast formation as witnessed by aSMA induction (Figure 35). Thus, we analyzed expression of 15-PGDH with both qPCR as well as Western blot and found that neither protein, nor mRNA was expressed in fibroblasts from IPF patients or healthy donors (data not shown). This finding is consistent with the results of 15-PGDH mRNA expression in lung tissue that showed almost no signal in vimentin expressing cells (cf. Figure 20 C)

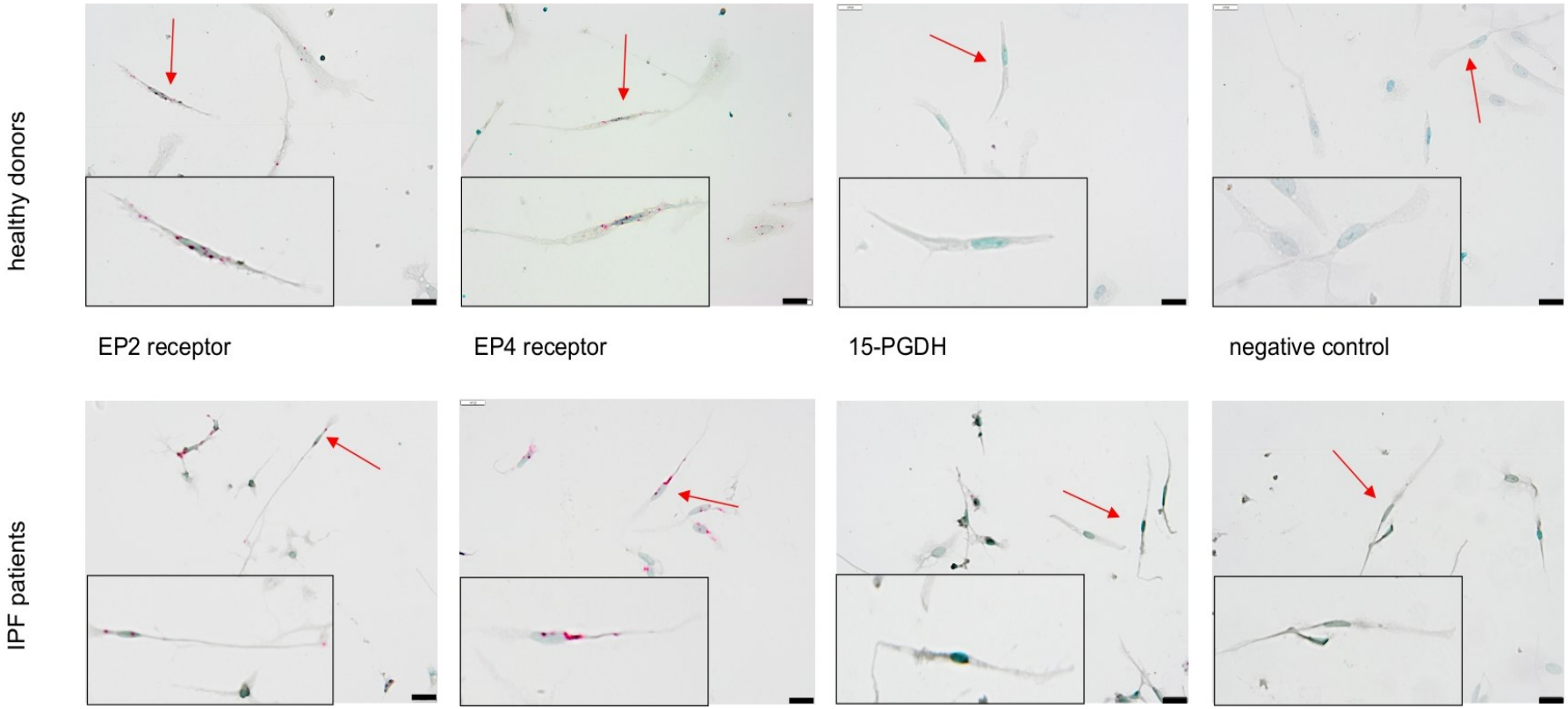

Figure 34. Fibrocytes from healthy controls and IPF patients express EP2 and EP4 receptors but not 15-PGDH mRNA.*In situ hybridization for the indicated targets (red dots) on fibrocytes from (upper row) healthy donors and (lower row) IPF patients was performed. Photomicrographs are representative for 4 donors/patients. Scale bars show 20 µm. Fibrocytes are indicated by red arrows, insets show these cells.*

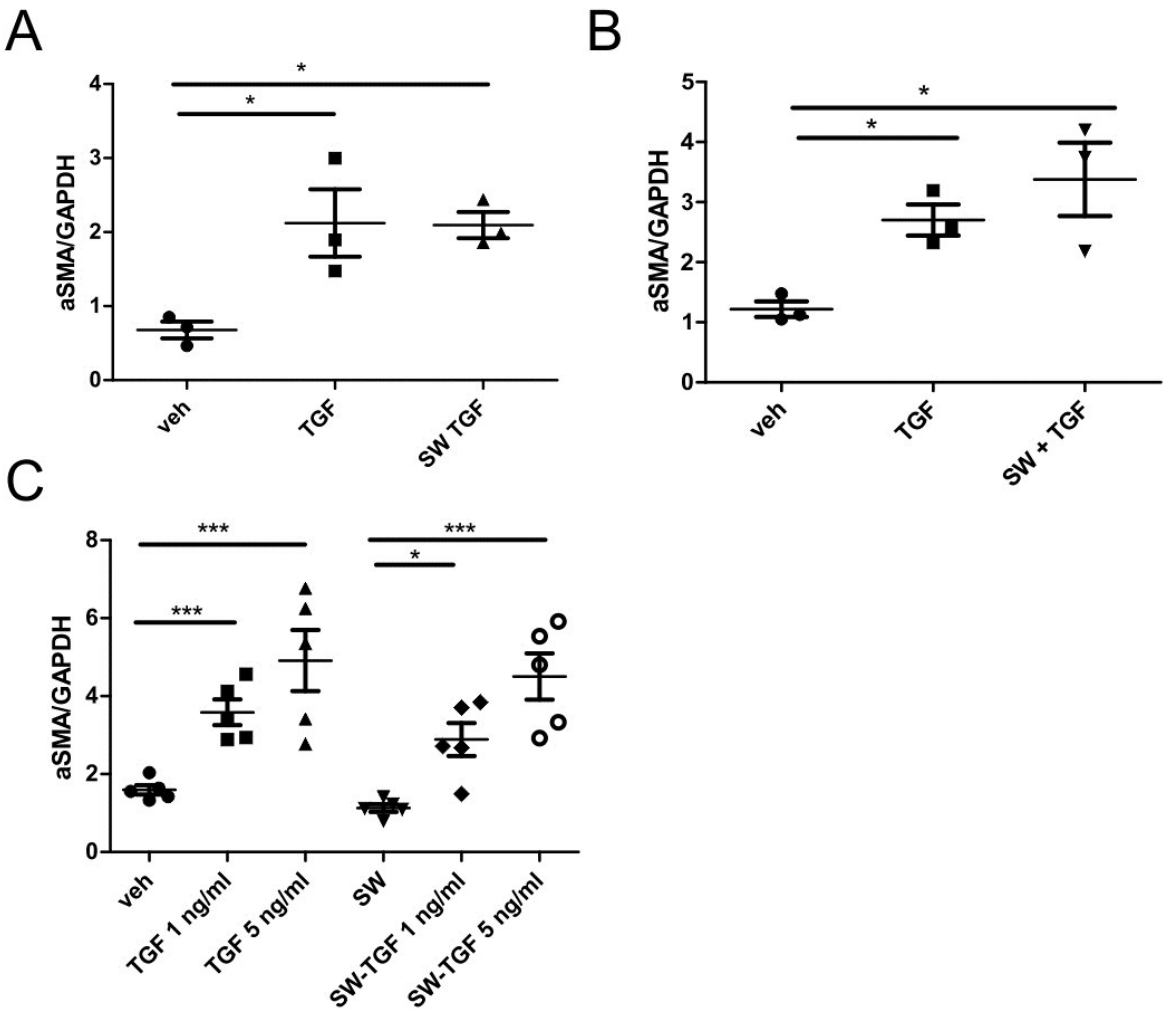

Figure 35. Inhibition of 15-PGDH shows no effect on TGFβ1-induced myofibroblast formation. *(**A,B**) Primary lung fibroblasts isolated from (**A**) healthy donors and (**B**) IPF patients were treated with TGFβ1 (TGF, 2ng/ml) and the 15-PGDH inhibitor (SW, SW033291, 1 µM) or respective vehicles for three days and aSMA induction was investigated by Western blot. (**C**) MRC5 cells were treated with TGFβ1 (TGF) and a 15-PGDH inhibitor (SW, SW033291, 1 µM) or respective vehicles for three days and aSMA induction was investigated by Western blot. For (**A,B**) One-way ANOVA, followed by Newman-Keuls test was used, while One-way ANOVA, followed by Tukey's test was employed for (**C**). *=p<0.05,, ***=p<0.001*

3.2.13 15-PGDH inhibition ameliorates established fibrosis in the bleomycin model

Considering the multiple beneficial findings of our preventive approach in the bleomycin model, we wanted to assess the effects of this treatment in a more relevant model. It has been shown that the early phase of the bleomycin model until day 7- 9 is predominantly characterized by inflammation (239). Thus, we applied a bleomycin model, where treatment with the 15-PGDH inhibitor was started at day 11 after bleomycin instillation, the timepoint where the acute inflammatory phase is considered to have passed (239). Also in this therapeutic model, we

saw a profound anti-fibrotic effect of 15-PGDH inhibition. Not only was histologic fibrosis reduced, but we could also observe that the initial weight loss was abrogated, once 15-PGDH inhibitor treatment was started (Figure 36). As decreased lung function is a crucial factor in the pathophysiology of IPF, we also investigated it in the bleomycin model. Also in this model, we found fundamental improvements in 15-PGDH inhibitor-treated mice as compared to mice that were treated with bleomycin only (Figure 37). To determine, whether the changes we could observe at the cellular level (i.e. increased ATII cell survival and decreased fibroblast proliferation) in the protective model, we analyzed pro-SP-C and COL1a1 gene expression as well as hydroxyproline levels in the mouse lungs. We could show that also in this therapeutic model, inhibition of 15-PGDH resulted in a reduction of fibrosis as assessed by reduced collagen and increased pro-SP-C in the inhibitor-treated mice (Figure 38).

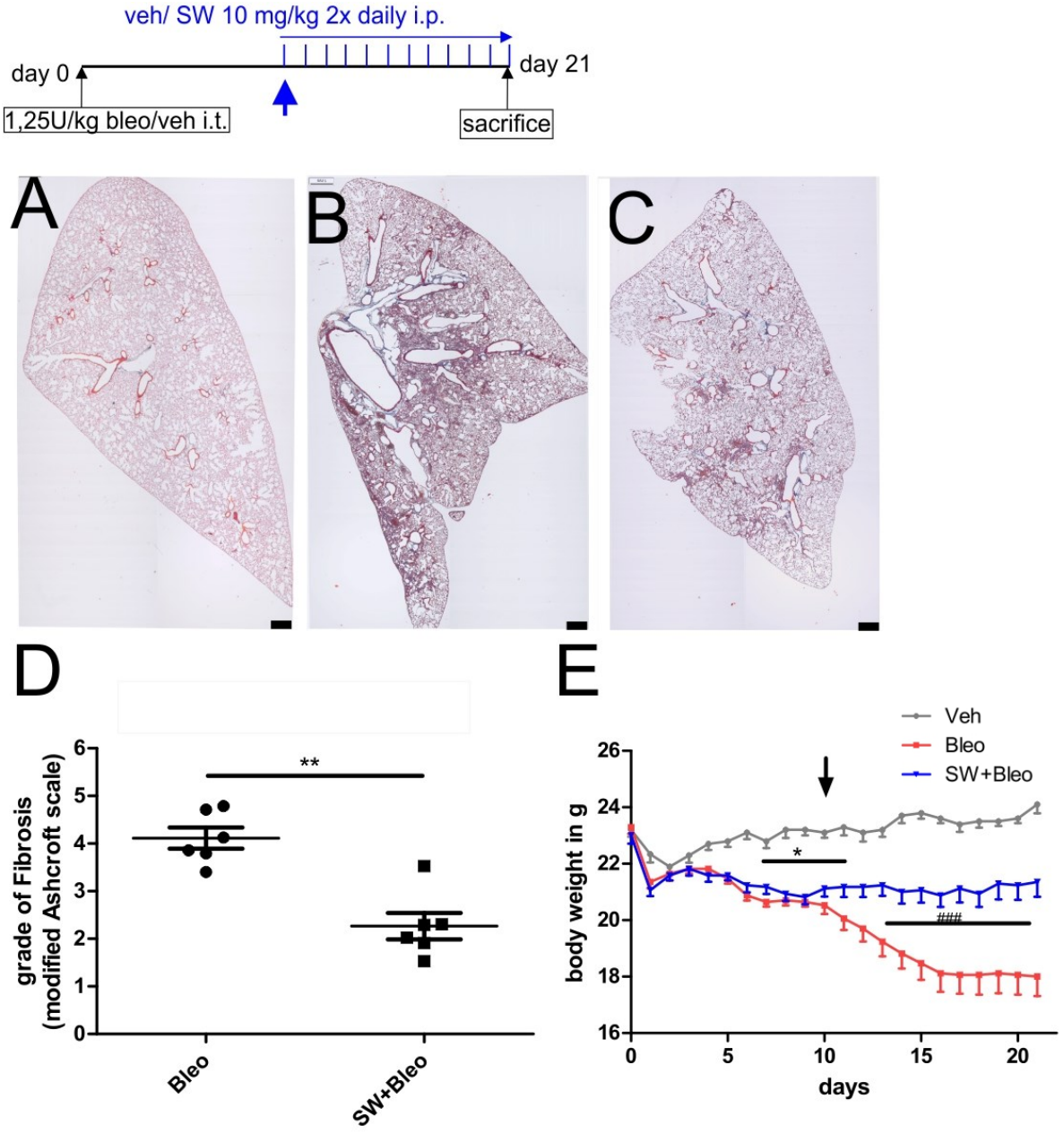

Figure 36. Inhibition of 15-PGDH decreases histological features of established fibrosis and abrogates weight loss*. Lobes from (**A**) vehicle, (**B**) bleomycin (1,25 U/kg, Bleo) and (**C**) 15-PGDH inhibitor ((SW+Bleo; SW033291 10 mg/kg twice daily, start at day 11) treated mice were stained with Masson's trichrome staining and (**D**) 60-70 photomicrographs were scored using modified Ashcroft scale. (**A-C**) Scale bar is 1 mm. (**E**) Weight was measured once daily and the last observation was carried forward for deceased mice. (**D**) Mann-Whitney test was performed (n=6). (**E**) Two-way ANOVA for repeated measurements followed by Bonferroni's post-hoc test was applied(n=9-16). *=p<0.05, **=p<0.01, in (**E**) ###=p<0.001 SW+ Bleo vs Bleo*

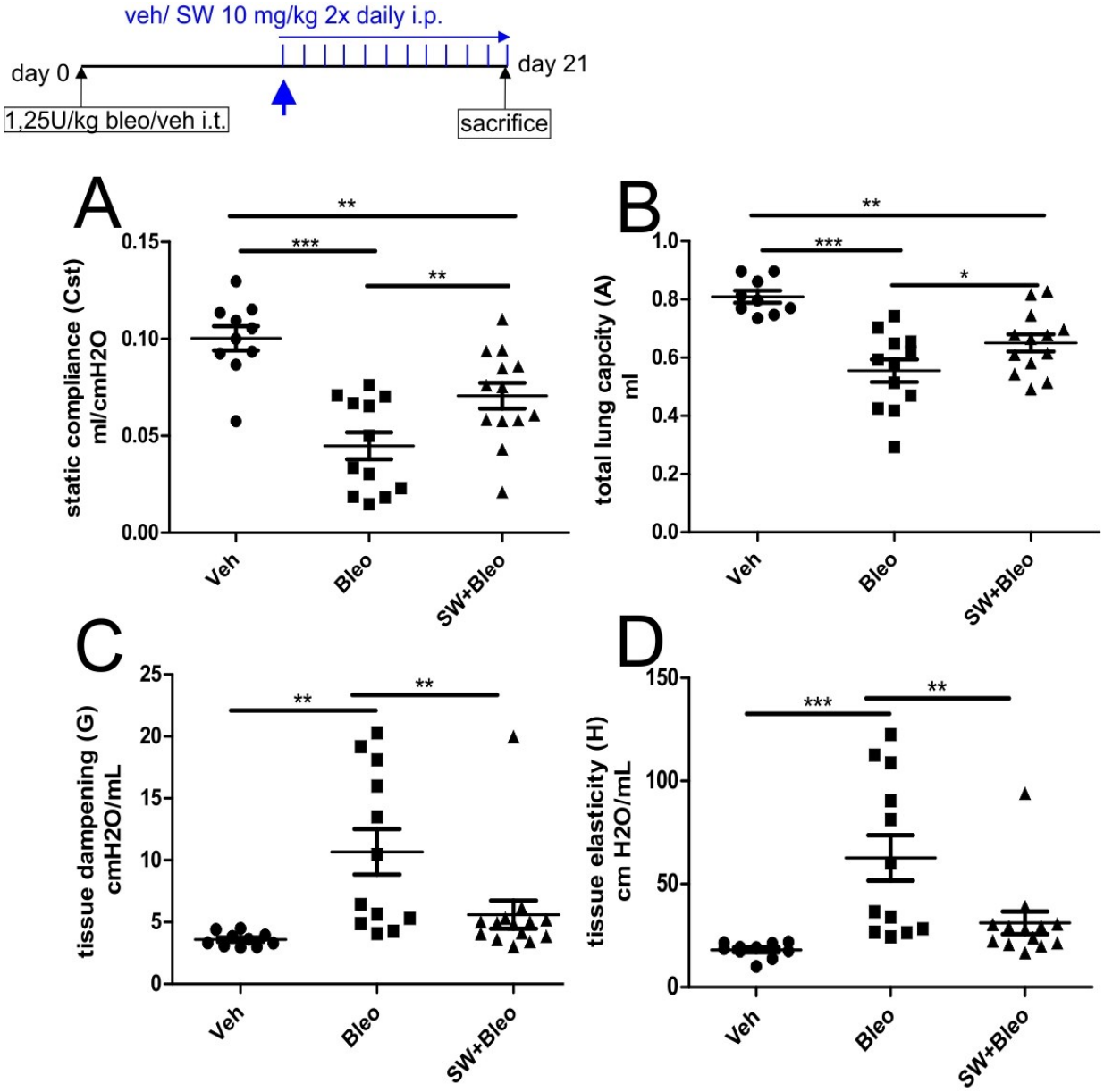

Figure 37. Inhibition of 15-PGDH ameliorates bleomycin-induced pulmonary fibrosis-associated changes in lung function in a therapeutic model. *(**A**) Static compliance, (**B**) Total lung capacity, (**C**) tissue dampening and (**D**) tissue elasticity were measured on day 21. One-way ANOVA, followed by Newman-Keuls-test was used for **A-D** (n=9-16), *=p<0.05, **=p<0.01, ***=p<0.001*

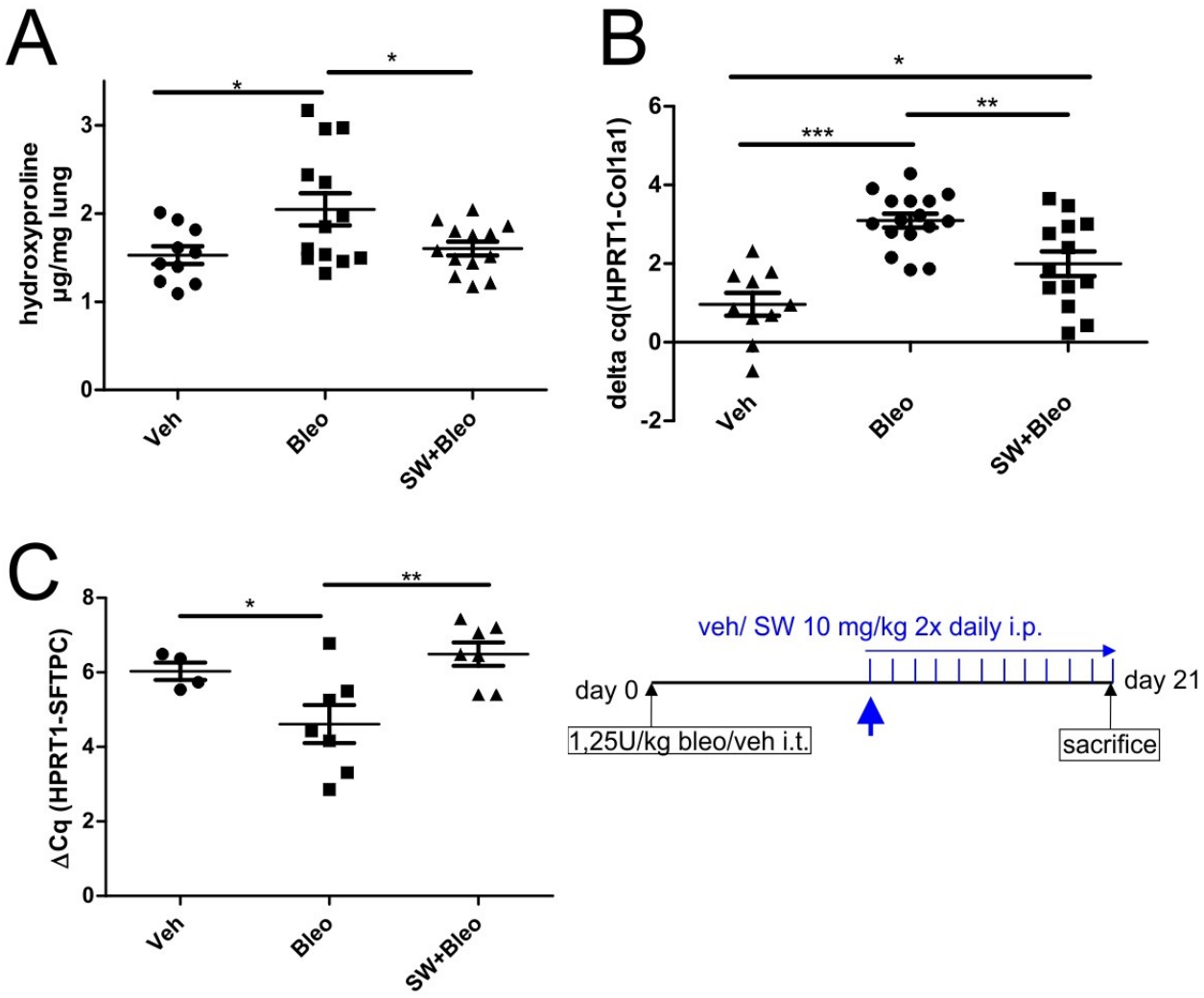

Figure 38. Inhibition of 15-PGDH ameliorates bleomycin-induced pulmonary fibrosis in a therapeutic model. *(**A**) Hydroxyproline levels, as a measure for lung collagen, were assayed from pulverized lung homogenates. (**B,C**) qPCR for (**B**) collagen type 1 alpha 1 and (**C**) pro-surfactant protein C were performed from lung homogenates and normalized to HPRT1 as a housekeeping gene. One-way ANOVA, followed by Newman-Keuls-test was used. *=p<0.05, **=p<0.01, ***=p<0.001*

3.2.14 miRNA 218-5p regulates 15-PGDH expression

Next we wanted to investigate which processes might be responsible for the selective upregulation of 15-PGDH in the alveolar walls. Although TGFβ1 has been described to increase 15-PGDH levels (129), we found evidence in the literature that 15-PGDH levels are suppressed by certain miRNAs in cell culture (228). Interestingly, the very same miRNA (miRNA 218-5p) has been shown to be downregulated in IPF (226, 227). We therefore set out to investigate, whether the described effects of this miRNA might also be present in lung epithelial cells. To this end, we used A549 cells and transfected them with inhibitors and mimics of miRNA 218-5p. As expected, inhibiting miRNA 218-5p led to an upregulation of 15-PGDH,

while mimics suppressed its expression (Figure 39 A,B,D). As A549 cells are a cancer cell line and might thus not represent truly physiologic circumstances, we also performed in vivo transfection experiments. Also in murine lungs, transfection with a mimic of miRNA 218-5p caused a decrease of 15-PGDH protein after 24 hours (Figure 39 C,E). Thus, we set out to investigate the situation in human lungs. We found by employing double in situ hybridization that cells which express 15-PGDH mRNA also show expression of pre-miRNA 218 (Figure 40). Interestingly, miRNA 26a-5p also has been shown to be decreased in IPF and TargetScan (version 7.2, http://www.targetscan.org) (263) revealed it as a potential regulator of 15-PGDH. In A549 cells, a mimic of this miRNA also showed suppression of 15-PGDH (Figure 41).

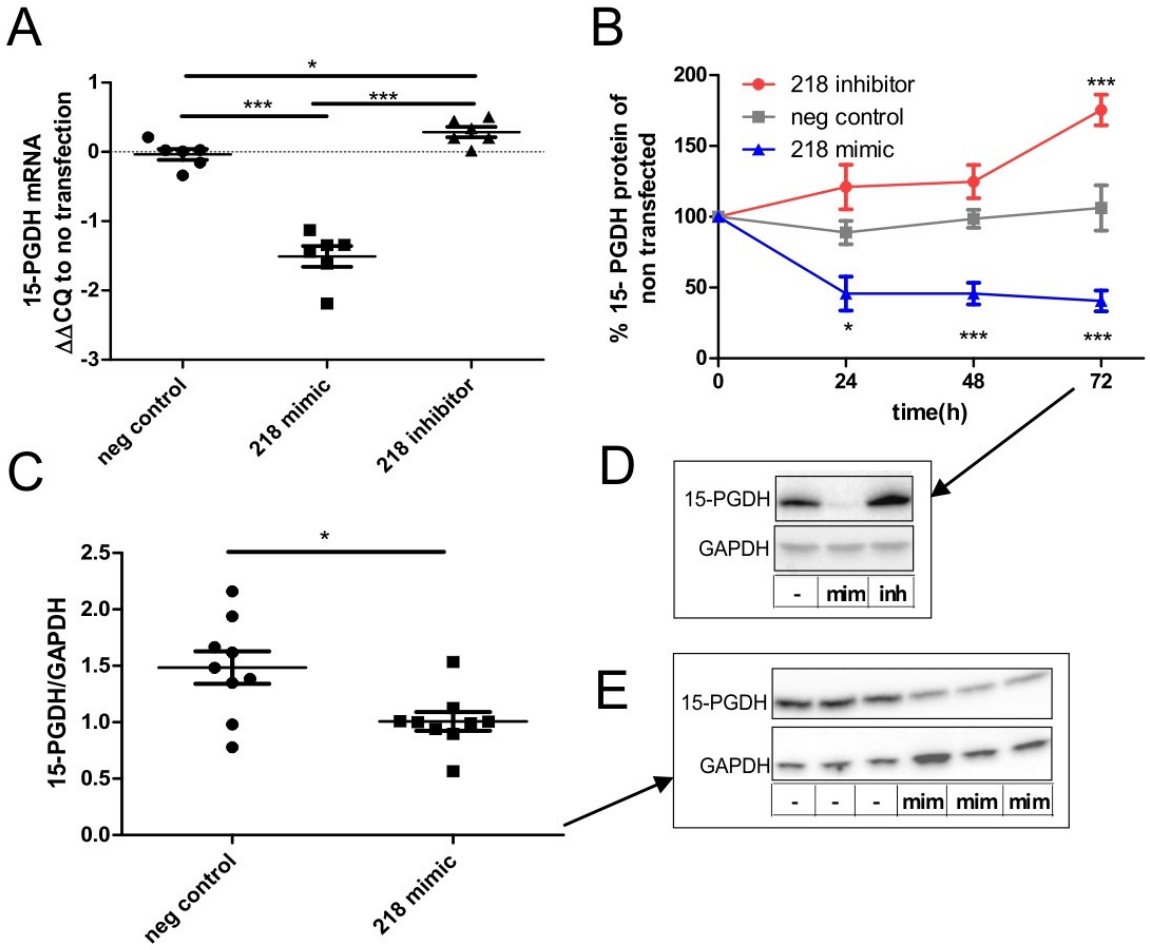

Figure 39. miRNA 218-5p is a regulator of 15-PGDH in vitro and in vivo. *(**A**,**B**) A549 cells were transfected with an inhibitor (inh) or a mimic (mim) of miRNA 218-5p or a respective negative control (neg control), the mRNA expression levels were measured (**A**) 24 h later, and (**B**) a time course for 15-PGDH protein expression was performed. (**D**) A representative blot for the 72 h time point is shown. (**C**) Mouse lungs were transfected with a mimic of miRNA 218-5p or a respective negative control (neg control) and 24 h later, lungs were harvested, pulverized on liquid nitrogen, and analysed for 15-PGDH protein levels on Western blot. In (**E**) a representative blot is shown. (**A**) One-way ANOVA, followed by Newman-Keuls-test was performed, while for **B** two-way-ANOVA,*

*followed by a Bonferroni post hoc test was done and for **C** a student's t-test was used. *=p<0.05, **=p<0.01, ***=p<0.001*

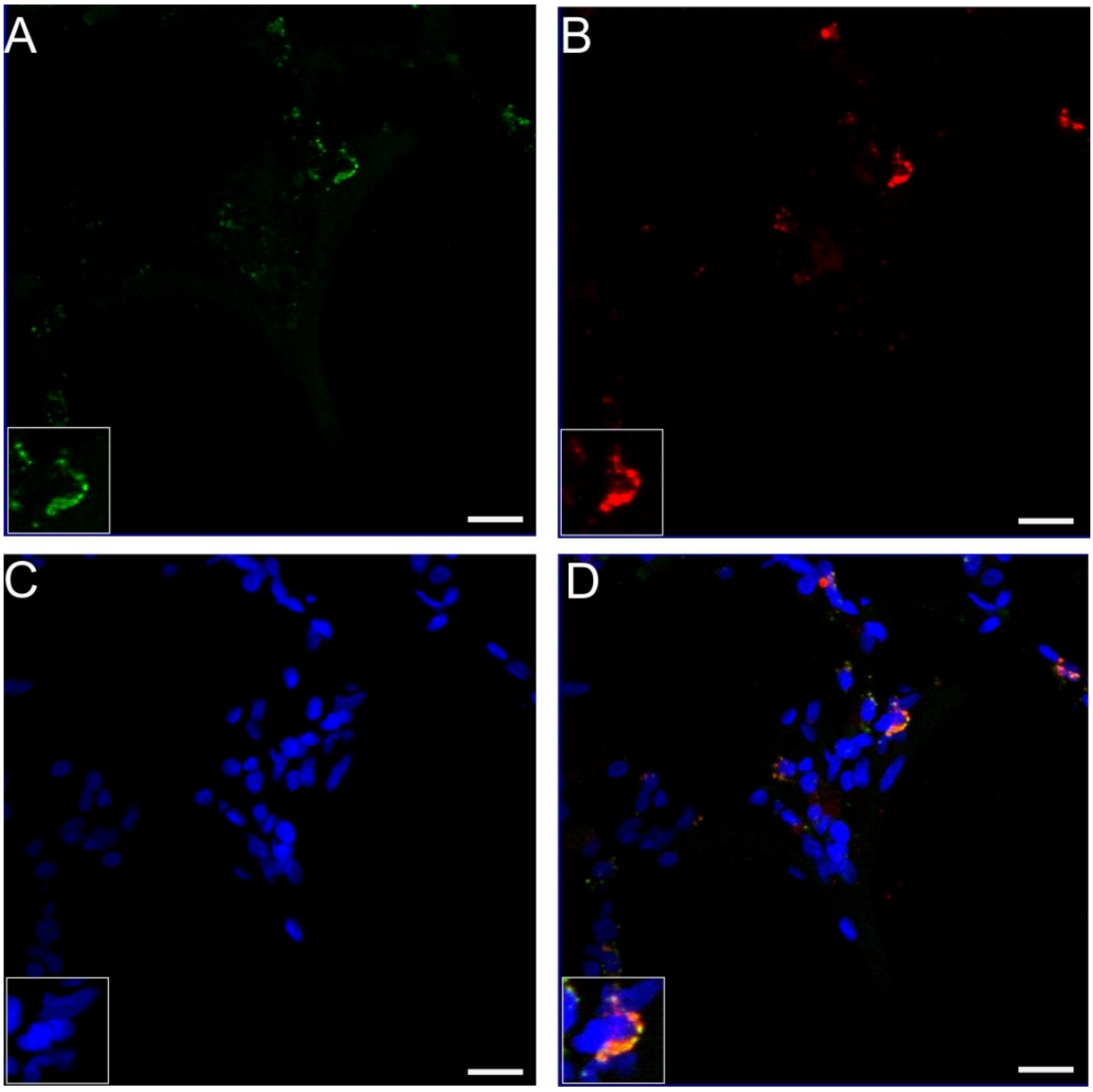

***Figure 40. 15-PGDH mRNA and pre-miRNA-218 are expressed in the same cells in healthy human lungs**. (**A-D**) In situ hybridization for (**A**) pre-miRNA 218a and (**B**) 15-PGDH mRNA was performed, sections were counterstained with (**C**) DAPI and (**D**) an overlay is shown. The photomicrograph is representative for 5 healthy lungs. Scale bars indicate 20 µm, insets show a double positive cell.*

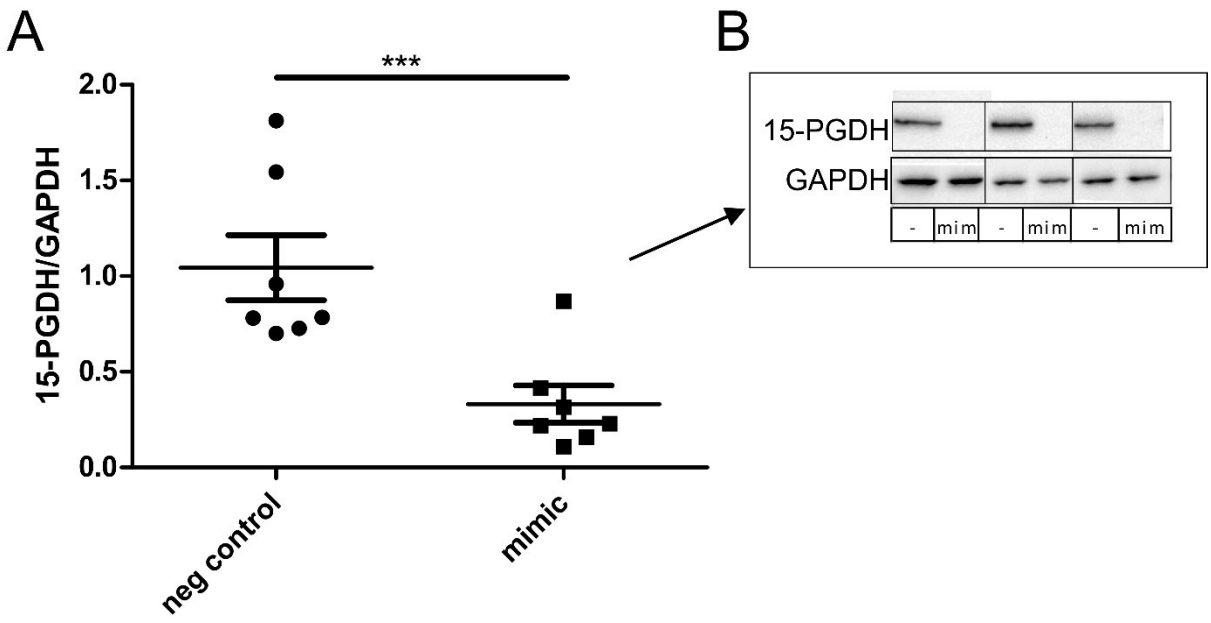

Figure 41. miRNA 26a-5p regulates 15-PGDH in vitro. *(**A**) A549 cells were transfected with a mimic of miRNA 26a-5p or a negative control, harvested after 72h and Western blot was performed. (**B**) shows a representative Western blot. (**A**) Statistical differences were tested by Student's t-test. ***p<0.001*

3.2.15 Inhibition of 15-PGDH increases eicosanoid and decreases collagen secretion in IPF precision-cut lung slices

Since we could observe that, although 15-PGDH is partly upregulated in IPF lungs, there are fibrotic areas that show almost no expression, and these do very likely increase as the disease progresses, we wanted to know whether inhibition of 15-PGDH might still be a valid approach. To this end, we used precision-cut lung slices (PCLS) from IPF lungs of patients who received a donor lung (i.e. representing end stage disease). To our surprise, we observed up to 10-fold increased PGE_2 levels upon addition of the 15-PGDH inhibitor as compared to vehicle treated controls (Figure 42 A). Furthermore, collagen secretion was significantly reduced upon 15-PGDH inhibition (Figure 42 B) and showed an inverse correlation to PGE_2 levels (Figure 42 C). Reduced collagen staining on PCLS was also observed (Figure 43). Mass spectrometry revealed the presence of other prostanoids, some of which also showed a trend towards increased levels after 15-PGDH inhibition (Figure 42 D). Of note, we could not detect specialized pro-resolving mediators (SPM). We also stained PCLS for collagen and found reduced staining, consistent with an anti-fibrotic action of the 15-PGDH inhibitor (Figure 43).

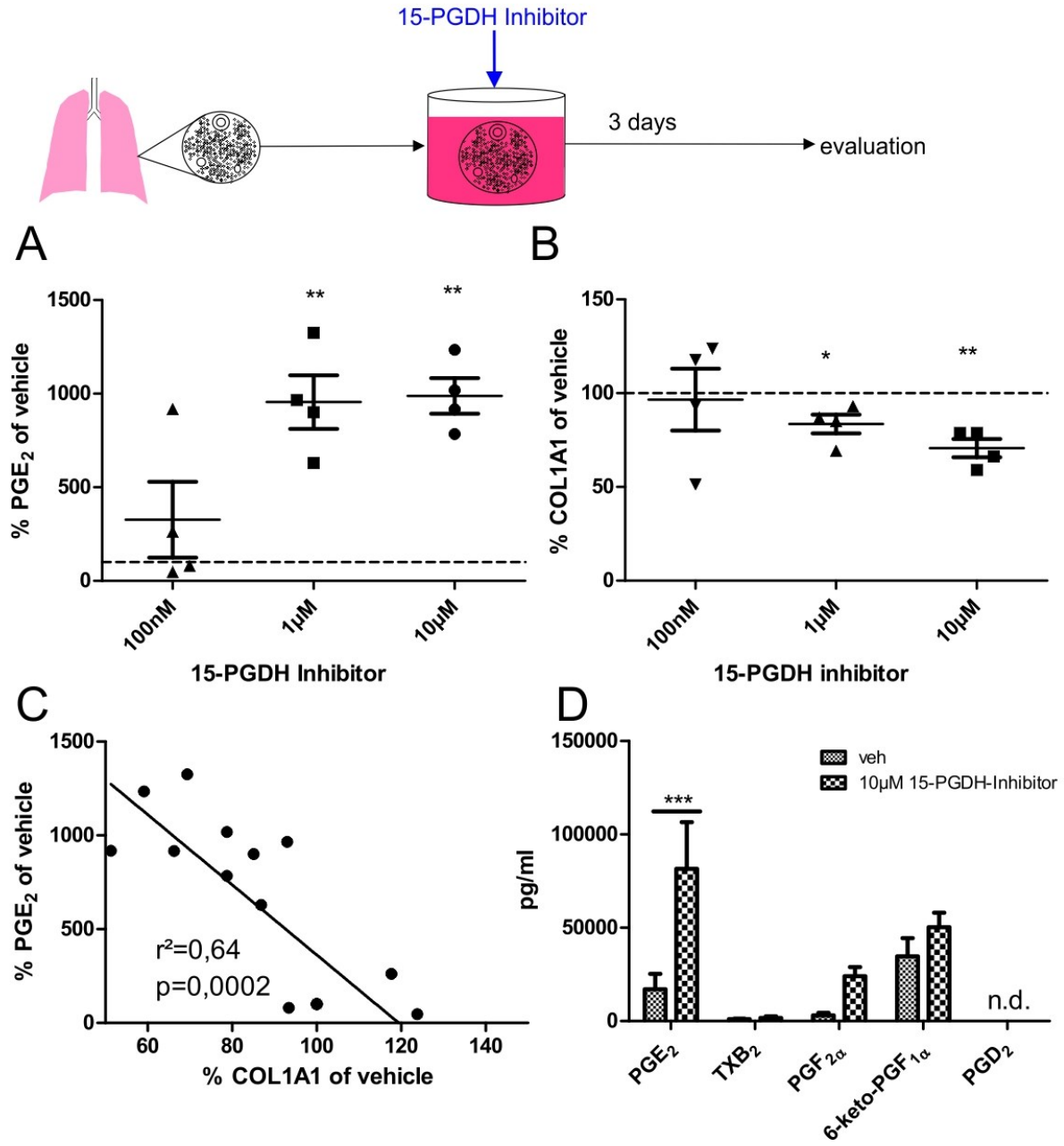

Figure 42. Inhibition of 15-PGDH increases PGE_2 levels and decreases collagen secretion in precision-cut lung slices (PCLS) from patients with IPF. *PCLS from IPF patients were incubated with a 15-PGDH inhibitor (SW033291) at the indicated concentrations for 72 hours, and thereafter (**A**) PGE_2 and (**B**) collagen 1a1 levels were measured in the supernatants. (**C**) Linear regression analysis was performed. (**D**) Eicosanoids were measured by mass spectrometry. For **A** and **B**, a two-tailed one-sample t-test against 100 % was performed while for **D** two-way ANOVA for repeated measurements followed by Bonferoni's post-hoc test was applied. *=p<0.05, **=p<0.01, ***=p<0.001, n.d. not detected*

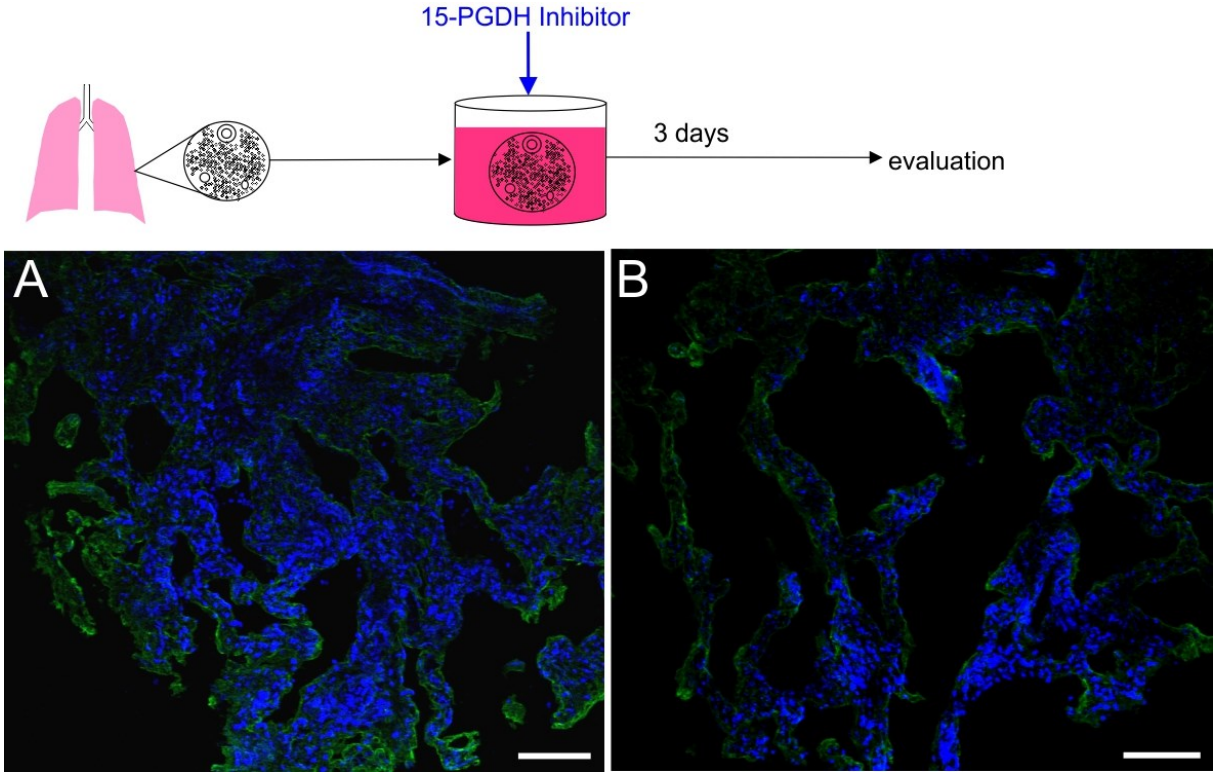

Figure 43. Morphology of vehicle and 15-PGDH inhibitor treated PCLS*. Collagen 1a1 was stained by immunofluorescence on PCLS treated with (**A**) vehicle or (**B**) 15-PGDH inhibitor (SW033291, 10µM), scale bar is 100µm. Photomicrographs are representative for 2 patients.*

4 Discussion

Taken together, we show herein conclusive further evidence for the beneficial role of eicosanoids and, more specifically PGE_2, in the lungs.

The first part of this thesis focused on the production of PGE_2 by alveolar epithelial cells and its influence on neighboring cells. These data expand earlier knowledge, concerning the central role of PGE_2 as a locally acting mediator that influences various lung cells. These include macrophages (253) as well as alveolar epithelial cells in an autocrine manner (102) and, probably most importantly, fibroblasts (165, 215). In a set of experiments we could show that alveolar epithelial cells in mice express COX-2 (18), as has been described also in men (19), although COX-1 was also present. This is of particular interest as our investigations revealed that PGE_2 production by isolated alveolar epithelial cells and in a human cell line primarily depends upon COX-2, as underpinned by the fact that its inhibition via NS398 almost completely abrogated PGE_2 synthesis, similar to a non-selective COX-inhibitor. When we further examined the possibility of COX-2 induction during culture conditions in alveolar epithelial cells, we found that the glucocorticoid dexamethasone did not reduce baseline COX-2 expression, but prevented the LPS-induced increase of both COX-2 protein and PGE_2 levels. This was in contrast to A549 cells, where dexamethasone even reduced baseline COX-2 levels and PGE_2 production. Furthermore, in these cells, we were not able to detect COX-1, as described by others (251). Therefore, our data show that in primary alveolar epithelial cells isolated from adult mice, baseline COX-2 and PGE_2 is only marginally influenced by dexamethasone treatment. This is in stark contrast to the data obtained from fetal rat ATII cells, where dexamethasone was shown to upregulate PGE_2 production (165). Interestingly, in this study, PGE_2 increased lipofibroblast free fatty acid release that resulted in increased SP-C production by alveolar epithelial cells. Thus, this process might represent a specific mechanism that is important in lung maturation (as witnessed by the routine application of corticosteroids to induce SP-C production) which can no longer be observed in adults. Alternatively, differences in culture conditions could be responsible for the observed alterations. While our protocol with 6 days in culture resulted in the formation of ATI-like cells, the shorter duration in the study by Torday et. al. might better preserve the ATII cell phenotype (250). Hence, these data show a complex regulatory role of glucocorticoid signaling on COX-2 and PGE_2, depending upon the exact cell type and probably also developmental stage. However, we do think that the difference between murine ATI-like and human A549 cells in PGE_2 secretion rather reflects the phenotypic characteristics of A549 cells associated with their identity, e.g. A549 being a cancer cell line. Although A549 cells are often used as a surrogate for ATII cells,

they do show discrepancies. For example, it has been described that SP-C production, a hallmark of ATII cells, is quite low in A549 cells (264). In our hands, in contrast to primary cells, these cells produced relatively low levels of PGE_2 and show complete abrogation of PGE_2 synthesis in response to dexamethasone (12). The data presented herein thus urge caution when using A549 cells to model the alveolar epithelium.

In our subsequent experiments on human microvascular endothelial cells, we wanted to investigate whether PGE_2 secreted by alveolar epithelial cells might be responsible for the earlier described barrier enhancing effect of alveolar epithelial cell-conditioned medium (249). We could reproduce the findings that addition of conditioned medium leads to increased barrier function and we could also show that this is blunted by the pre-incubation of epithelial cells with COX-inhibitors. Consistent with our data on PGE_2 synthesis, both the selective COX-2- and the non-selective COX-inhibitor showed similar efficacy. The observation that IP-antagonism did not prevent conditioned medium-induced increases in barrier function was somewhat surprising, as PGI_2 has been shown to increase endothelial barrier function (255, 265) and its metabolite, 6-keto-PGF_{1alpha} was present in the supernatants. Analysis of the effects of a specific agonist revealed only minor increases in barrier function upon IP receptor activation and led us to hypothesize that this receptor might be more relevant in pulmonary artery endothelial cells (255, 265). However, the fact that EP4 receptor-antagonism also prevented the effects of conditioned medium, establishes PGE_2 as the agent that mediates this epithelial-to-endothelial crosstalk. The possible COX-2-dependent synthesis of PGE_2 *in vivo* under physiologic conditions is corroborated by the fact that we also observed COX-2 and COX-1 in alveolar epithelial cells *in situ* in specific-pathogen free mice, where COX-2-inducing subclinical infections are highly unlikely. These data hint towards a remarkable contribution of PGE_2 to the maintenance of pulmonary endothelial barrier function via activation of the EP4 receptor. Indeed, a study using ATII cell-specific COX-2 knockout mice found that their deficiency in PG-synthesis results in a greater influx of inflammatory cells in LPS-induced lung injury. Furthermore, these mice showed exaggerated inflammation as assessed by histopathology, consistent with endothelial barrier dysfunction (256). These findings are similar to preliminary data from our lab that show increased neutrophil influx and edema formation in the LPS model in diclofenac-treated mice (data not shown). Therefore, it seems reasonable to deduce that ATII cell derived PGE_2 protects the pulmonary endothelial barrier from injury, and thus contributes to host protection. This might also be true for its effects on alveolar macrophages, where potent anti-inflammatory effects have also been described (253), suggesting a two-pronged approach. Together with observations from our lab (67), these data add to the recognized beneficial effects of PGE_2 in the lungs (69). Thus, further investigations

into its potential in the treatment of human disease characterized by exaggerated inflammation and loss of endothelial barrier function, such as acute respiratory distress syndrome are warranted.

Subsequently, we wanted to investigate, whether we would be able to increase PGE_2 synthesis by alveolar epithelial cells. We could show that isolated alveolar epithelial cells as well as mouse lungs express 15-PGDH, as has been described (248).Of note, we found slight increases of PGE_2 in alveolar epithelial cells upon treatment with a specific 15-PGDH inhibitor (SW033291) (231). SW033291 has previously been shown to increase PG levels in the lungs, colon, bone marrow and liver. Furthermore it exerted beneficial effects in mouse models of DSS-induced colitis, liver regeneration and stem cell engraftment in bone marrow transplantation and tissue repair in general (231) and increases bone formation (266). These data provided us with the rationale to further investigate the effects of 15-PGDH inhibition and its expression in idiopathic pulmonary fibrosis.

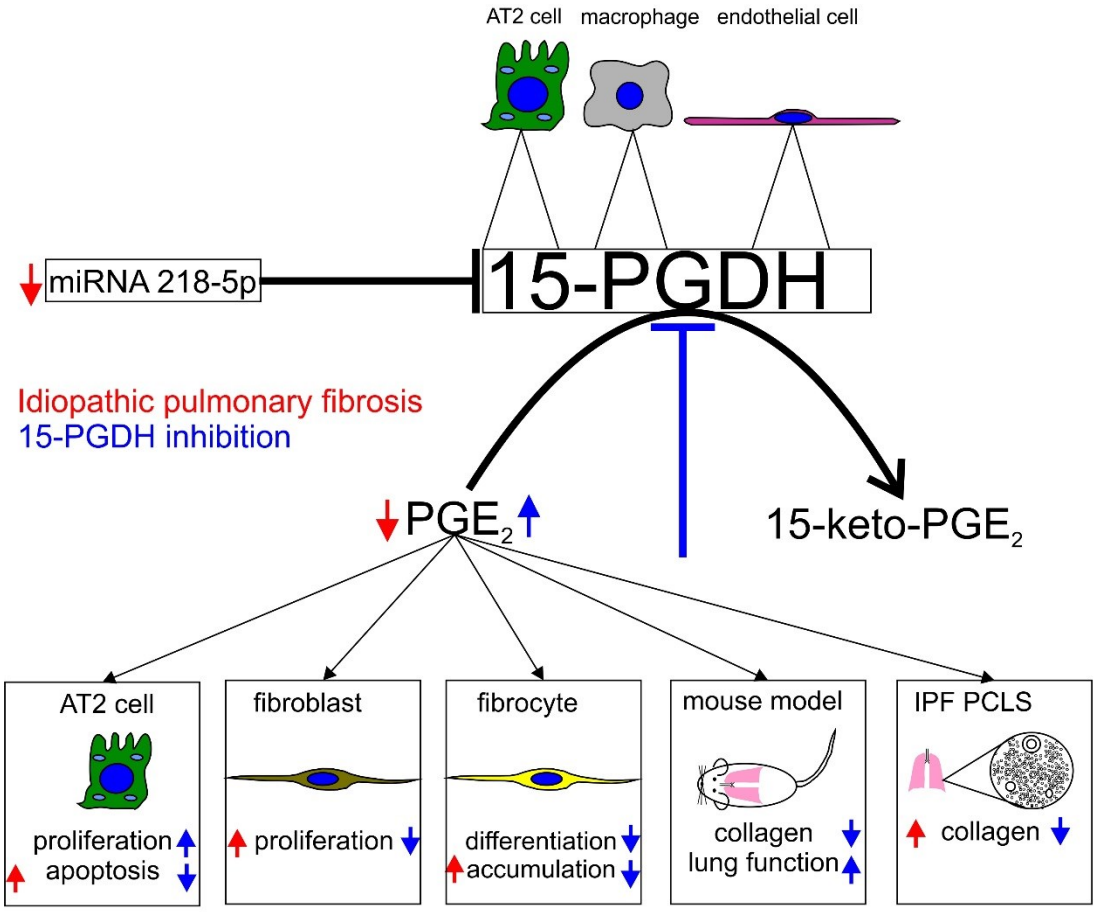

Figure 44. Graphical Abstract.

In the main chapter of this thesis, we could show that 15-PGDH expression in IPF is altered and one likely explanation for this is represented by miRNA-dependent pathways. In both mouse models and human tissue explants, inhibition of 15-PGDH increased PGE_2 levels and reduced hallmarks of pulmonary fibrosis.

When investigating 15-PGDH expression in IPF and human donor lungs, we observed vast discrepancies between the two different readouts we used. When applying a histologic approach (i.e. ISH and IHC) we detected abundant expression of 15-PGDH in biopsies (IHC) and post-explant samples (ISH) from IPF lungs in still intact tissue, predominantly in alveolar walls, that was much more pronounced than in healthy controls. However, areas of pronounced fibrosis and fibroblastic foci showed almost no detectable 15-PGDH in IHC as corroborated by the fact that vimentin expressing cells did not express 15-PGDH mRNA in ISH. When we subsequently measured 15-PGDH activity of lung tissue lysates from healthy controls and IPF patients, we found that there was no difference at all. Although we hypothesized that this variance might be explained by the predominance of fibrotic tissue at later stages, as the lung tissue used for activity assays was from patients receiving lung transplants (i.e. end-stage disease) we could not prove our assumption by histology alone. However, a recent study (267) examined the transcriptome of IPF lungs and compared scarred and non-scarred tissue to healthy lungs. Interestingly, these data support our findings as, in accordance to our results, they found increased levels of 15-PGDH in intact but decreased levels in scarred IPF tissue as compared to healthy controls. Consequently, these findings highlight the long recognized fact that IPF is a highly heterogeneous disease, both in a temporal and spatial context and that this should be taken into account when comparing different readouts. The data concerning the expression patterns of 15-PGDH complement earlier findings that reported diminished COX-2 expression in IPF tissue and fibroblasts (221-223, 268) but pronounced COX-2 staining especially in the metaplastic epithelium covering fibrotic foci and in non-fibrotic areas (19, 229). We therefore hypothesize that the combination of lowered PGE_2 synthesis by IPF fibroblasts and the increased expression of 15-PGDH in intact tissue, predominantly alveolar walls, ultimately leads to the decreased PGE_2 levels that have been reported in the BAL of IPF patients (209). The dynamics of IPF might lead to different priorities of these two factors, depending upon the disease stage: initial increases in 15-PGDH in alveolar walls might at first decrease PGE_2 levels, while later on, the hampered capacity for PGE_2 synthesis by the expanding fibroblasts plays the major role. Of note, the seemingly contradictory results that PGE-MUM is increased (229) while BAL PGE_2 is decreased in IPF patients cannot possibly be caused by decreased synthesis alone. In contrast, our data provide a reasonable explanation wherein increased catabolism of PGE_2,

together with locally increased COX-2 expression (and therefore probably increased PGE_2 formation) leads to the observed findings.

Another pathway for regulating PGE_2 levels, which we did not address in this study, is the trans-membrane-transport of this compound. Interestingly, deletion of SLCO2A1, the transporter that mediates cellular uptake of PGE_2, the step usually thought to precede its inactivation (117), was shown to worsen pulmonary fibrosis in the bleomycin model (248). The mechanisms involved remain unclear, especially as, contrary to prior expectations, deletion led to decreased pulmonary PGE_2 levels. The worsened phenotype was explained by altered distribution of PGE_2 in the lungs, as BAL levels were increased, although later studies failed to reproduce the reduction of PGE_2 in lung homogenates of SLCO2A1 knockout mice and showed increased levels instead (269). Furthermore, no cell membrane-associated expression of MRP4 in pulmonary epithelial cells has been described so far, as would be required for directed transport (270). Therefore, these data in fact hint towards involvement of PGE_2 distribution at least in mouse models, but some inconsistencies remain and the existing knowledge does not support SLCO2A1 inhibition as a valid strategy to increase PGE_2 in IPF.

Of note, we recently described the potent thromboxane-synthase inhibiting properties of imatinib and nilotinib, two BCR-ABL tyrosine kinase inhibitors, used in the treatment of chronic myeloid leukemia, at concentrations that are routinely achieved in patients. This in turn resulted in an increased PGE_2 secretion by immune cells via substrate shift of PGH_2 from TX- to PGE-synthase (230). Interestingly, imatinib also showed great promise in mouse models of pulmonary fibrosis (271), but did not achieve therapeutic effects in humans suffering from IPF (272). One of the reasons for this could be the fact that, in contrast to immune cells, TX-synthesis in IPF lungs is quite low, as observed in PCLS, and further inhibition does not increase the already much higher PGE_2 levels. However, at least some of the beneficial effects of imatinib in the bleomycin model are mediated via tyrosine kinase inhibition, a mechanism shared with nintedanib, albeit the affinity for specific receptors differs (202).

After we found considerable expression of 15-PGDH in human lungs, we further investigated its expression and activity in mouse lungs. Investigations by *in situ* hybridization and activity measurements revealed expression at the mRNA level and functionality of this enzyme. When comparing to either mouse kidneys or human lungs, murine lungs showed the highest activity. However, the discrepancy to human tissue, where activity was lower, might be due to delays in the homogenization process and freeze-thaw steps, both caused by the necessary transport of samples from the transplantation center, rather than true differences in activity. Following these findings, we tested whether 15-PGDH inhibition would prevent the pathological changes

in the bleomycin model. Although this model has been criticized, as it does not exactly recapitulate the pathognomonic features described in IPF, it is still the most widely used model to assess new therapeutic approaches (239). Major differences are represented by the facts that distribution of fibrosis is rather peri-bronchial (as compared to sub-pleural in IPF) and that it is usually self-limiting and fibrosis resolves over time (as compared to the chronic progressive disease in humans). However, both antifibrotic drugs, nintedanib and pirfenidone that are used for the treatment of IPF patients, show potent effects in the bleomycin model. We found a variety of beneficial effects of 15-PGDH inhibition in the protective model; the 15-PGDH inhibitor did not only prevent weight loss in response to bleomycin, but also reduced mortality and, most importantly, protected from fibrosis as assessed by histologic and biochemical readouts. Many of these effects have already been published for PGE_2 (211, 213, 268, 273) and were thus conclusive with the fact that PGE_2 in the lungs was increased by the inhibitor treatment in bleomycin treated mice. Besides these assays, we also wanted to investigate on which cells are involved in these effects. The conceptual framework for these investigations was the so-called apoptosis paradox, referring to the increased epithelial and decreased fibroblast apoptosis/increased fibroblast proliferation that is considered one of the driving factors in IPF. Importantly, PGE_2 has been implicated as a mediator that could counteract these processes by exerting differential effects on fibroblasts and alveolar epithelial cells, thereby restoring physiologic conditions (102). However, while *in vitro* data show inhibition of fibroblast proliferation and ATII cell apoptosis by PGE_2 (18, 102), to the best of our knowledge, the presence of these effects in the bleomycin model has not been investigated so far. By co-staining cell markers for fibroblasts or ATII cells with those for proliferation or apoptosis, we indeed unraveled a regulation of these parameters by 15-PGDH inhibitor treatment. We found a pronounced decrease in apoptotic ATII cells and proliferating fibroblasts in the bleomycin-mice receiving 15-PGDH inhibitor treatment. Especially ATII cell apoptosis was almost reversed to vehicle levels. Interestingly, ATII cell proliferation was slightly increased by bleomycin alone, but further increased by blocking 15-PGDH. Beneficial effects of increased ATII cell proliferation were revealed by studies using keratinocyte growth factor (258). Thus, we could show that blocking of 15-PGDH reverts the bleomycin induced pro-fibrotic changes in fibroblast and alveolar epithelial cell apoptosis/proliferation. As these alterations are deemed the hallmarks and driving forces of disease-progression in IPF (274), the potential of a single compound that acts on both of them can hardly be overstated. This is in line with earlier work, as targeting both epithelial cells and fibroblasts has been considered crucial for the effective treatment of IPF (204). However, current drugs are focused predominantly on suppression of

fibroblasts, and considerations concerning the long term safety of this one-sided approach have arisen (142).

Interestingly, we were not able to assess the effect of 15-PGDH inhibition on lung fibroblasts, as - contrary to earlier reports (262) – neither primary lung fibroblasts form IPF patients and donors nor MRC5 cells did express this enzyme. This is in accordance with the data from ISH experiments where we detected negligible co-localization of vimentin and 15-PGDH mRNA. Consistent with these results, addition of the 15-PGDH inhibitor did not cause any observable changes in TGFβ1-induced myofibroblast formation. Furthermore, TGFβ1 treatment did not result in increased 15-PGDH expression in primary lung fibroblasts as has been described for A549 cells, as neither mRNA nor protein could be detected (225). In contrast, PGE_2 itself was described to exert multiple suppressing effects on fibroblasts, including the reversion of a myofibroblast phenotype (170). These disappointing *in vitro* results in the presence of such potent *in vivo* effects highlight the importance of *in vivo* testing for specific problems that involve complex paracrine processes which are still not completely understood.

A somewhat unexpected finding was the revelation that 15-PGDH inhibitor-treated mice show pronounced inhibition of bleomycin-induced pulmonary fibrocyte accumulation. Although EP receptor expression on this cell type has been described (261), to the best of our knowledge, no effect of PGE_2 has been shown on these cells so far. In subsequent experiments, we found a pronounced inhibition of fibrocyte differentiation from healthy human peripheral blood mononuclear cells by PGE_2, with almost complete suppression at a concentration of 100 nM. These results are similar to that observed for nintedanib and pirfenidone, which were used as positive controls. Further investigations showed that this effect was mediated via EP2 and EP4 receptors. As EP2 receptor signaling was shown to be impaired in IPF fibroblasts (216) we obtained blood from IPF patients and therein investigated again the impact of PGE_2 on fibrocyte differentiation. We found that PGE_2 was still able to suppress fibrocyte differentiation with similar potency as observed in healthy donors and this was probably independent from the treatment that IPF patients received. By using ISH, we could show that cells with the phenotypic characteristics of fibrocytes express EP2 and EP4 receptors but not 15-PGDH in both healthy donors and IPF patients. Together with the fact that also already differentiated fibrocytes were reduced by PGE_2 treatment, these data provide a further rational for the use of EP-receptor agonists in IPF.

The fact that we could not find increased fibrocyte differentiation in IPF patients as compared to healthy donors might seem surprising at first but could be caused by multiple factors. First, our study was not designed to detect such differences but only wanted to assess the potential

of PGE_2 to act on fibrocytes also in patients. Thus, healthy donors were chosen randomly from a donor pool, mainly composed of students (20-25 years old) and these were not matched in any way to the much older (mean age 74.5 ± 10.4) and predominantly male (7:2) IPF patients. As fibrocytes have been implicated in wound healing under physiologic conditions, the slightly increased levels of differentiation in the donors might simply be reflective of the higher regenerative capacity of younger individuals (275).

In order to further strengthen our investigations, we decided to assess 15-PGDH inhibition in a different model of bleomycin-induced pulmonary fibrosis. As described above, the early phase of this model until day 9 is primarily characterized by acute and ongoing inflammation. This results in the fact that some anti-inflammatory treatments lead to prevention of fibrosis if given early enough, but do neither reduce fibrosis once established nor are beneficial in patients (276). In contrast, antifibrotics, such as pirfenidone that are used for the treatment of IPF also exert beneficial functions in established fibrosis (271, 277). This is especially relevant for strategies that interfere with eicosanoid signaling, such as PGE_2, as we and others have described potent anti-inflammatory effects of PGE_2 in the lungs (69, 278). However, also in the therapeutic approach, we found considerable amelioration of bleomycin-induced pulmonary fibrosis in 15-PGDH inhibitor-treated mice. Although we did not reassess in depth the effects on fibroblast and ATII cell proliferation/apoptosis, we found an abrogation of the bleomycin effects on COL1A1 and SFTPC levels at the mRNA level, consistent with findings in the preventive model. Earlier reports describe improvements in methacholine-induced hyperresponsiveness in global 15-PGDH knock out (KO) mice (121). As decreased lung function and ultimately respiratory failure are the most clinically relevant manifestations of IPF, the abrogation of the detrimental bleomycin-induced changes on respiratory parameters by 15-PGDH inhibition further strengthens the feasibility of this therapeutic approach.

One finding in our mouse model differs from earlier reports. A study comparing the aforementioned 15-PGDH-KO mice with wild type mice found no effect on static compliance, tissue elastance and septal thickening in bleomycin-induced lung fibrosis (89). An important caveat in the interpretation of data from KO mice is the vast discrepancy of findings concerning the genetic alteration of prostaglandin biosynthesis. For example, whereas some studies found considerable pro-fibrotic effects in COX-2-KO mice (89), others report merely effects on lung function but not fibrosis (279) while another even shows increased levels of PGE_2 and no effect on fibrosis (280). Similar concerns are true for the receptors involved, where different groups came to partly contradictory conclusions. These include findings showing contribution of FP, but not IP, DP or EP receptors (101), while another study describes effects of IP but not EP

receptors (89) and others report involvement of DP receptors (80) in the bleomycin mouse model. This is further complicated by the fact that pharmacologic inhibition of COX (281) or agonism at PG-receptors yield partly opposing results, with clear beneficial roles for PGI_2 (217, 282), PGE_2 (211-213, 268) and some evidence for a role of PGD_2 (283). One likely explanation for this discrepancy could be that compensatory mechanisms are activated by deletion of a single gene, as has been shown for PGE_2 levels in COX-2-KO mice (256, 280) and a recent report asked for cautious interpretation of data from genetically modified mice (239). However, our data clearly demonstrate that pharmacologic inhibition of 15-PGDH is beneficial in a therapeutic model in mice which is in accordance with the limited data on post treatment with a non 15-PGDH-degradable PGE_2 analogue (212) and that inhibition of 15-PGDH also ameliorates lung function and reduces hydroxyproline content, the gold standard of fibrosis evaluation (239).

In addition to the data already obtained, we wanted to assess the mechanisms that might govern 15-PGDH expression. A recent publication described profound suppressing effects of a microRNA, miRNA 218-5p on the levels of 15-PGDH protein and subsequent PGE_2 catabolism in synovial mesenchymal stem cells (228). The fact that miRNA 218-5p is decreased in IPF lungs (226) made it an interesting target for further investigations, as we hypothesized that the subsequent lack of 15-PGDH mRNA inhibition might contribute to increased 15-PGDH levels. We could indeed observe a regulatory role of a specific inhibitor and mimic of this miRNA in A549 cells. However, with regard to the above mentioned differences of A549 cells to normal alveolar epithelial cells, especially concerning prostanoid synthesis, we wanted to confirm our data in a more relevant model. Although the binding site for miRNA 218-5p in the 15-PGDH 3' untranslated region shows a slightly different sequence in mice (thereby reducing likelihood of binding) (263), we could observe a reduction in pulmonary 15-PGDH levels upon intratracheal transfection with the miRNA mimic. Interestingly, TGFβ1 stimulation has been shown to both increase 15-PGDH levels (225) and decrease miRNA 218-5p in A549 cells (284). Thus, together with these observations, our data suggest that 15-PGDH expression is regulated by miRNA 218-5p. Interestingly, both decreased miRNA-218-5p and increased 15-PGDH expression have been associated with a downregulation of epithelial, and upregulation of mesenchymal, markers (284, 285), features that are hypothesized to play a role in IPF, although probably not as epithelial to mesenchymal transition *sensu stricto* (181, 286). Of note, miRNA 26a-5p has been shown to have beneficial effects in the bleomycin model and is downregulated in IPF (287). Also, miRNA 26a-5p was identified as a potential regulator of 15-PGDH as was confirmed in A549 cells. Taken together, these data provide further evidence for the dysregulation of 15-PGDH under fibrotic conditions

in the lung and unravel a novel mechanism in this context. Anyhow, further studies assessing the therapeutic effect of miRNA-218-5p mimics on bleomycin induced fibrosis are warranted. However, the fact that miRNAs show incredible versatility and thus possibly influence thousands of mRNAs due to their short binding sequence might complicate future investigations.

As overall levels of 15-PGDH showed a tendency to decrease in end-stage IPF lungs, as suggested by histology and activity assays and confirmed by transcriptomics (267) we wanted to investigate PCLS from explant IPF lungs. The fact that also in these lungs inhibition of 15-PGDH caused increases in eicosanoids and decreases in collagen secretion show that this approach is a valid therapeutic strategy even when intact tissue, harboring the areas of increased 15-PGDH expression, is almost gone. The finding that PGE_2 and collagen levels are inversely correlated in the supernatants is consistent with, but not proof of a suppressing effect of PGE_2 on collagen secretion as has been described in fibroblasts (288). Mass spectrometry analysis of the supernatants revealed a trend towards increased PGF_{2alpha} levels, as 15-PGDH is also a katabolic enzyme for this prostanoid, even though with nearly tripled K_m and lower V_{max} (109). PGF_{2alpha} has been shown to exert detrimental effects in IPF and the bleomycine model (101). In our study we found that its levels were much lower than PGE_2 and far below the stimulatory concentration required for increased collagen transcription (101). Furthermore, collagen synthesis was decreased in PCLS in response to 15-PGDH inhibition and not increased. These facts hint towards negligible effects of PGF_{2alpha} in our PCLS model. Furthermore, later observations found even decreased PGF_{2alpha} levels after bleomycin treatment, casting some doubt on the relevance of these findings (248). However, a combination of an antagonist for the FP receptor and a 15-PGDH inhibitor might represent an even better therapeutic option. Further, 6-keto-PGF_{1alpha}, the stable metabolite of PGI_2, showed a trend towards an increase upon 15-PGDH inhibition, also in line with earlier observation (112) and was present at the highest concentrations at baseline conditions. This is of special interest in the light of recent findings that describe beneficial effects of IP receptor-agonism in IPF (88). Finally, the surprising fact that no detectable levels of specialized pro-resolving mediators were present in PCLS supernatants, although LXA_4 is a substrate of 15-PGDH (289), is probably best explained by the transcellular pathway of lipoxin synthesis that usually involves peripheral blood cells such as neutrophils and platelets (290, 291). However, most platelets and neutrophils would be expected to be flushed out during the washing steps in PCLS preparation. In addition, neutrophils undergo rapid apoptosis if no further stimuli are present and would accordingly not be expected to survive during further culture (292). Furthermore, only very low levels of these mediators are present without additional stimuli (e.g. LPS) (293). Last, although

alveolar macrophages are known to produce LXs (293) these cells might also be removed during the necessary washing steps and percentages of these cells are lower in IPF BAL (294).

One important caveat in our studies might be the pro-carcinogenic effect of 15-PGDH inhibition. However, although there is evidence of decreased 15-PGDH in multiple human cancer types (122, 127-129), there is not a single documented case of unusual cancer manifestations in humans with a 15-PGDH loss of function mutation. While these mutations are not very common and it might be argued that n-numbers are too low, alterations in SLCO2A1, which are equally rare, are associated with a highly increased risk of gastrointestinal adenomas (132, 133). Furthermore, other consistent phenotypic changes, except PHO and digital clubbing have not been described in 15-PGDH mutations. Nevertheless, it can be difficult to infer the effects of pharmacological treatments from knock-out phenotypes as has also been shown in this study. Moreover, even if 15-PGDH inhibitor treatment might lead to an increased risk for colon carcinoma, these tumors can often be detected early on by colonoscopy (295). In addition, these tumors are thought to take a decade or more to arise (295), and current median survival in IPF is at about 3.8 years (141). Other side effects of 15-PGDH inhibition could be related to pregnancy and reproduction but are highly unlikely to play a role in the treatment of IPF as this affects predominantly males and is rare in people less than 50 years old (146). Furthermore, there might be effects on blood pressure, as also the PGI_2 metabolite 6-keto-PGF_{1alpha} was slightly increased and PGE_2 itself acts vasodilatory in some vascular beds (48). However, PGI_2 is hydrolyzed to its much less active metabolite in a non-enzymatic manner (84) and we did not observe hypotension in our mouse experiments, which is in stark contrast to EP4 agonists (296).

In conclusion, our data show pronounced beneficial effects of 15-PGDH inhibition in pulmonary fibrosis models in mice and human IPF tissue. Not only could we demonstrate an amelioration of biochemical (hydroxyproline content) and functional (lung function) readouts in the bleomycin model upon inhibitor treatment, but we could also provide evidence of a restoration of physiological homeostasis on a cellular level. Besides the reduction of fibrocyte accumulation, 15-PGDH inhibition governs opposing effects on fibroblast proliferation and alveolar epithelial cell apoptosis, resulting in disruption of the fibrotic *circulus vitiosus*. Together with the alterations in 15-PGDH expression observed in IPF, these data provide considerable evidence for a causal involvement of this enzyme in disease-associated reductions of PGE_2 levels. We therefore suggest 15-PGDH as a therapeutic target in IPF, a condition that still has limited therapeutic options and high mortality.

5 References

1. Goldblatt MW. Properties of human seminal plasma. J Physiol. 1935;84(2):208-18.

2. von Euler US. On the specific vaso-dilating and plain muscle stimulating substances from accessory genital glands in man and certain animals (prostaglandin and vesiglandin). J Physiol. 1936;88(2):213-34.

3. Hamberg M, Svensson J, Samuelsson B. Thromboxanes: a new group of biologically active compounds derived from prostaglandin endoperoxides. Proc Natl Acad Sci U S A. 1975;72(8):2994-8.

4. Raz A, Minkes MS, Needleman P. Endoperoxides and thromboxanes. Structural determinants for platelet aggregation and vasoconstriction. Biochim Biophys Acta. 1977;488(2):305-11.

5. Levin G, Duffin KL, Obukowicz MG, Hummert SL, Fujiwara H, Needleman P, et al. Differential metabolism of dihomo-gamma-linolenic acid and arachidonic acid by cyclo-oxygenase-1 and cyclo-oxygenase-2: implications for cellular synthesis of prostaglandin E1 and prostaglandin E2. Biochem J. 2002;365(Pt 2):489-96.

6. Hla T, Bishop-Bailey D, Liu CH, Schaefers HJ, Trifan OC. Cyclooxygenase-1 and -2 isoenzymes. Int J Biochem Cell Biol. 1999;31(5):551-7.

7. Goodman LS, Gilman A, Brunton LL. Goodman & Gilman's the pharmacological basis of therapeutics. 11. ed. New York: McGraw-Hill; 2006. 2021 s. p.

8. Smith WL, DeWitt DL, Garavito RM. Cyclooxygenases: structural, cellular, and molecular biology. Annu Rev Biochem. 2000;69:145-82.

9. Kozak KR, Prusakiewicz JJ, Marnett LJ. Oxidative metabolism of endocannabinoids by COX-2. Curr Pharm Des. 2004;10(6):659-67.

10. Simmons DL, Botting RM, Hla T. Cyclooxygenase isozymes: the biology of prostaglandin synthesis and inhibition. Pharmacol Rev. 2004;56(3):387-437.

11. Diaz A, Chepenik KP, Korn JH, Reginato AM, Jimenez SA. Differential regulation of cyclooxygenases 1 and 2 by interleukin-1 beta, tumor necrosis factor-alpha, and transforming growth factor-beta 1 in human lung fibroblasts. Exp Cell Res. 1998;241(1):222-9.

12. Barnthaler T, Maric J, Platzer W, Konya V, Theiler A, Hasenohrl C, et al. The Role of PGE2 in Alveolar Epithelial and Lung Microvascular Endothelial Crosstalk. Sci Rep. 2017;7(1):7923.

13. Harris RC. COX-2 and the kidney. J Cardiovasc Pharmacol. 2006;47 Suppl 1:S37-42.

14. Zidar N, Odar K, Glavac D, Jerse M, Zupanc T, Stajer D. Cyclooxygenase in normal human tissues--is COX-1 really a constitutive isoform, and COX-2 an inducible isoform? J Cell Mol Med. 2009;13(9B):3753-63.

15. Warner TD, Giuliano F, Vojnovic I, Bukasa A, Mitchell JA, Vane JR. Nonsteroid drug selectivities for cyclo-oxygenase-1 rather than cyclo-oxygenase-2 are associated with human gastrointestinal toxicity: a full in vitro analysis. Proc Natl Acad Sci U S A. 1999;96(13):7563-8.

16. Bresalier RS, Sandler RS, Quan H, Bolognese JA, Oxenius B, Horgan K, et al. Cardiovascular events associated with rofecoxib in a colorectal adenoma chemoprevention trial. N Engl J Med. 2005;352(11):1092-102.

17. Gierse JK, McDonald JJ, Hauser SD, Rangwala SH, Koboldt CM, Seibert K. A single amino acid difference between cyclooxygenase-1 (COX-1) and -2 (COX-2) reverses the selectivity of COX-2 specific inhibitors. J Biol Chem. 1996;271(26):15810-4.

18. Lama V, Moore BB, Christensen P, Toews GB, Peters-Golden M. Prostaglandin E2 synthesis and suppression of fibroblast proliferation by alveolar epithelial cells is cyclooxygenase-2-dependent. American journal of respiratory cell and molecular biology. 2002;27(6):752-8.

19. Lappi-Blanco E, Kaarteenaho-Wiik R, Maasilta PK, Anttila S, Paakko P, Wolff HJ. COX-2 is widely expressed in metaplastic epithelium in pulmonary fibrous disorders. Am J Clin Pathol. 2006;126(5):717-24.

20. Ozaki T, Rennard SI, Crystal RG. Cyclooxygenase metabolites are compartmentalized in the human lower respiratory tract. J Appl Physiol (1985). 1987;62(1):219-22.

21. Vane JR, Botting RM. The mechanism of action of aspirin. Thromb Res. 2003;110(5-6):255-8.

22. Vane JR. Inhibition of prostaglandin synthesis as a mechanism of action for aspirin-like drugs. Nat New Biol. 1971;231(25):232-5.

23. Hara S. Prostaglandin terminal synthases as novel therapeutic targets. Proc Jpn Acad Ser B Phys Biol Sci. 2017;93(9):703-23.

24. Choi SH, Langenbach R, Bosetti F. Cyclooxygenase-1 and -2 enzymes differentially regulate the brain upstream NF-kappa B pathway and downstream enzymes involved in prostaglandin biosynthesis. J Neurochem. 2006;98(3):801-11.

25. Smith WL, Urade Y, Jakobsson PJ. Enzymes of the cyclooxygenase pathways of prostanoid biosynthesis. Chem Rev. 2011;111(10):5821-65.

26. Alzamil HA, Pawade J, Fortier MA, Bernal AL. Expression of the prostaglandin F synthase AKR1B1 and the prostaglandin transporter SLCO2A1 in human fetal membranes in relation to spontaneous term and preterm labor. Front Physiol. 2014;5:272.

27. Lovgren AK, Kovarova M, Koller BH. cPGES/p23 is required for glucocorticoid receptor function and embryonic growth but not prostaglandin E2 synthesis. Mol Cell Biol. 2007;27(12):4416-30.

28. Jania LA, Chandrasekharan S, Backlund MG, Foley NA, Snouwaert J, Wang IM, et al. Microsomal prostaglandin E synthase-2 is not essential for in vivo prostaglandin E2 biosynthesis. Prostaglandins Other Lipid Mediat. 2009;88(3-4):73-81.

29. Church RJ, Jania LA, Koller BH. Prostaglandin E(2) produced by the lung augments the effector phase of allergic inflammation. J Immunol. 2012;188(8):4093-102.

30. Baragatti B, Sodini D, Uematsu S, Coceani F. Role of microsomal prostaglandin E synthase-1 (mPGES1)-derived PGE2 in patency of the ductus arteriosus in the mouse. Pediatr Res. 2008;64(5):523-7.

31. Baroody RA, Bito LZ. The impermeability of the basic cell membrane to thromboxane-B2' prostacyclin and 6-keto-PGF 1 alpha. Prostaglandins. 1981;21(1):133-42.

32. Johnson MC, Saunders L. Physical studies of aqueous solutions of two prostaglandins. Biochim Biophys Acta. 1970;218(3):543-5.

33. Reid G, Wielinga P, Zelcer N, van der Heijden I, Kuil A, de Haas M, et al. The human multidrug resistance protein MRP4 functions as a prostaglandin efflux transporter and is inhibited by nonsteroidal antiinflammatory drugs. Proc Natl Acad Sci U S A. 2003;100(16):9244-9.

34. Russel FG, Koenderink JB, Masereeuw R. Multidrug resistance protein 4 (MRP4/ABCC4): a versatile efflux transporter for drugs and signalling molecules. Trends Pharmacol Sci. 2008;29(4):200-7.

35. Kochel TJ, Reader JC, Ma X, Kundu N, Fulton AM. Multiple drug resistance-associated protein (MRP4) exports prostaglandin E2 (PGE2) and contributes to metastasis in basal/triple negative breast cancer. Oncotarget. 2017;8(4):6540-54.

36. Furugen A, Yamaguchi H, Tanaka N, Shiida N, Ogura J, Kobayashi M, et al. Contribution of multidrug resistance-associated proteins (MRPs) to the release of prostanoids from A549 cells. Prostaglandins Other Lipid Mediat. 2013;106:37-44.

37. Hilger D, Masureel M, Kobilka BK. Structure and dynamics of GPCR signaling complexes. Nat Struct Mol Biol. 2018;25(1):4-12.

38. Hanlon CD, Andrew DJ. Outside-in signaling--a brief review of GPCR signaling with a focus on the Drosophila GPCR family. J Cell Sci. 2015;128(19):3533-42.

39. Wettschureck N, Offermanns S. Mammalian G proteins and their cell type specific functions. Physiol Rev. 2005;85(4):1159-204.

40. Stock JL, Shinjo K, Burkhardt J, Roach M, Taniguchi K, Ishikawa T, et al. The prostaglandin E2 EP1 receptor mediates pain perception and regulates blood pressure. J Clin Invest. 2001;107(3):325-31.

41. Katoh H, Watabe A, Sugimoto Y, Ichikawa A, Negishi M. Characterization of the signal transduction of prostaglandin E receptor EP1 subtype in cDNA-transfected Chinese hamster ovary cells. Biochim Biophys Acta. 1995;1244(1):41-8.

42. Norel X, de Montpreville V, Brink C. Vasoconstriction induced by activation of EP1 and EP3 receptors in human lung: effects of ONO-AE-248, ONO-DI-004, ONO-8711 or ONO-8713. Prostaglandins Other Lipid Mediat. 2004;74(1-4):101-12.

43. Morsy MA, Isohama Y, Miyata T. Prostaglandin E(2) increases surfactant secretion via the EP(1) receptor in rat alveolar type II cells. Eur J Pharmacol. 2001;426(1-2):21-4.

44. Savla U, Appel HJ, Sporn PH, Waters CM. Prostaglandin E(2) regulates wound closure in airway epithelium. Am J Physiol Lung Cell Mol Physiol. 2001;280(3):L421-31.

45. Fujino H, West KA, Regan JW. Phosphorylation of glycogen synthase kinase-3 and stimulation of T-cell factor signaling following activation of EP2 and EP4 prostanoid receptors by prostaglandin E2. J Biol Chem. 2002;277(4):2614-9.

46. Regan JW. EP2 and EP4 prostanoid receptor signaling. Life Sci. 2003;74(2-3):143-53.

47. Chun KS, Lao HC, Trempus CS, Okada M, Langenbach R. The prostaglandin receptor EP2 activates multiple signaling pathways and beta-arrestin1 complex formation during mouse skin papilloma development. Carcinogenesis. 2009;30(9):1620-7.

48. Kennedy CR, Zhang Y, Brandon S, Guan Y, Coffee K, Funk CD, et al. Salt-sensitive hypertension and reduced fertility in mice lacking the prostaglandin EP2 receptor. Nat Med. 1999;5(2):217-20.

49. Nataraj C, Thomas DW, Tilley SL, Nguyen MT, Mannon R, Koller BH, et al. Receptors for prostaglandin E(2) that regulate cellular immune responses in the mouse. J Clin Invest. 2001;108(8):1229-35.

50. Kay LJ, Gilbert M, Pullen N, Skerratt S, Farrington J, Seward EP, et al. Characterization of the EP receptor subtype that mediates the inhibitory effects of prostaglandin E2 on IgE-dependent secretion from human lung mast cells. Clin Exp Allergy. 2013;43(7):741-51.

51. Kolodsick JE, Peters-Golden M, Larios J, Toews GB, Thannickal VJ, Moore BB. Prostaglandin E2 inhibits fibroblast to myofibroblast transition via E. prostanoid receptor 2 signaling and cyclic adenosine monophosphate elevation. Am J Respir Cell Mol Biol. 2003;29(5):537-44.

52. White ES, Atrasz RG, Dickie EG, Aronoff DM, Stambolic V, Mak TW, et al. Prostaglandin E(2) inhibits fibroblast migration by E-prostanoid 2 receptor-mediated increase in PTEN activity. Am J Respir Cell Mol Biol. 2005;32(2):135-41.

53. Sheller JR, Mitchell D, Meyrick B, Oates J, Breyer R. EP(2) receptor mediates bronchodilation by PGE(2) in mice. J Appl Physiol (1985). 2000;88(6):2214-8.

54. Buckley J, Birrell MA, Maher SA, Nials AT, Clarke DL, Belvisi MG. EP4 receptor as a new target for bronchodilator therapy. Thorax. 2011;66(12):1029-35.

55. Philipose S, Konya V, Sreckovic I, Marsche G, Lippe IT, Peskar BA, et al. The prostaglandin E2 receptor EP4 is expressed by human platelets and potently inhibits platelet aggregation and thrombus formation. Arterioscler Thromb Vasc Biol. 2010;30(12):2416-23.

56. Yamaoka K, Yano A, Kuroiwa K, Morimoto K, Inazumi T, Hatae N, et al. Prostaglandin EP3 receptor superactivates adenylyl cyclase via the Gq/PLC/Ca2+ pathway in a lipid raft-dependent manner. Biochem Biophys Res Commun. 2009;389(4):678-82.

57. Hatae N, Sugimoto Y, Ichikawa A. Prostaglandin receptors: advances in the study of EP3 receptor signaling. J Biochem. 2002;131(6):781-4.

58. Ichikawa A, Negishi M, Hasegawa H. Three isoforms of the prostaglandin E receptor EP3 subtype different in agonist-independent constitutive Gi activity and agonist-dependent Gs activity. Adv Exp Med Biol. 1997;433:239-42.

59. Ichikawa A, Sugimoto Y, Tanaka S. Molecular biology of histidine decarboxylase and prostaglandin receptors. Proc Jpn Acad Ser B Phys Biol Sci. 2010;86(8):848-66.

60. Negishi M, Sugimoto Y, Irie A, Narumiya S, Ichikawa A. Two isoforms of prostaglandin E receptor EP3 subtype. Different COOH-terminal domains determine sensitivity to agonist-induced desensitization. J Biol Chem. 1993;268(13):9517-21.

61. Kunikata T, Yamane H, Segi E, Matsuoka T, Sugimoto Y, Tanaka S, et al. Suppression of allergic inflammation by the prostaglandin E receptor subtype EP3. Nat Immunol. 2005;6(5):524-31.

62. Maher SA, Birrell MA, Belvisi MG. Prostaglandin E2 mediates cough via the EP3 receptor: implications for future disease therapy. Am J Respir Crit Care Med. 2009;180(10):923-8.

63. Yokoyama U, Iwatsubo K, Umemura M, Fujita T, Ishikawa Y. The prostanoid EP4 receptor and its signaling pathway. Pharmacol Rev. 2013;65(3):1010-52.

64. Konya V, Marsche G, Schuligoi R, Heinemann A. E-type prostanoid receptor 4 (EP4) in disease and therapy. Pharmacol Ther. 2013;138(3):485-502.

65. Fujino H, Regan JW. EP(4) prostanoid receptor coupling to a pertussis toxin-sensitive inhibitory G protein. Mol Pharmacol. 2006;69(1):5-10.

66. Luschnig-Schratl P, Sturm EM, Konya V, Philipose S, Marsche G, Frohlich E, et al. EP4 receptor stimulation down-regulates human eosinophil function. Cell Mol Life Sci. 2011;68(21):3573-87.

67. Konya V, Maric J, Jandl K, Luschnig P, Aringer I, Lanz I, et al. Activation of EP receptors prevents endotoxin-induced neutrophil infiltration into the airways and enhances microvascular barrier function. Br J Pharmacol. 2015;172(18).

68. Huang SK, White ES, Wettlaufer SH, Grifka H, Hogaboam CM, Thannickal VJ, et al. Prostaglandin E(2) induces fibroblast apoptosis by modulating multiple survival pathways. FASEB J. 2009;23(12):4317-26.

69. Vancheri C, Mastruzzo C, Sortino MA, Crimi N. The lung as a privileged site for the beneficial actions of PGE2. Trends Immunol. 2004;25(1):40-6.

70. Hashemi Goradel N, Najafi M, Salehi E, Farhood B, Mortezaee K. Cyclooxygenase-2 in cancer: A review. J Cell Physiol. 2019;234(5):5683-99.

71. Pannunzio A, Coluccia M. Cyclooxygenase-1 (COX-1) and COX-1 Inhibitors in Cancer: A Review of Oncology and Medicinal Chemistry Literature. Pharmaceuticals (Basel). 2018;11(4).

72. Peinhaupt M, Roula D, Theiler A, Sedej M, Schicho R, Marsche G, et al. DP1 receptor signaling prevents the onset of intrinsic apoptosis in eosinophils and functions as a transcriptional modulator. J Leukoc Biol. 2018;104(1):159-71.

73. Cheng K, Wu TJ, Wu KK, Sturino C, Metters K, Gottesdiener K, et al. Antagonism of the prostaglandin D2 receptor 1 suppresses nicotinic acid-induced vasodilation in mice and humans. Proc Natl Acad Sci U S A. 2006;103(17):6682-7.

74. Jandl K, Stacher E, Balint Z, Sturm EM, Maric J, Peinhaupt M, et al. Activated prostaglandin D2 receptors on macrophages enhance neutrophil recruitment into the lung. J Allergy Clin Immunol. 2016;137(3):833-43.

75. Maher SA, Birrell MA, Adcock JJ, Wortley MA, Dubuis ED, Bonvini SJ, et al. Prostaglandin D2 and the role of the DP1, DP2 and TP receptors in the control of airway reflex events. Eur Respir J. 2015;45(4):1108-18.

76. Kostenis E, Ulven T. Emerging roles of DP and CRTH2 in allergic inflammation. Trends Mol Med. 2006;12(4):148-58.

77. Hirai H, Tanaka K, Yoshie O, Ogawa K, Kenmotsu K, Takamori Y, et al. Prostaglandin D2 selectively induces chemotaxis in T helper type 2 cells, eosinophils, and basophils via seven-transmembrane receptor CRTH2. J Exp Med. 2001;193(2):255-61.

78. Domingo C, Palomares O, Sandham DA, Erpenbeck VJ, Altman P. The prostaglandin D2 receptor 2 pathway in asthma: a key player in airway inflammation. Respir Res. 2018;19(1):189.

79. Ando M, Murakami Y, Kojima F, Endo H, Kitasato H, Hashimoto A, et al. Retrovirally introduced prostaglandin D2 synthase suppresses lung injury induced by bleomycin. Am J Respir Cell Mol Biol. 2003;28(5):582-91.

80. Ueda S, Fukunaga K, Takihara T, Shiraishi Y, Oguma T, Shiomi T, et al. Deficiency of CRTH2, a Prostaglandin D2 Receptor, Aggravates Bleomycin-induced Pulmonary Inflammation and Fibrosis. Am J Respir Cell Mol Biol. 2019;60(3):289-98.

81. Murata T, Aritake K, Tsubosaka Y, Maruyama T, Nakagawa T, Hori M, et al. Anti-inflammatory role of PGD2 in acute lung inflammation and therapeutic application of its signal enhancement. Proc Natl Acad Sci U S A. 2013;110(13):5205-10.

82. Midgett C, Stitham J, Martin K, Hwa J. Prostacyclin receptor regulation--from transcription to trafficking. Curr Mol Med. 2011;11(7):517-28.

83. Lang IM, Gaine SP. Recent advances in targeting the prostacyclin pathway in pulmonary arterial hypertension. Eur Respir Rev. 2015;24(138):630-41.

84. Cho MJ, Allen MA. Chemical stability of prostacyclin (PGI2) in aqueous solutions. Prostaglandins. 1978;15(6):943-54.

85. Whittle BJ, Silverstein AM, Mottola DM, Clapp LH. Binding and activity of the prostacyclin receptor (IP) agonists, treprostinil and iloprost, at human prostanoid receptors: treprostinil is a potent DP1 and EP2 agonist. Biochem Pharmacol. 2012;84(1):68-75.

86. Tateson JE, Moncada S, Vane JR. Effects of prostacyclin (PGX) on cyclic AMP concentrations in human platelets. Prostaglandins. 1977;13(3):389-97.

87. Willis AL, Smith DL, Vigo C, Kluge AF. Effects of prostacyclin and orally active stable mimetic agent RS-93427-007 on basic mechanisms of atherogenesis. Lancet. 1986;2(8508):682-3.

88. Zmajkovicova K, Menyhart K, Bauer Y, Studer R, Renault B, Schnoebelen M, et al. The Antifibrotic Activity of Prostacyclin Receptor Agonism Is Mediated through Inhibition of YAP/TAZ. Am J Respir Cell Mol Biol. 2019;60(5):578-91.

89. Lovgren AK, Jania LA, Hartney JM, Parsons KK, Audoly LP, Fitzgerald GA, et al. COX-2-derived prostacyclin protects against bleomycin-induced pulmonary fibrosis. Am J Physiol Lung Cell Mol Physiol. 2006;291(2):L144-56.

90. Nakahata N. Thromboxane A2: physiology/pathophysiology, cellular signal transduction and pharmacology. Pharmacol Ther. 2008;118(1):18-35.

91. Moers A, Wettschureck N, Gruner S, Nieswandt B, Offermanns S. Unresponsiveness of platelets lacking both Galpha(q) and Galpha(13). Implications for collagen-induced platelet activation. J Biol Chem. 2004;279(44):45354-9.

92. Verstraete M. Introduction: thromboxane in biological systems and the possible impact of its inhibition. Br J Clin Pharmacol. 1983;15 Suppl 1:7S-11S.

93. Smyth EM. Thromboxane and the thromboxane receptor in cardiovascular disease. Clin Lipidol. 2010;5(2):209-19.

94. Safholm J, Manson ML, Bood J, Delin I, Orre AC, Bergman P, et al. Prostaglandin E2 inhibits mast cell-dependent bronchoconstriction in human small airways through the E prostanoid subtype 2 receptor. J Allergy Clin Immunol. 2015;136(5):1232-9 e1.

95. Kobayashi K, Horikami D, Omori K, Nakamura T, Yamazaki A, Maeda S, et al. Thromboxane A2 exacerbates acute lung injury via promoting edema formation. Sci Rep. 2016;6:32109.

96. Zhang J, Gong Y, Yu Y. PG F(2alpha) Receptor: A Promising Therapeutic Target for Cardiovascular Disease. Front Pharmacol. 2010;1:116.

97. Fujino H, Srinivasan D, Pierce KL, Regan JW. Differential regulation of prostaglandin F(2alpha) receptor isoforms by protein kinase C. Mol Pharmacol. 2000;57(2):353-8.

98. Rice KM, Uddemarri S, Desai DH, Morrison RG, Harris R, Wright GL, et al. PGF2alpha-associated vascular smooth muscle hypertrophy is ROS dependent and involves the activation of mTOR, p70S6k, and PTEN. Prostaglandins Other Lipid Mediat. 2008;85(1-2):49-57.

99. Sugimoto Y, Yamasaki A, Segi E, Tsuboi K, Aze Y, Nishimura T, et al. Failure of parturition in mice lacking the prostaglandin F receptor. Science. 1997;277(5326):681-3.

100. Yamagishi-Kimura R, Honjo M, Aihara M. Contribution of prostanoid FP receptor and prostaglandins in transient inflammatory ocular hypertension. Sci Rep. 2018;8(1):11098.

101. Oga T, Matsuoka T, Yao C, Nonomura K, Kitaoka S, Sakata D, et al. Prostaglandin F(2alpha) receptor signaling facilitates bleomycin-induced pulmonary fibrosis independently of transforming growth factor-beta. Nat Med. 2009;15(12):1426-30.

102. Maher TM, Evans IC, Bottoms SE, Mercer PF, Thorley AJ, Nicholson AG, et al. Diminished prostaglandin E2 contributes to the apoptosis paradox in idiopathic pulmonary fibrosis. Am J Respir Crit Care Med. 2010;182(1):73-82.

103. Schuligoi R, Schmidt R, Geisslinger G, Kollroser M, Peskar BA, Heinemann A. PGD2 metabolism in plasma: kinetics and relationship with bioactivity on DP1 and CRTH2 receptors. Biochem Pharmacol. 2007;74(1):107-17.

104. Lands WEM, Smith WL, Colowick SP, Kaplan NO. Prostaglandins and arachidonate metabolites. New York: Academic Press; 1982. xxv, 705 pages : illustrations ; 24 cm. p.

105. Bito LZ, Baroody RA. Impermeability of rabbit erythrocytes to prostaglandins. Am J Physiol. 1975;229(6):1580-4.

106. Kanai N, Lu R, Satriano JA, Bao Y, Wolkoff AW, Schuster VL. Identification and characterization of a prostaglandin transporter. Science. 1995;268(5212):866-9.

107. Hagenbuch B, Meier PJ. Organic anion transporting polypeptides of the OATP/ SLC21 family: phylogenetic classification as OATP/ SLCO superfamily, new nomenclature and molecular/functional properties. Pflugers Arch. 2004;447(5):653-65.

108. Fagerberg L, Hallstrom BM, Oksvold P, Kampf C, Djureinovic D, Odeberg J, et al. Analysis of the human tissue-specific expression by genome-wide integration of transcriptomics and antibody-based proteomics. Mol Cell Proteomics. 2014;13(2):397-406.

109. Nakano J, Anggard E, Samuelsson B. 15-Hydroxy-prostanoate dehydrogenase. Prostaglandins as substrates and inhibitors. Eur J Biochem. 1969;11(2):386-9.

110. Tai HH. Enzymatic synthesis of (15s)-[15-3h]prostaglandins and their use in the development of a simple and sensitive assay for 15-hydroxyprostaglandin dehydrogenase. Biochemistry. 1976;15(21):4586-92.

111. Serhan CN, Maddox JF, Petasis NA, Akritopoulou-Zanze I, Papayianni A, Brady HR, et al. Design of lipoxin A4 stable analogs that block transmigration and adhesion of human neutrophils. Biochemistry. 1995;34(44):14609-15.

112. Jarabak J, Fried J. Comparison of substrate specificities of the human placental NAD- and NADP-linked 15-hydroxyprostaglandin dehydrogenases. Prostaglandins. 1979;18(2):241-6.

113. Watanabe K, Shimizu T, Iguchi S, Wakatsuka H, Hayashi M, Hayaishi O. An NADP-linked prostaglandin D dehydrogenase in swine brain. J Biol Chem. 1980;255(5):1779-82.

114. Miura T, Nishinaka T, Terada T. Different functions between human monomeric carbonyl reductase 3 and carbonyl reductase 1. Mol Cell Biochem. 2008;315(1-2):113-21.

115. Uppal S, Diggle CP, Carr IM, Fishwick CW, Ahmed M, Ibrahim GH, et al. Mutations in 15-hydroxyprostaglandin dehydrogenase cause primary hypertrophic osteoarthropathy. Nat Genet. 2008;40(6):789-93.

116. Ferreira SH, Vane JR. Prostaglandins: their disappearance from and release into the circulation. Nature. 1967;216(5118):868-73.

117. Nomura T, Lu R, Pucci ML, Schuster VL. The two-step model of prostaglandin signal termination: in vitro reconstitution with the prostaglandin transporter and prostaglandin 15 dehydrogenase. Mol Pharmacol. 2004;65(4):973-8.

118. Coggins KG, Latour A, Nguyen MS, Audoly L, Coffman TM, Koller BH. Metabolism of PGE2 by prostaglandin dehydrogenase is essential for remodeling the ductus arteriosus. Nat Med. 2002;8(2):91-2.

119. Loftin CD, Trivedi DB, Tiano HF, Clark JA, Lee CA, Epstein JA, et al. Failure of ductus arteriosus closure and remodeling in neonatal mice deficient in cyclooxygenase-1 and cyclooxygenase-2. Proc Natl Acad Sci U S A. 2001;98(3):1059-64.

120. Nguyen M, Camenisch T, Snouwaert JN, Hicks E, Coffman TM, Anderson PA, et al. The prostaglandin receptor EP4 triggers remodelling of the cardiovascular system at birth. Nature. 1997;390(6655):78-81.

121. Hartney JM, Coggins KG, Tilley SL, Jania LA, Lovgren AK, Audoly LP, et al. Prostaglandin E2 protects lower airways against bronchoconstriction. Am J Physiol Lung Cell Mol Physiol. 2006;290(1):L105-13.

122. Tai HH. Prostaglandin catabolic enzymes as tumor suppressors. Cancer Metastasis Rev. 2011;30(3-4):409-17.

123. Bergmann C, Wobser M, Morbach H, Falkenbach A, Wittenhagen D, Lassay L, et al. Primary hypertrophic osteoarthropathy with digital clubbing and palmoplantar hyperhidrosis caused by 15-PGHD/HPGD loss-of-function mutations. Exp Dermatol. 2011;20(6):531-3.

124. Seifert W, Beninde J, Hoffmann K, Lindner TH, Bassir C, Aksu F, et al. HPGD mutations cause cranioosteoarthropathy but not autosomal dominant digital clubbing. Eur J Hum Genet. 2009;17(12):1570-6.

125. Yuan L, Chen L, Liao RX, Lin YY, Jiang Y, Wang O, et al. A Common Mutation and a Novel Mutation in the HPGD Gene in Nine Patients with Primary Hypertrophic Osteoarthropathy. Calcif Tissue Int. 2015;97(4):336-42.

126. Sinibaldi L, Harifi G, Bottillo I, Iannicelli M, El Hassani S, Brancati F, et al. A novel homozygous splice site mutation in the HPGD gene causes mild primary hypertrophic osteoarthropathy. Clin Exp Rheumatol. 2010;28(2):153-7.

127. Arima K, Komohara Y, Bu L, Tsukamoto M, Itoyama R, Miyake K, et al. Downregulation of 15-hydroxyprostaglandin dehydrogenase by interleukin-1beta from

activated macrophages leads to poor prognosis in pancreatic cancer. Cancer Sci. 2018;109(2):462-70.

128. Lehtinen L, Vainio P, Wikman H, Reemts J, Hilvo M, Issa R, et al. 15-Hydroxyprostaglandin dehydrogenase associates with poor prognosis in breast cancer, induces epithelial-mesenchymal transition, and promotes cell migration in cultured breast cancer cells. J Pathol. 2012;226(4):674-86.

129. Yan M, Rerko RM, Platzer P, Dawson D, Willis J, Tong M, et al. 15-Hydroxyprostaglandin dehydrogenase, a COX-2 oncogene antagonist, is a TGF-beta-induced suppressor of human gastrointestinal cancers. Proc Natl Acad Sci U S A. 2004;101(50):17468-73.

130. Tariq M, Azeem Z, Ali G, Chishti MS, Ahmad W. Mutation in the HPGD gene encoding NAD+ dependent 15-hydroxyprostaglandin dehydrogenase underlies isolated congenital nail clubbing (ICNC). J Med Genet. 2009;46(1):14-20.

131. Schmidleithner L, Thabet Y, Schonfeld E, Kohne M, Sommer D, Abdullah Z, et al. Enzymatic Activity of HPGD in Treg Cells Suppresses Tconv Cells to Maintain Adipose Tissue Homeostasis and Prevent Metabolic Dysfunction. Immunity. 2019;50(5):1232-48 e14.

132. Guda K, Fink SP, Milne GL, Molyneaux N, Ravi L, Lewis SM, et al. Inactivating mutation in the prostaglandin transporter gene, SLCO2A1, associated with familial digital clubbing, colon neoplasia, and NSAID resistance. Cancer Prev Res (Phila). 2014;7(8):805-12.

133. Umeno J, Hisamatsu T, Esaki M, Hirano A, Kubokura N, Asano K, et al. A Hereditary Enteropathy Caused by Mutations in the SLCO2A1 Gene, Encoding a Prostaglandin Transporter. PLoS Genet. 2015;11(11):e1005581.

134. Harmon GS, Dumlao DS, Ng DT, Barrett KE, Dennis EA, Dong H, et al. Pharmacological correction of a defect in PPAR-gamma signaling ameliorates disease severity in Cftr-deficient mice. Nat Med. 2010;16(3):313-8.

135. Tai HH, Ensor CM, Tong M, Zhou H, Yan F. Prostaglandin catabolizing enzymes. Prostaglandins Other Lipid Mediat. 2002;68-69:483-93.

136. Hamberg M, Samuelsson B. On the metabolism of prostaglandins E 1 and E 2 in man. J Biol Chem. 1971;246(22):6713-21.

137. Rosas IO, Dellaripa PF, Lederer DJ, Khanna D, Young LR, Martinez FJ. Interstitial lung disease: NHLBI Workshop on the Primary Prevention of Chronic Lung Diseases. Ann Am Thorac Soc. 2014;11 Suppl 3:S169-77.

138. Homolka J. Idiopathic pulmonary fibrosis: a historical review. CMAJ. 1987;137(11):1003-5.

139. Nalysnyk L, Cid-Ruzafa J, Rotella P, Esser D. Incidence and prevalence of idiopathic pulmonary fibrosis: review of the literature. Eur Respir Rev. 2012;21(126):355-61.

140. Hutchinson J, Fogarty A, Hubbard R, McKeever T. Global incidence and mortality of idiopathic pulmonary fibrosis: a systematic review. Eur Respir J. 2015;46(3):795-806.

141. Raghu G, Chen SY, Yeh WS, Maroni B, Li Q, Lee YC, et al. Idiopathic pulmonary fibrosis in US Medicare beneficiaries aged 65 years and older: incidence, prevalence, and survival, 2001-11. Lancet Respir Med. 2014;2(7):566-72.

142. George G, Vaid U, Summer R. Therapeutic advances in idiopathic pulmonary fibrosis. Clin Pharmacol Ther. 2016;99(1):30-2.

143. Hewson T, McKeever TM, Gibson JE, Navaratnam V, Hubbard RB, Hutchinson JP. Timing of onset of symptoms in people with idiopathic pulmonary fibrosis. Thorax. 2017.

144. Roger VL. Epidemiology of heart failure. Circ Res. 2013;113(6):646-59.

145. Terzikhan N, Verhamme KM, Hofman A, Stricker BH, Brusselle GG, Lahousse L. Prevalence and incidence of COPD in smokers and non-smokers: the Rotterdam Study. Eur J Epidemiol. 2016;31(8):785-92.

146. Raghu G, Collard HR, Egan JJ, Martinez FJ, Behr J, Brown KK, et al. An official ATS/ERS/JRS/ALAT statement: idiopathic pulmonary fibrosis: evidence-based guidelines for diagnosis and management. Am J Respir Crit Care Med. 2011;183(6):788-824.

147. Lederer DJ, Martinez FJ. Idiopathic Pulmonary Fibrosis. N Engl J Med. 2018;378(19):1811-23.

148. Sgalla G, Iovene B, Calvello M, Ori M, Varone F, Richeldi L. Idiopathic pulmonary fibrosis: pathogenesis and management. Respir Res. 2018;19(1):32.

149. Schneider JP, Wrede C, Hegermann J, Weibel ER, Muhlfeld C, Ochs M. On the Topological Complexity of Human Alveolar Epithelial Type 1 Cells. Am J Respir Crit Care Med. 2019;199(9):1153-6.

150. Lüllmann-Rauch R, Lüllmann-Rauch R. Histologie. Bruxelles: De Boeck; 2008. XX, 679 p. p.

151. Crapo JD, Barry BE, Gehr P, Bachofen M, Weibel ER. Cell number and cell characteristics of the normal human lung. Am Rev Respir Dis. 1982;126(2):332-7.

152. Dobbs LG, Johnson MD, Vanderbilt J, Allen L, Gonzalez R. The great big alveolar TI cell: evolving concepts and paradigms. Cell Physiol Biochem. 2010;25(1):55-62.

153. Wong MH, Johnson MD. Differential response of primary alveolar type I and type II cells to LPS stimulation. PLoS One. 2013;8(1):e55545.

154. Fehrenbach H. Alveolar epithelial type II cell: defender of the alveolus revisited. Respir Res. 2001;2(1):33-46.

155. Desai TJ, Brownfield DG, Krasnow MA. Alveolar progenitor and stem cells in lung development, renewal and cancer. Nature. 2014;507(7491):190-4.

156. Snetselaar R, van Batenburg AA, van Oosterhout MFM, Kazemier KM, Roothaan SM, Peeters T, et al. Short telomere length in IPF lung associates with fibrotic lesions and predicts survival. PLoS One. 2017;12(12):e0189467.

157. Naikawadi RP, Disayabutr S, Mallavia B, Donne ML, Green G, La JL, et al. Telomere dysfunction in alveolar epithelial cells causes lung remodeling and fibrosis. JCI Insight. 2016;1(14):e86704.

158. Yu G, Tzouvelekis A, Wang R, Herazo-Maya JD, Ibarra GH, Srivastava A, et al. Thyroid hormone inhibits lung fibrosis in mice by improving epithelial mitochondrial function. Nat Med. 2018;24(1):39-49.

159. Burman A, Tanjore H, Blackwell TS. Endoplasmic reticulum stress in pulmonary fibrosis. Matrix Biol. 2018;68-69:355-65.

160. Charbeneau RP, Christensen PJ, Chrisman CJ, Paine R, 3rd, Toews GB, Peters-Golden M, et al. Impaired synthesis of prostaglandin E2 by lung fibroblasts and alveolar epithelial cells from GM-CSF-/- mice: implications for fibroproliferation. Am J Physiol Lung Cell Mol Physiol. 2003;284(6):L1103-11.

161. Katzenstein AL, Myers JL. Idiopathic pulmonary fibrosis: clinical relevance of pathologic classification. Am J Respir Crit Care Med. 1998;157(4 Pt 1):1301-15.

162. Habiel DM, Hogaboam CM. Heterogeneity of Fibroblasts and Myofibroblasts in Pulmonary Fibrosis. Curr Pathobiol Rep. 2017;5(2):101-10.

163. Chen L, Acciani T, Le Cras T, Lutzko C, Perl AK. Dynamic regulation of platelet-derived growth factor receptor alpha expression in alveolar fibroblasts during realveolarization. Am J Respir Cell Mol Biol. 2012;47(4):517-27.

164. McGowan SE, Torday JS. The pulmonary lipofibroblast (lipid interstitial cell) and its contributions to alveolar development. Annu Rev Physiol. 1997;59:43-62.

165. Torday JS, Sun H, Qin J. Prostaglandin E2 integrates the effects of fluid distension and glucocorticoid on lung maturation. Am J Physiol. 1998;274(1):L106-11.

166. El Agha E, Moiseenko A, Kheirollahi V, De Langhe S, Crnkovic S, Kwapiszewska G, et al. Two-Way Conversion between Lipogenic and Myogenic Fibroblastic Phenotypes Marks the Progression and Resolution of Lung Fibrosis. Cell Stem Cell. 2017;20(2):261-73 e3.

167. Moore MW, Herzog EL. Regulation and Relevance of Myofibroblast Responses in Idiopathic Pulmonary Fibrosis. Curr Pathobiol Rep. 2013;1(3):199-208.

168. Hinz B, Phan SH, Thannickal VJ, Prunotto M, Desmouliere A, Varga J, et al. Recent developments in myofibroblast biology: paradigms for connective tissue remodeling. Am J Pathol. 2012;180(4):1340-55.

169. Huang SK, Fisher AS, Scruggs AM, White ES, Hogaboam CM, Richardson BC, et al. Hypermethylation of PTGER2 confers prostaglandin E2 resistance in fibrotic fibroblasts from humans and mice. Am J Pathol. 2010;177(5):2245-55.

170. Garrison G, Huang SK, Okunishi K, Scott JP, Kumar Penke LR, Scruggs AM, et al. Reversal of myofibroblast differentiation by prostaglandin E(2). Am J Respir Cell Mol Biol. 2013;48(5):550-8.

171. Uhal BD, Joshi I, True AL, Mundle S, Raza A, Pardo A, et al. Fibroblasts isolated after fibrotic lung injury induce apoptosis of alveolar epithelial cells in vitro. Am J Physiol. 1995;269(6 Pt 1):L819-28.

172. Bucala R, Spiegel LA, Chesney J, Hogan M, Cerami A. Circulating fibrocytes define a new leukocyte subpopulation that mediates tissue repair. Mol Med. 1994;1(1):71-81.

173. Pilling D, Fan T, Huang D, Kaul B, Gomer RH. Identification of markers that distinguish monocyte-derived fibrocytes from monocytes, macrophages, and fibroblasts. PLoS One. 2009;4(10):e7475.

174. Abe R, Donnelly SC, Peng T, Bucala R, Metz CN. Peripheral blood fibrocytes: differentiation pathway and migration to wound sites. J Immunol. 2001;166(12):7556-62.

175. Kao HK, Chen B, Murphy GF, Li Q, Orgill DP, Guo L. Peripheral blood fibrocytes: enhancement of wound healing by cell proliferation, re-epithelialization, contraction, and angiogenesis. Ann Surg. 2011;254(6):1066-74.

176. Heukels P, van Hulst JAC, van Nimwegen M, Boorsma CE, Melgert BN, van den Toorn LM, et al. Fibrocytes are increased in lung and peripheral blood of patients with idiopathic pulmonary fibrosis. Respir Res. 2018;19(1):90.

177. Moeller A, Gilpin SE, Ask K, Cox G, Cook D, Gauldie J, et al. Circulating fibrocytes are an indicator of poor prognosis in idiopathic pulmonary fibrosis. Am J Respir Crit Care Med. 2009;179(7):588-94.

178. Kleaveland KR, Moore BB, Kim KK. Paracrine functions of fibrocytes to promote lung fibrosis. Expert Rev Respir Med. 2014;8(2):163-72.

179. Kleaveland KR, Velikoff M, Yang J, Agarwal M, Rippe RA, Moore BB, et al. Fibrocytes are not an essential source of type I collagen during lung fibrosis. J Immunol. 2014;193(10):5229-39.

180. Moore BB, Murray L, Das A, Wilke CA, Herrygers AB, Toews GB. The role of CCL12 in the recruitment of fibrocytes and lung fibrosis. Am J Respir Cell Mol Biol. 2006;35(2):175-81.

181. Rock JR, Barkauskas CE, Cronce MJ, Xue Y, Harris JR, Liang J, et al. Multiple stromal populations contribute to pulmonary fibrosis without evidence for epithelial to mesenchymal transition. Proc Natl Acad Sci U S A. 2011;108(52):E1475-83.

182. Wilson CL, Stephenson SE, Higuero JP, Feghali-Bostwick C, Hung CF, Schnapp LM. Characterization of human PDGFR-beta-positive pericytes from IPF and non-IPF lungs. Am J Physiol Lung Cell Mol Physiol. 2018;315(6):L991-L1002.

183. Yoshimura S, Nishimura Y, Nishiuma T, Yamashita T, Kobayashi K, Yokoyama M. Overexpression of nitric oxide synthase by the endothelium attenuates bleomycin-induced lung fibrosis and impairs MMP-9/TIMP-1 balance. Respirology. 2006;11(5):546-56.

184. Zhang L, Wang Y, Wu G, Xiong W, Gu W, Wang CY. Macrophages: friend or foe in idiopathic pulmonary fibrosis? Respir Res. 2018;19(1):170.

185. Raghu G, Weycker D, Edelsberg J, Bradford WZ, Oster G. Incidence and prevalence of idiopathic pulmonary fibrosis. Am J Respir Crit Care Med. 2006;174(7):810-6.

186. Idiopathic Pulmonary Fibrosis Clinical Research N, Raghu G, Anstrom KJ, King TE, Jr., Lasky JA, Martinez FJ. Prednisone, azathioprine, and N-acetylcysteine for pulmonary fibrosis. N Engl J Med. 2012;366(21):1968-77.

187. Baughman RP, Lower EE. Immunosuppressant Therapy for Idiopathic Pulmonary Fibrosis. Clin Immunother. 1996;6(6):431-42.

188. Meyer KC, Nathan SD. Idiopathic pulmonary fibrosis : a comprehensive clinical guide. xv, 451 pages p.

189. Kim ES, Keating GM. Pirfenidone: a review of its use in idiopathic pulmonary fibrosis. Drugs. 2015;75(2):219-30.

190. Noble PW, Albera C, Bradford WZ, Costabel U, Glassberg MK, Kardatzke D, et al. Pirfenidone in patients with idiopathic pulmonary fibrosis (CAPACITY): two randomised trials. Lancet. 2011;377(9779):1760-9.

191. King TE, Jr., Bradford WZ, Castro-Bernardini S, Fagan EA, Glaspole I, Glassberg MK, et al. A phase 3 trial of pirfenidone in patients with idiopathic pulmonary fibrosis. N Engl J Med. 2014;370(22):2083-92.

192. Conte E, Gili E, Fagone E, Fruciano M, Iemmolo M, Vancheri C. Effect of pirfenidone on proliferation, TGF-beta-induced myofibroblast differentiation and fibrogenic activity of primary human lung fibroblasts. Eur J Pharm Sci. 2014;58:13-9.

193. Oku H, Shimizu T, Kawabata T, Nagira M, Hikita I, Ueyama A, et al. Antifibrotic action of pirfenidone and prednisolone: different effects on pulmonary cytokines and growth factors in bleomycin-induced murine pulmonary fibrosis. Eur J Pharmacol. 2008;590(1-3):400-8.

194. Misra HP, Rabideau C. Pirfenidone inhibits NADPH-dependent microsomal lipid peroxidation and scavenges hydroxyl radicals. Mol Cell Biochem. 2000;204(1-2):119-26.

195. Oku H, Nakazato H, Horikawa T, Tsuruta Y, Suzuki R. Pirfenidone suppresses tumor necrosis factor-alpha, enhances interleukin-10 and protects mice from endotoxic shock. Eur J Pharmacol. 2002;446(1-3):167-76.

196. Inomata M, Kamio K, Azuma A, Matsuda K, Kokuho N, Miura Y, et al. Pirfenidone inhibits fibrocyte accumulation in the lungs in bleomycin-induced murine pulmonary fibrosis. Respir Res. 2014;15:16.

197. Hilberg F, Roth GJ, Krssak M, Kautschitsch S, Sommergruber W, Tontsch-Grunt U, et al. BIBF 1120: triple angiokinase inhibitor with sustained receptor blockade and good antitumor efficacy. Cancer Res. 2008;68(12):4774-82.

198. Richeldi L, du Bois RM, Raghu G, Azuma A, Brown KK, Costabel U, et al. Efficacy and safety of nintedanib in idiopathic pulmonary fibrosis. N Engl J Med. 2014;370(22):2071-82.

199. Hostettler KE, Zhong J, Papakonstantinou E, Karakiulakis G, Tamm M, Seidel P, et al. Anti-fibrotic effects of nintedanib in lung fibroblasts derived from patients with idiopathic pulmonary fibrosis. Respir Res. 2014;15:157.

200. Wollin L, Maillet I, Quesniaux V, Holweg A, Ryffel B. Antifibrotic and anti-inflammatory activity of the tyrosine kinase inhibitor nintedanib in experimental models of lung fibrosis. J Pharmacol Exp Ther. 2014;349(2):209-20.

201. Lehmann M, Buhl L, Alsafadi HN, Klee S, Hermann S, Mutze K, et al. Differential effects of Nintedanib and Pirfenidone on lung alveolar epithelial cell function in ex vivo murine and human lung tissue cultures of pulmonary fibrosis. Respir Res. 2018;19(1):175.

202. Sato S, Shinohara S, Hayashi S, Morizumi S, Abe S, Okazaki H, et al. Anti-fibrotic efficacy of nintedanib in pulmonary fibrosis via the inhibition of fibrocyte activity. Respir Res. 2017;18(1):172.

203. Idiopathic Pulmonary Fibrosis Clinical Research N, Martinez FJ, de Andrade JA, Anstrom KJ, King TE, Jr., Raghu G. Randomized trial of acetylcysteine in idiopathic pulmonary fibrosis. N Engl J Med. 2014;370(22):2093-101.

204. Warsinske HC, Wheaton AK, Kim KK, Linderman JJ, Moore BB, Kirschner DE. Computational Modeling Predicts Simultaneous Targeting of Fibroblasts and Epithelial Cells Is Necessary for Treatment of Pulmonary Fibrosis. Front Pharmacol. 2016;7:183.

205. Dowman LM, McDonald CF, Bozinovski S, Vlahos R, Gillies R, Pouniotis D, et al. Greater endurance capacity and improved dyspnoea with acute oxygen supplementation in idiopathic pulmonary fibrosis patients without resting hypoxaemia. Respirology. 2017;22(5):957-64.

206. Dowman LM, McDonald CF, Hill CJ, Lee AL, Barker K, Boote C, et al. The evidence of benefits of exercise training in interstitial lung disease: a randomised controlled trial. Thorax. 2017;72(7):610-9.

207. Laporta Hernandez R, Aguilar Perez M, Lazaro Carrasco MT, Ussetti Gil P. Lung Transplantation in Idiopathic Pulmonary Fibrosis. Med Sci (Basel). 2018;6(3).

208. Weill D, Benden C, Corris PA, Dark JH, Davis RD, Keshavjee S, et al. A consensus document for the selection of lung transplant candidates: 2014--an update from the Pulmonary Transplantation Council of the International Society for Heart and Lung Transplantation. J Heart Lung Transplant. 2015;34(1):1-15.

209. Borok Z, Gillissen A, Buhl R, Hoyt RF, Hubbard RC, Ozaki T, et al. Augmentation of functional prostaglandin E levels on the respiratory epithelial surface by aerosol administration of prostaglandin E. Am Rev Respir Dis. 1991;144(5):1080-4.

210. Ko SD, Page RC, Narayanan AS. Fibroblast heterogeneity and prostaglandin regulation of subpopulations. Proc Natl Acad Sci U S A. 1977;74(8):3429-32.

211. Dackor RT, Cheng J, Voltz JW, Card JW, Ferguson CD, Garrett RC, et al. Prostaglandin E(2) protects murine lungs from bleomycin-induced pulmonary fibrosis and lung dysfunction. Am J Physiol Lung Cell Mol Physiol. 2011;301(5):L645-55.

212. Failla M, Genovese T, Mazzon E, Fruciano M, Fagone E, Gili E, et al. 16,16-Dimethyl prostaglandin E2 efficacy on prevention and protection from bleomycin-induced lung injury and fibrosis. Am J Respir Cell Mol Biol. 2009;41(1):50-8.

213. Ivanova V, Garbuzenko OB, Reuhl KR, Reimer DC, Pozharov VP, Minko T. Inhalation treatment of pulmonary fibrosis by liposomal prostaglandin E2. Eur J Pharm Biopharm. 2013;84(2):335-44.

214. Choung J, Taylor L, Thomas K, Zhou X, Kagan H, Yang X, et al. Role of EP2 receptors and cAMP in prostaglandin E2 regulated expression of type I collagen alpha1, lysyl oxidase, and cyclooxygenase-1 genes in human embryo lung fibroblasts. J Cell Biochem. 1998;71(2):254-63.

215. Moore BB, Peters-Golden M, Christensen PJ, Lama V, Kuziel WA, Paine R, 3rd, et al. Alveolar epithelial cell inhibition of fibroblast proliferation is regulated by MCP-1/CCR2 and mediated by PGE2. Am J Physiol Lung Cell Mol Physiol. 2003;284(2):L342-9.

216. Moore BB, Ballinger MN, White ES, Green ME, Herrygers AB, Wilke CA, et al. Bleomycin-induced E prostanoid receptor changes alter fibroblast responses to prostaglandin E2. J Immunol. 2005;174(9):5644-9.

217. Zhu Y, Liu Y, Zhou W, Xiang R, Jiang L, Huang K, et al. A prostacyclin analogue, iloprost, protects from bleomycin-induced pulmonary fibrosis in mice. Respir Res. 2010;11:34.

218. Roach KM, Feghali-Bostwick CA, Amrani Y, Bradding P. Lipoxin A4 Attenuates Constitutive and TGF-beta1-Dependent Profibrotic Activity in Human Lung Myofibroblasts. J Immunol. 2015;195(6):2852-60.

219. Martins V, Valenca SS, Farias-Filho FA, Molinaro R, Simoes RL, Ferreira TP, et al. ATLa, an aspirin-triggered lipoxin A4 synthetic analog, prevents the inflammatory and fibrotic effects of bleomycin-induced pulmonary fibrosis. J Immunol. 2009;182(9):5374-81.

220. Grimminger F, von Kurten I, Walmrath D, Seeger W. Type II alveolar epithelial eicosanoid metabolism: predominance of cyclooxygenase pathways and transcellular lipoxygenase metabolism in co-culture with neutrophils. Am J Respir Cell Mol Biol. 1992;6(1):9-16.

221. Wilborn J, Crofford LJ, Burdick MD, Kunkel SL, Strieter RM, Peters-Golden M. Cultured lung fibroblasts isolated from patients with idiopathic pulmonary fibrosis have a diminished capacity to synthesize prostaglandin E2 and to express cyclooxygenase-2. J Clin Invest. 1995;95(4):1861-8.

222. Xaubet A, Roca-Ferrer J, Pujols L, Ramirez J, Mullol J, Marin-Arguedas A, et al. Cyclooxygenase-2 is up-regulated in lung parenchyma of chronic obstructive pulmonary disease and down-regulated in idiopathic pulmonary fibrosis. Sarcoidosis Vasc Diffuse Lung Dis. 2004;21(1):35-42.

223. Evans IC, Barnes JL, Garner IM, Pearce DR, Maher TM, Shiwen X, et al. Epigenetic regulation of cyclooxygenase-2 by methylation of c8orf4 in pulmonary fibrosis. Clin Sci (Lond). 2016;130(8):575-86.

224. Petkova DK, Clelland CA, Ronan JE, Lewis S, Knox AJ. Reduced expression of cyclooxygenase (COX) in idiopathic pulmonary fibrosis and sarcoidosis. Histopathology. 2003;43(4):381-6.

225. Tong M, Ding Y, Tai HH. Histone deacetylase inhibitors and transforming growth factor-beta induce 15-hydroxyprostaglandin dehydrogenase expression in human lung adenocarcinoma cells. Biochem Pharmacol. 2006;72(6):701-9.

226. Pandit KV, Corcoran D, Yousef H, Yarlagadda M, Tzouvelekis A, Gibson KF, et al. Inhibition and role of let-7d in idiopathic pulmonary fibrosis. Am J Respir Crit Care Med. 2010;182(2):220-9.

227. Berschneider B, Ellwanger DC, Baarsma HA, Thiel C, Shimbori C, White ES, et al. miR-92a regulates TGF-beta1-induced WISP1 expression in pulmonary fibrosis. Int J Biochem Cell Biol. 2014;53:432-41.

228. Cong R, Tao K, Fu P, Lou L, Zhu Y, Chen S, et al. MicroRNA218 promotes prostaglandin E2 to inhibit osteogenic differentiation in synovial mesenchymal stem cells by targeting 15hydroxyprostaglandin dehydrogenase [NAD(+)]. Mol Med Rep. 2017;16(6):9347-54.

229. Horikiri T, Hara H, Saito N, Araya J, Takasaka N, Utsumi H, et al. Increased levels of prostaglandin E-major urinary metabolite (PGE-MUM) in chronic fibrosing interstitial pneumonia. Respir Med. 2017;122:43-50.

230. Barnthaler T, Jandl K, Sill H, Uhl B, Schreiber Y, Grill M, et al. Imatinib stimulates prostaglandin E2 and attenuates cytokine release via EP4 receptor activation. J Allergy Clin Immunol. 2019;143(2):794-7 e10.

231. Zhang Y, Desai A, Yang SY, Bae KB, Antczak MI, Fink SP, et al. TISSUE REGENERATION. Inhibition of the prostaglandin-degrading enzyme 15-PGDH potentiates tissue regeneration. Science. 2015;348(6240):aaa2340.

232. Jablonska E, Markart P, Zakrzewicz D, Preissner KT, Wygrecka M. Transforming growth factor-beta1 induces expression of human coagulation factor XII via Smad3 and JNK signaling pathways in human lung fibroblasts. J Biol Chem. 2010;285(15):11638-51.

233. Pilling D, Gomer RH. Differentiation of circulating monocytes into fibroblast-like cells. Methods Mol Biol. 2012;904:191-206.

234. Konya V, Ullen A, Kampitsch N, Theiler A, Philipose S, Parzmair GP, et al. Endothelial E-type prostanoid 4 receptors promote barrier function and inhibit neutrophil trafficking. J Allergy Clin Immunol. 2013;131(2):532-40 e1-2.

235. Rayamajhi M, Redente EF, Condon TV, Gonzalez-Juarrero M, Riches DW, Lenz LL. Non-surgical intratracheal instillation of mice with analysis of lungs and lung draining lymph nodes by flow cytometry. J Vis Exp. 2011(51).

236. Sturm EM, Schratl P, Schuligoi R, Konya V, Sturm GJ, Lippe IT, et al. Prostaglandin E2 inhibits eosinophil trafficking through E-prostanoid 2 receptors. J Immunol. 2008;181(10):7273-83.

237. Theiler A, Barnthaler T, Platzer W, Richtig G, Peinhaupt M, Rittchen S, et al. Butyrate ameliorates allergic airway inflammation by limiting eosinophil trafficking and survival. J Allergy Clin Immunol. 2019.

238. Moeller A, Ask K, Warburton D, Gauldie J, Kolb M. The bleomycin animal model: a useful tool to investigate treatment options for idiopathic pulmonary fibrosis? Int J Biochem Cell Biol. 2008;40(3):362-82.

239. Jenkins RG, Moore BB, Chambers RC, Eickelberg O, Konigshoff M, Kolb M, et al. An Official American Thoracic Society Workshop Report: Use of Animal Models for the Preclinical Assessment of Potential Therapies for Pulmonary Fibrosis. Am J Respir Cell Mol Biol. 2017;56(5):667-79.

240. Hubner RH, Gitter W, El Mokhtari NE, Mathiak M, Both M, Bolte H, et al. Standardized quantification of pulmonary fibrosis in histological samples. Biotechniques. 2008;44(4):507-11, 14-7.

241. Pfister R, Hagemeister J, Esser S, Hellmich M, Erdmann E, Schneider CA. NT-pro-BNP for diagnostic and prognostic evaluation in patients hospitalized for syncope. Int J Cardiol. 2012;155(2):268-72.

242. Vanoirbeek JA, Rinaldi M, De Vooght V, Haenen S, Bobic S, Gayan-Ramirez G, et al. Noninvasive and invasive pulmonary function in mouse models of obstructive and restrictive respiratory diseases. Am J Respir Cell Mol Biol. 2010;42(1):96-104.

243. Schlosser K, Taha M, Stewart DJ. Systematic Assessment of Strategies for Lung-targeted Delivery of MicroRNA Mimics. Theranostics. 2018;8(5):1213-26.

244. Tai HH, Hollander CS. Kinetic evidence of a distinct regulatory site on 15-hydroxyprostaglandin dehydrogenase. Adv Prostaglandin Thromboxane Res. 1976;1:171-5.

245. Ulcar R, Peskar BA, Schuligoi R, Heinemann A, Kessler HH, Santner BI, et al. Cyclooxygenase inhibition in human monocytes increases endotoxin-induced TNF alpha without affecting cyclooxygenase-2 expression. Eur J Pharmacol. 2004;501(1-3):9-17.

246. Martin C, Uhlig S, Ullrich V. Videomicroscopy of methacholine-induced contraction of individual airways in precision-cut lung slices. Eur Respir J. 1996;9(12):2479-87.

247. Seaman MA, Levin JR, Serlin RC. New Developments in Pairwise Multiple Comparisons - Some Powerful and Practicable Procedures. Psychol Bull. 1991;110(3):577-86.

248. Nakanishi T, Hasegawa Y, Mimura R, Wakayama T, Uetoko Y, Komori H, et al. Prostaglandin Transporter (PGT/SLCO2A1) Protects the Lung from Bleomycin-Induced Fibrosis. PLoS One. 2015;10(4):e0123895.

249. Wang L, Taneja R, Wang W, Yao LJ, Veldhuizen RA, Gill SE, et al. Human alveolar epithelial cells attenuate pulmonary microvascular endothelial cell permeability under septic conditions. PLoS One. 2013;8(2):e55311.

250. Demaio L, Tseng W, Balverde Z, Alvarez JR, Kim KJ, Kelley DG, et al. Characterization of mouse alveolar epithelial cell monolayers. Am J Physiol Lung Cell Mol Physiol. 2009;296(6):L1051-8.

251. Mitchell JA, Belvisi MG, Akarasereenont P, Robbins RA, Kwon OJ, Croxtall J, et al. Induction of cyclo-oxygenase-2 by cytokines in human pulmonary epithelial cells: regulation by dexamethasone. Br J Pharmacol. 1994;113(3):1008-14.

252. Schuligoi R, Amann R, Prenn C, Peskar BA. Effects of the cyclooxygenase-2 inhibitor NS-398 on thromboxane and leukotriene synthesis in rat peritoneal cells. Inflamm Res. 1998;47(5):227-30.

253. Speth JM, Bourdonnay E, Penke LR, Mancuso P, Moore BB, Weinberg JB, et al. Alveolar Epithelial Cell-Derived Prostaglandin E2 Serves as a Request Signal for Macrophage Secretion of Suppressor of Cytokine Signaling 3 during Innate Inflammation. J Immunol. 2016;196(12):5112-20.

254. Konya V, Ullen A, Kampitsch N, Theiler A, Philipose S, Parzmair GP, et al. Endothelial E-type prostanoid 4 receptors promote barrier function and inhibit neutrophil trafficking. J Allergy Clin Immunol. 2012;131(2):532-40 e1-2.

255. Konya V, Sturm EM, Schratl P, Beubler E, Marsche G, Schuligoi R, et al. Endothelium-derived prostaglandin I(2) controls the migration of eosinophils. J Allergy Clin Immunol. 2010;125(5):1105-13.

256. Cheng J, Dackor RT, Bradbury JA, Li H, DeGraff LM, Hong LK, et al. Contribution of alveolar type II cell-derived cyclooxygenase-2 to basal airway function, lung inflammation, and lung fibrosis. FASEB J. 2016;30(1):160-73.

257. Safaeian L, Jafarian-Dehkordi A, Rabbani M, Sadeghi HM, Afshar-Moghaddam N, Sarahroodi S. Comparison of bleomycin-induced pulmonary apoptosis between NMRI mice and C57BL/6 mice. Res Pharm Sci. 2013;8(1):43-50.

258. Aguilar S, Scotton CJ, McNulty K, Nye E, Stamp G, Laurent G, et al. Bone marrow stem cells expressing keratinocyte growth factor via an inducible lentivirus protects against bleomycin-induced pulmonary fibrosis. PLoS One. 2009;4(11):e8013.

259. Jordana M, Schulman J, McSharry C, Irving LB, Newhouse MT, Jordana G, et al. Heterogeneous proliferative characteristics of human adult lung fibroblast lines and clonally derived fibroblasts from control and fibrotic tissue. Am Rev Respir Dis. 1988;137(3):579-84.

260. Mikamo M, Kitagawa K, Sakai S, Uchida C, Ohhata T, Nishimoto K, et al. Inhibiting Skp2 E3 Ligase Suppresses Bleomycin-Induced Pulmonary Fibrosis. Int J Mol Sci. 2018;19(2).

261. Nikam VS, Wecker G, Schermuly R, Rapp U, Szelepusa K, Seeger W, et al. Treprostinil inhibits the adhesion and differentiation of fibrocytes via the cyclic adenosine monophosphate-dependent and Ras-proximate protein-dependent inactivation of extracellular regulated kinase. Am J Respir Cell Mol Biol. 2011;45(4):692-703.

262. Liu X, Nelson A, Wang X, Farid M, Gunji Y, Ikari J, et al. Vitamin D modulates prostaglandin E2 synthesis and degradation in human lung fibroblasts. Am J Respir Cell Mol Biol. 2014;50(1):40-50.

263. Agarwal V, Bell GW, Nam JW, Bartel DP. Predicting effective microRNA target sites in mammalian mRNAs. Elife. 2015;4.

264. Rucka Z, Vanhara P, Koutna I, Tesarova L, Potesilova M, Stejskal S, et al. Differential effects of insulin and dexamethasone on pulmonary surfactant-associated genes and proteins in A549 and H441 cells and lung tissue. Int J Mol Med. 2013;32(1):211-8.

265. Birukova AA, Wu T, Tian Y, Meliton A, Sarich N, Tian X, et al. Iloprost improves endothelial barrier function in lipopolysaccharide-induced lung injury. Eur Respir J. 2013;41(1):165-76.

266. Chen H, Hu B, Lv X, Zhu S, Zhen G, Wan M, et al. Prostaglandin E2 mediates sensory nerve regulation of bone homeostasis. Nat Commun. 2019;10(1):181.

267. Luzina IG, Salcedo MV, Rojas-Pena ML, Wyman AE, Galvin JR, Sachdeva A, et al. Transcriptomic evidence of immune activation in macroscopically normal-appearing and scarred lung tissues in idiopathic pulmonary fibrosis. Cell Immunol. 2018;325:1-13.

268. Bauman KA, Wettlaufer SH, Okunishi K, Vannella KM, Stoolman JS, Huang SK, et al. The antifibrotic effects of plasminogen activation occur via prostaglandin E2 synthesis in humans and mice. J Clin Invest. 2010;120(6):1950-60.

269. Gose T, Nakanishi T, Kamo S, Shimada H, Otake K, Tamai I. Prostaglandin transporter (OATP2A1/SLCO2A1) contributes to local disposition of eicosapentaenoic acid-derived PGE3. Prostaglandins Other Lipid Mediat. 2016;122:10-7.

270. Torky AR, Stehfest E, Viehweger K, Taege C, Foth H. Immuno-histochemical detection of MRPs in human lung cells in culture. Toxicology. 2005;207(3):437-50.

271. Chaudhary NI, Schnapp A, Park JE. Pharmacologic differentiation of inflammation and fibrosis in the rat bleomycin model. Am J Respir Crit Care Med. 2006;173(7):769-76.

272. Daniels CE, Lasky JA, Limper AH, Mieras K, Gabor E, Schroeder DR, et al. Imatinib treatment for idiopathic pulmonary fibrosis: Randomized placebo-controlled trial results. Am J Respir Crit Care Med. 2010;181(6):604-10.

273. Yoon YS, Lee YJ, Choi YH, Park YM, Kang JL. Macrophages programmed by apoptotic cells inhibit epithelial-mesenchymal transition in lung alveolar epithelial cells via PGE2, PGD2, and HGF. Sci Rep. 2016;6:20992.

274. Sakai N, Tager AM. Fibrosis of two: Epithelial cell-fibroblast interactions in pulmonary fibrosis. Biochim Biophys Acta. 2013;1832(7):911-21.

275. Yun MH. Changes in Regenerative Capacity through Lifespan. Int J Mol Sci. 2015;16(10):25392-432.

276. Cortijo J, Iranzo A, Milara X, Mata M, Cerda-Nicolas M, Ruiz-Sauri A, et al. Roflumilast, a phosphodiesterase 4 inhibitor, alleviates bleomycin-induced lung injury. Br J Pharmacol. 2009;156(3):534-44.

277. Cross J, Stenton GR, Harwig C, Szabo C, Genovese T, Di Paola R, et al. AQX-1125, small molecule SHIP1 activator inhibits bleomycin-induced pulmonary fibrosis. Br J Pharmacol. 2017;174(18):3045-57.

278. Konya V, Maric J, Jandl K, Luschnig P, Aringer I, Lanz I, et al. Activation of EP receptors prevents endotoxin-induced neutrophil infiltration into the airways and enhances microvascular barrier function. Br J Pharmacol. 2015.

279. Card JW, Voltz JW, Carey MA, Bradbury JA, Degraff LM, Lih FB, et al. Cyclooxygenase-2 deficiency exacerbates bleomycin-induced lung dysfunction but not fibrosis. Am J Respir Cell Mol Biol. 2007;37(3):300-8.

280. Hodges RJ, Jenkins RG, Wheeler-Jones CP, Copeman DM, Bottoms SE, Bellingan GJ, et al. Severity of lung injury in cyclooxygenase-2-deficient mice is dependent on reduced prostaglandin E(2) production. Am J Pathol. 2004;165(5):1663-76.

281. Hodges RJ. The Role of Cyclooxygenase-2 and Prostaglandin E2 in the Pathogenesis of Pulmonary Fibrosis. Ann Arbor, Michigan: University of London.

282. Corboz MR, Zhang J, LaSala D, DiPetrillo K, Li Z, Malinin V, et al. Therapeutic administration of inhaled INS1009, a treprostinil prodrug formulation, inhibits bleomycin-induced pulmonary fibrosis in rats. Pulm Pharmacol Ther. 2018;49:95-103.

283. van den Brule S, Wallemme L, Uwambayinema F, Huaux F, Lison D. The D prostanoid receptor agonist BW245C [(4S)-(3-[(3R,S)-3-cyclohexyl-3-hydroxypropyl]-2,5-dioxo)-4-imidazolidineheptanoi c acid] inhibits fibroblast proliferation and bleomycin-induced lung fibrosis in mice. J Pharmacol Exp Ther. 2010;335(2):472-9.

284. Shi ZM, Wang L, Shen H, Jiang CF, Ge X, Li DM, et al. Downregulation of miR-218 contributes to epithelial-mesenchymal transition and tumor metastasis in lung cancer by targeting Slug/ZEB2 signaling. Oncogene. 2017;36(18):2577-88.

285. Tai HH, Tong M, Ding Y. 15-hydroxyprostaglandin dehydrogenase (15-PGDH) and lung cancer. Prostaglandins Other Lipid Mediat. 2007;83(3):203-8.

286. Nieto MA, Huang RY, Jackson RA, Thiery JP. Emt: 2016. Cell. 2016;166(1):21-45.

287. Liang H, Xu C, Pan Z, Zhang Y, Xu Z, Chen Y, et al. The antifibrotic effects and mechanisms of microRNA-26a action in idiopathic pulmonary fibrosis. Mol Ther. 2014;22(6):1122-33.

288. Thomas PE, Peters-Golden M, White ES, Thannickal VJ, Moore BB. PGE(2) inhibition of TGF-beta1-induced myofibroblast differentiation is Smad-independent but involves cell shape and adhesion-dependent signaling. Am J Physiol Lung Cell Mol Physiol. 2007;293(2):L417-28.

289. Clish CB, Levy BD, Chiang N, Tai HH, Serhan CN. Oxidoreductases in lipoxin A4 metabolic inactivation: a novel role for 15-onoprostaglandin 13-reductase/leukotriene B4 12-hydroxydehydrogenase in inflammation. J Biol Chem. 2000;275(33):25372-80.

290. Bannenberg G, Serhan CN. Specialized pro-resolving lipid mediators in the inflammatory response: An update. Biochim Biophys Acta. 2010;1801(12):1260-73.

291. Gronert K, Clish CB, Romano M, Serhan CN. Transcellular regulation of eicosanoid biosynthesis. Methods Mol Biol. 1999;120:119-44.

292. McCracken JM, Allen LA. Regulation of human neutrophil apoptosis and lifespan in health and disease. J Cell Death. 2014;7:15-23.

293. Bhavsar PK, Levy BD, Hew MJ, Pfeffer MA, Kazani S, Israel E, et al. Corticosteroid suppression of lipoxin A4 and leukotriene B4 from alveolar macrophages in severe asthma. Respir Res. 2010;11:71.

294. Krombach F, Gerlach JT, Padovan C, Burges A, Behr J, Beinert T, et al. Characterization and quantification of alveolar monocyte-like cells in human chronic inflammatory lung disease. Eur Respir J. 1996;9(5):984-91.

295. Pickhardt PJ, Pooler BD, Kim DH, Hassan C, Matkowskyj KA, Halberg RB. The Natural History of Colorectal Polyps: Overview of Predictive Static and Dynamic Features. Gastroenterol Clin North Am. 2018;47(3):515-36.

296. Aringer I, Artinger K, Kirsch AH, Schabhuttl C, Jandl K, Barnthaler T, et al. Blockade of prostaglandin E2 receptor 4 ameliorates nephrotoxic serum nephritis. Am J Physiol Renal Physiol. 2018;315(6):F1869-F80.